

NATHAN REMANS

June 2024

CFD ANALYSIS OF CLT COMPARTMENT FIRES



COMPUTATIONAL FLUID DYNAMICS ANALYSIS OF CROSS LAMINATED TIMBER COMPARTMENT FIRE BEHAVIOUR BASED ON CHEMICAL REACTIONS

Investigating the influence of exposed cross laminated timber on compartment fire dynamics with computational fluid dynamics software by modelling the burning behaviour of wood through chemical reactions.

MASTER THESIS REPORT

In partial fulfilment of the requirements for the degree of:

MASTER OF SCIENCE IN CIVIL ENGINEERING

Specialisation:

BUILDING ENGINEERING STRUCTURAL DESIGN

BY

NATHAN REMANS



Faculty of Civil Engineering and Geosciences
Delft University of Technology

JUNE 2024

Graduation Committee

Prof.dr.ir. J.W.G. van de Kuilen

Chairman Graduation Committee – Biobased Structures and
Materials

Dr.ir. G.J.P. Ravenshorst

Supervisor TU Delft – Biobased Structures and Materials

Dr. Z. Nan

Postdoc TU Delft – 3MD department

Ir. R. van Herpen

Supervisor Eindhoven University of Technology – Built Environment

Ir. N. Castelein

Supervisor Sweco – Engineering & Consultancy Bouw

Graduate Student

Nathan Remans

ACKNOWLEDGEMENTS

For me, this research has been captivating and versatile from start to finish. I would like to thank the following people for helping me successfully complete this research over the last 9 months:

- I would like to thank my supervisors for their wide range of expertises that led to invaluable feedback over the course of my research. Geert Ravenshorst, thank you for helping me define my research scope at the start of the process. Additionally, your approachability for questions and feedback was greatly appreciated in helping me explore new aspects within my research scope. Jan-Willem van de Kuilen, thank you for taking the time abroad in Munich to attend my progress meetings and provide me with valuable feedback. Ruud van Herpen, thank you for the new insights you shared over the course of my thesis. Your critical thoughts on CFD modelling have provided me with a better understanding of the current limitations in the research field. Zhuojun Nan, thank you for being my supervisor while having only just arrived in Delft. Your feedback on setting up and validating the FDS model has proven to be extremely useful for the final result of my thesis. Last but not least, I would like to thank Niels Castelein as my supervisor from Sweco. Your knowledge of current challenges in the timber building industry has taught me a lot about the relevance of my research topic. Additionally, you have made my time at Sweco fun and interactive, especially with the efforts you put into involving me within the team of Sjaak.
- I would like to thank everyone at Sweco for the social and challenging work environment. It was a joy coming into the office in de Bilt. Special thanks to Ersin Ferad for introducing me to CFD software and providing me with invaluable feedback for setting up the FDS model. Additionally, I want to thank Sander Goesten for his continuous feedback on my report and presentations during the last months.
- I would like to thank Gerhard Olivier for providing me with the experimental data which was required for validating the FDS model. Your enthusiastic and thoughtful ideas have increased my motivation for this thesis even further.
- I would like to thank my friends for helping me maintain a good balance between working and enjoying some time for myself. This has definitely been helpful in shutting off my thoughts about my thesis after working hours.
- Lastly, I would like to thank my family for providing me with their continuous support from start to end.

SUMMARY

In recent years, the building industry is experiencing a shift towards timber buildings driven by the need for a sustainable building industry. A popular building typology consists of Cross-Laminated Timber (CLT) panels that function as structural elements. Due to the excellent mechanical properties of CLT panels, the use of this building typology is gaining popularity. There is an ongoing trend for leaving CLT panels exposed, meaning without protective fire-resistant cladding. This enhances the aesthetical appeal of the building but raises questions regarding fire safety.

Following upon this trend, the Dutch government initiated a literature study conducted by RISE for assessing the applicability of the current Dutch building decree for timber buildings. It was concluded that the building decree is not always adequate for guaranteeing fire safety in timber buildings due to the additional fire load that comes with timber elements. Additionally, little knowledge is available to formulate guidelines for the use of exposed CLT panels within a compartment. For bridging this regulatory gap, new methods need to be developed for increasing the knowledge in the timber fire safety engineering industry. Ultimately, this knowledge can be implemented in the Dutch building decree to enhance the possibilities of using exposed CLT panels, while guaranteeing a fire-safe structure.

In the last decade, several experimental series have been conducted aiming to increase the understanding of fire dynamics within a CLT compartment. The overarching goal of these experiments was to assess the impact of exposed CLT surfaces on the temperature development and the energy release within the compartment (HRR). Based on these experiments, it was concluded that leaving CLT exposed does not notably influence the maximum compartment temperatures but does result in a significant increase in released energy within the compartment. This poses additional risks for e.g. external flaming.

The experiments are time-consuming and costly to set up for full-scale compartments. Therefore, computational tools are explored for simulating the fire dynamics within a CLT compartment. Computational Fluid Dynamics (CFD) software is commonly used for simulating the fire behaviour in a structure. However, this type of software is currently focused on non-combustible structural materials which means that solely the interior fuel load contributes to the fire. For compartments with exposed CLT panels it is crucial to include the contribution of the burning CLT to the compartment fire dynamics. Limited existing research is available for this topic. Current research mostly models the burning behaviour of wood in CFD software by using the ignition temperature method, which specifies an ignition temperature and subsequently a predefined burning rate. This simplifies the real burning behaviour of wood, excluding the pyrolysis and combustion processes that occur in fire-exposed wood.

This thesis attempts to model the fire dynamics within a CLT compartment with Fire Dynamics Simulator (FDS), which is a CFD software. Hereby, special attention is given to modelling the pyrolysis and combustion reaction for the fire exposed CLT panels. The ability to model the burning behaviour of wood in FDS is a big step forward to be able to move from large-scale experiments to computational models. The research goal of this thesis is as follows:

“Develop a computational modelling tool applicable for simulating the fire dynamics within a Cross-Laminated Timber (CLT) compartment using chemical reactions, specifically examining the impact of exposed CLT surfaces on compartment fire dynamics.”

A model in FDS consists of three-dimensional meshes built up from a large number of cubical cells. The required computational time is one of the main limitations of FDS, which increases with an increasing number of cells within the computational domain. The second challenge is modelling the

pyrolysis behaviour of wood which is complex to imitate due to the natural origin of wood. The last most important limitation of FDS models is the validation. An FDS model needs to be benchmarked against reference experiments to replicate the experimental results. Even after validation of the model, extrapolation to different test configurations should be done carefully due to the mesh dependency of the model and the impact of other input parameters.

This thesis validates the FDS model by comparing the simulated results with the experimental series by Olivier (2019). This series assessed small-scale cubical compartments with 0,5 m sides and an opening factor of $0,042 \text{ m}^{0.5}$ to allow for oxygen to flow into the compartment. Subsequently, the amount and orientation of exposed CLT surfaces was varied to assess its impact on the compartment fire dynamics. In this thesis three simulations are performed with one wall, two walls and a ceiling exposed respectively. The simulated HRR and gas temperatures are compared with the experimental results for validating the FDS model.

Extensive analyses of the simulated results shows that the HRR due to the burning CLT is overestimated by approximately 50% in the fully developed fire phase in all three small-scale simulations. Therefore, the pyrolysis reaction and the burning rate are overestimated in the FDS model. The simulated burning rates range from 1,15 – 1,33 mm/min, while experimentally measured burning rates are approximately 0,60 mm/min which is more commonly assumed in practice. The HRR is approximated well in the growth phase, thus adequately simulating the ignition and fire development. However, in the decay phase the validation is extremely poor due to the immediate extinguishment of the burning CLT as soon as the gas burner is turned off. This is attributed to the fast inflow of cold ambient air which results in the gas temperatures dropping below the pyrolysis range that is specified between 200 – 400°C. Subsequently, combustion of pyrolysis gases stops as well.

The simulated gas temperatures vary significantly more locally compared to the experimental data. Simulated gas temperatures in the middle of the compartment are underestimated by approximately 30% in the small-scale simulations. On the other hand, gas temperatures near the burning CLT surfaces are either approximated well or slightly overestimated. It is therefore concluded that the radiation from the burning CLT is poorly approximated and has a further reach in real-life experiments.

Extensive sensitivity analyses have shown that the simulated results in the FDS model are highly sensitive to the mesh cell size and the heat of combustion of wood. It is concluded that the three-dimensional mesh should consist of 20 mm cubical cells positioned within a proximity of 10 – 20 cm from the CLT surfaces. Larger cell sizes result in a poor approximation of the fire dynamics, while smaller cells do not notably refine the simulated results but do require significantly longer computing time. In the remainder of the computational domain 100 mm cubical cells should be used to minimise the number of cells in the simulation while maintaining simulation accuracy.

The most challenging part of the FDS model is the char layer that results from the pyrolysis process due to incomplete combustion. Including the formation of a physical char layer results in a highly fluctuating and unrealistic fire behaviour. Therefore, the choice is made to exclude the char layer from the FDS model. Instead, the incomplete combustion is considered by applying an effective heat of combustion value of 10 MJ/kg to the wood material. Hereby, an overestimation of the burning behaviour of the fire exposed CLT surfaces is avoided to the best extent possible in the small-scale simulations.

After validating the FDS model with small-scale experiments, the practical applications of the model are explored. Equation (2) as presented in prEN 1995-1-2 is used for determining the charring depth of a fire-exposed timber element based on the compartment gas temperatures. Based on an extensive analysis, it is concluded that this formula is only suitable for determining the final charring depth after a complete burning phase. Due to the lack of a realistic decay phase in the simulations, the

implementation of the simulated gas temperatures from the FDS model is not recommended. Utilising Equation (2) to determine the charring depth at intermediate points during a fire results in a significant overestimation of the charring depth. Therefore, applying this formula to delamination sensitive CLT is not recommended due to the inability of predicting the moment at which the char layer reaches the glue layer bonding two CLT lamellae.

Furthermore, the FDS model is applied to a full-scale compartment corresponding to the fully exposed CLT experiment by McGregor (2013). Based on the results of the discussed full-scale compartment simulation, it is concluded that the size of the simulated geometry significantly influences the correspondence between experimental and simulated results. Especially the decay phase is a notable point of attention, which depicts sustained burning in the full-scale simulation while resulting in immediate extinguishment in the small-scale simulations. Additionally, the underestimation of the HRR in the full-scale simulation versus the overestimation in the small-scale simulations is a point of attention that needs to be further investigated. It is recommended to apply the FDS model to a larger variety of full-scale CLT compartments to analyse if similar trends are observed.

Conclusively, this thesis provides significant added value by enhancing the knowledge within the CFD modelling research field for FSE. The presented FDS model has potential for serving as a tool to roughly predict the fire dynamics within a CLT compartment. However, further optimisation of the model is required before practical applications in daily engineering can be justified.

CONTENTS

SUMMARY	5
1 INTRODUCTION	16
2 RESEARCH DEFINITION	18
2.1 RESEARCH GOAL	18
2.2 RESEARCH QUESTIONS	18
2.3 RELEVANCE OF THE WORK	19
2.4 METHODOLOGY	19
2.5 REPORT OUTLINE	21
2.6 SCOPE LIMITATIONS	22
3 CROSS-LAMINATED TIMBER	24
3.1 CLT ELEMENTS	24
3.2 MECHANICAL PROPERTIES	24
3.3 FIRE RISK	25
4 FIRE DYNAMICS	26
4.1 FUNDAMENTALS OF WOOD COMBUSTION	26
4.1.1 Combustion	26
4.1.2 Pyrolysis	27
4.1.3 Charring	28
4.2 HEAT RELEASE	33
4.3 HEAT TRANSFER	34
4.4 EFFECTS OF FIRE EXPOSURE ON MECHANICAL PROPERTIES OF TIMBER	34
4.5 COMPARTMENT FIRES	35
4.5.1 Fire development	35
4.5.2 Influencing factors	38
4.5.3 Influence of combustible construction	39
5 FIRE REGULATIONS	40
5.1 FIRE SAFETY	40
5.2 FIRE RESISTANCE	40
5.3 REGULATORY GAP	41
5.4 CONCLUSION	42
6 EXPERIMENTAL CLT FIRE BEHAVIOUR	43
6.1 EXISTING CLT EXPERIMENTS	43
6.1.1 McGregor (2013): Contribution of CLT panels to a room fire	43

6.1.2	Medina Hevia (2014): Fire resistance of partially protected CLT.....	43
6.1.3	Crielaard (2015): Self-extinguishment of CLT	45
6.1.4	Emberley et al. (2017): Description of small and large-scale CLT fire tests.....	46
6.1.5	Hadden et al. (2017): Effects of exposed CLT on compartment fire dynamics.....	46
6.1.6	Su et al. (2018): CLT compartment fire tests	47
6.1.7	Just et al. (2018): CLT compartment fire.....	48
6.1.8	Olivier (2019): Fire performance of CLT.....	49
6.1.9	Mindeguia et al. (2020): Thermo-mechanical behaviour of CLT slabs	50
6.2	CONCLUSION	51
7	MODELLING IN FIRE SAFETY ENGINEERING	52
7.1	RELEVANCE	52
7.1.1	Integration in the building industry.....	52
7.1.2	Challenges and limitations.....	52
7.2	EXISTING SOFTWARE	53
7.2.1	Ozone.....	53
7.2.2	CFAST	54
7.2.3	FDS.....	55
7.2.4	Conclusion	56
7.3	RESEARCH ON CFD MODELLING OF WOOD COMBUSTION.....	57
7.3.1	Hejtmánek et al. (2017): Input data of burning wood for CFD modelling.....	57
7.3.2	Janardhan and Hostikka (2019): CFD simulation of fire spread on wood cribs.....	59
7.3.3	Brunkhorst and Zehfuß (2020): Compartment fires with immobile fire load	60
7.3.4	Dai et al. (2022): Engineering CFD model for fire spread on wood cribs	61
7.3.5	Sun et al. (2022): BIM and FDS framework for simulation of CLT compartments.....	62
7.3.6	Nakrani et al. (2023): Characterization of wood combustion through simulations	63
7.3.7	Hayajneh and Naser (2023): CFD study of fire spread in multi-storey timber building	64
7.4	CONCLUSION	66
8	MODEL DEVELOPMENT	68
8.1	STRUCTURE FDS FILE	68
8.2	MODEL GEOMETRY.....	68
8.2.1	Multiple meshes	68
8.2.2	Thermal boundary conditions	69
8.2.3	Reference experiments.....	70
8.3	MODELLING BURNING BEHAVIOUR OF WOOD.....	72
8.3.1	Pyrolysis.....	72
8.3.2	Combustion	73

8.4	FIRE MODELLING	73
8.5	OUTPUT	74
8.6	PYROSIM POST PROCESSING	75
8.7	CONCLUSION	76
9	SIMULATIONS	77
9.1	SIMULATION 1: LEFT SIDE WALL EXPOSED	77
9.1.1	Observations HRR	77
9.1.2	Observations temperature	79
9.2	SIMULATION 2: 2 SIDE WALLS EXPOSED.....	81
9.2.1	Observations HRR	81
9.2.2	Observations temperature	83
9.3	SIMULATION 3: CEILING EXPOSED.....	85
9.3.1	Observations HRR	85
9.3.2	Observations temperature	86
10	ANALYSIS.....	88
10.1	COMPARISON SIMULATIONS AND EXPERIMENTS	88
10.1.1	HRR	88
10.1.2	Compartment temperatures	90
10.2	SENSITIVITY ANALYSIS.....	94
10.2.1	Mesh size	94
10.2.2	Heat of combustion	96
10.2.3	Wood moisture content.....	98
10.2.4	Ventilation factor	100
11	MODELLING IMPLEMENTATION IN PRACTICE	104
11.1	CHARRING RATE FROM MODEL TO PRACTICE.....	104
11.2	EXTRAPOLATION MODEL TO LARGER COMPARTMENT	108
11.3	CONCLUSION	111
12	CONCLUSIONS	113
13	RECOMMENDATIONS AND FUTURE RESEARCH.....	116
13.1	RECOMMENDATIONS	116
13.2	FUTURE RESEARCH	117
	REFERENCES	118
	APPENDIX	124
A	INPUT DATA FDS MODEL SIMULATION 1	124
B	OVERVIEW FDS NAMELIST RECORDS.....	130
C	THERMAL PROPERTIES OF WOOD	133

D	OVERVIEW EXISTING CLT FIRE EXPERIMENTS.....	135
E	SIMULATION RESULTS.....	137
E.1	Overview results simulation 1	137
E.2	Overview results simulation 2	140
E.3	Overview results simulation 3	142
F	ANALYSIS NON-COMBUSTIBLE SURFACES FDS	145
G	ANALYSIS CHAR LAYER IN FDS MODEL.....	148

List of Figures

Figure 1: The Great Fire of Londen (Museum of Fine Arts, Budapest, n.d.)	16
Figure 2: Fire triangle (Bahrani, 2015)	26
Figure 3: Temperature development through various wood species (TU München, 2023)	28
Figure 4: Charring rate versus density (A. I. Bartlett et al., 2018)	29
Figure 5: Charring rate versus moisture content (A. I. Bartlett et al., 2018)	30
Figure 6: Influence of encapsulation on the char depth (Hakkarainen, 2002)	30
Figure 7: Influence of adhesive and CLT configuration on char depth (Frangi et al., 2009)	31
Figure 8: Charring rate initially unprotected CLT element (NEN, 2023)	32
Figure 9: Charring rate initially protected CLT element (NEN, 2023)	32
Figure 10: Reduction in mechanical properties of wood due to elevated temperatures (Östman, 1985)	35
Figure 11: Temperature development for a compartment fire (Karlsson & Quintiere, 1999)	36
Figure 12: Pressure development in and outside the compartment (Karlsson & Quintiere, 1999)	38
Figure 13: Standard fire curve (International Organisation for Standardization, 2014)	41
Figure 14: HRR comparison of fully protected, partially protected and fully exposed (Hevia & Ramón, 2018)	44
Figure 15: Comparison of compartment temperatures (Hevia & Ramón, 2018)	44
Figure 16: Hypothesis of fire development due to involved CLT (Crielaard, 2015)	45
Figure 17: Comparison of HRR between 6 test setups (Su et al., 2018)	48
Figure 18: Comparison of results (Hejtmánek et al., 2017)	58
Figure 19: Comparison of results (Janardhan & Hostikka, 2019)	59
Figure 20: Comparison of results (Brunkhorst & Zehfuß, 2020)	61
Figure 21: Comparison HRR and fire spread results (Dai et al., 2022)	62
Figure 22: Comparison of results (Sun et al., 2022)	63
Figure 23: Comparison of results (Nakrani et al., 2023)	64
Figure 24: FDS model multi-storey CLT building (Hayajneh & Naser, 2023)	65
Figure 25: Comparison of results (Hayajneh & Naser, 2023)	65
Figure 26: Ideal FDS mesh alignment	69
Figure 27: FDS alignment 2 mesh sizes	69
Figure 28: Incorrect FDS mesh alignment	69
Figure 29: Experimental setup (Olivier, 2019)	71
Figure 30: Thermal degradation of pine wood (Nakrani et al., 2023)	72
Figure 31: Example visualisation FDS model output	75
Figure 32: Visualisation FDS model in PyroSim	75
Figure 33: PyroSim fire and smoke visualisation	76
Figure 34: Simulation 1 visualisation burning rate after 500 seconds	78
Figure 35: Simulation 1 HRR development	79
Figure 36: Simulation 1 gas temperature comparison	80
Figure 37: Simulation 2 full HRR development	82
Figure 38: Simulation 2 HRR development first 3000 seconds	82
Figure 39: Simulation 2 gas temperature full comparison	83
Figure 40: Simulation 2 gas temperature comparison first 4000 seconds	84
Figure 41: Simulation 3 HRR development	86
Figure 42: Simulation 3 gas temperature comparison	87
Figure 43: HRR overview simulations 1 – 3	90
Figure 44: Top view compartment gas temperature slice at 0,2 m height simulation 1	91
Figure 45: Analysis gas temperature simulation 1 - 3 at 0,4 m height	92
Figure 46: Compartment oxygen concentration right before and after turning the gas burner off	93
Figure 47: HRR for varying mesh cell size in heating phase	95
Figure 48: Gas temperatures for varying mesh cell size in heating phase	95
Figure 49: HRR for varying heat of combustion in heating phase	97
Figure 50: Thickness exposed CLT wall over time for varying heat of combustion	98

Figure 51: HRR for varying wood moisture content in heating phase	99
Figure 52: Gas temperatures for varying wood moisture content in heating phase	99
Figure 53: Compartment configurations with varying ventilation factor	100
Figure 54: HRR development for varying ventilation factor	101
Figure 55: Gas temperatures for varying ventilation factor	102
Figure 56: Gas temperature above the surface of exposed left side wall	105
Figure 57: Charring depth simulation 1 vs configuration 3 according to EC5 formula	107
Figure 58: Charring depth simulation 2 vs configuration 2 according to EC5 formula	107
Figure 59: Floor plan full-scale compartment (McGregor, 2013)	108
Figure 60: Mesh size comparison for using in full-scale compartment	109
Figure 61: HRR fully exposed CLT compartment with propane burner (McGregor, 2013)	110
Figure 62: HRR simulation full-scale compartment	110
Figure 63: Specific heat capacity as function of temperature for CLT panels	133
Figure 64: Thermal conductivity as function of temperature for CLT panels	134
Figure 65: Simulation 1 HRR	137
Figure 66: Simulation 1 mass loss rate	137
Figure 67: Simulation 1 decreasing wall thickness	138
Figure 68: Simulation 1 gas temperatures in middle of compartment	138
Figure 69: Simulation 1 gas temperature near CLT surface	138
Figure 70: Simulation 1 CLT surface temperature	139
Figure 71: Simulation 1 thermocouples	139
Figure 72: Simulation 2 HRR	140
Figure 73: Simulation 2 mass loss rate	140
Figure 74: Simulation 2 decreasing wall thickness	140
Figure 75: Simulation 2 gas temperatures in middle of compartment	141
Figure 76: Simulation 2 gas temperature near CLT surface	141
Figure 77: Simulation 2 CLT surface temperatures	141
Figure 78: Simulation 2 thermocouples	142
Figure 79: Simulation 3 HRR	142
Figure 80: Simulation 3 mass loss rate	142
Figure 81: Simulation 3 decreasing ceiling thickness	143
Figure 82: Simulation 3 gas temperatures in middle of compartment	143
Figure 83: Simulation 3 CLT surface temperature	143
Figure 84: Simulation 3 thermocouples	144
Figure 85: HRR for varying non-combustible surfaces in heating phase	146
Figure 86: Gas temperatures for varying non-combustible surfaces	147
Figure 87: HRR for varying char ratio in heating phase	149
Figure 88: Mass loss rate exposed CLT wall for varying char ratio	150

List of Tables

Table 1: CLT charring rates in ETA-14/0349	33
Table 2: Overview research on CFD modelling	57
Table 3: Material properties FDS model (Hejtmánek et al., 2017)	57
Table 4: Input data FDS model by Janardhan and Hostikka (2019)	59
Table 5: Input data FDS model by Brunkhorst and Zehfuß (2020)	60
Table 6: Input data FDS model by Dai et al. (2022)	61
Table 7: Input data FDS model by Sun et al. (2022)	62
Table 8: Input data FDS model by Nakrani et al. (2023)	64
Table 9: Overview test setup (Olivier, 2019)	71
Table 10: FDS model output quantities	74
Table 11: Overview configurations for FDS simulations	77
Table 12: Overview simulation 1	77
Table 13: Observations HRR simulation 1	78
Table 14: Quantification HRR simulation 1 vs configuration 3 in heating phase	79
Table 15: Quantification gas temperatures simulation 1 vs configuration 3 in heating phase	80
Table 16: Overview simulation 2	81
Table 17: Observations HRR simulation 2	81
Table 18: Quantification HRR simulation 2 vs configuration 2 in heating phase	83
Table 19: Quantification gas temperatures simulation 2 vs configuration 2 in heating phase	84
Table 20: Overview simulation 3	85
Table 21: Observations HRR simulation 3	85
Table 22: Quantification HRR simulation 3 vs experiment in heating phase	86
Table 23: Quantification gas temperatures simulation 3 vs configuration 4 in heating phase	87
Table 24: HRR analysis simulation 1 – 3 in heating phase	89
Table 25: Gas temperature analysis simulation 1 - 3 in heating phase	91
Table 26: Default values FDS model before sensitivity analysis	94
Table 27: Results mesh size sensitivity analysis first 400 seconds	95
Table 28: Results heat of combustion sensitivity analysis heating phase	96
Table 29: Overview burning rate for varying heat of combustion in heating phase	97
Table 30: Results moisture content sensitivity analysis heating phase	99
Table 31: Results ventilation factor sensitivity analysis heating phase	101
Table 32: Overview EC5 charring left side wall	106
Table 33: Description namelist records FDS	130
Table 34: Thermal properties for CLT panels	133
Table 35: Overview existing CLT fire experiments	135
Table 36: Properties PromatectH surface in FDS model	145
Table 37: Overview simulation results for varying non-combustible surfaces	146
Table 38: FDS input properties char layer	148
Table 39: HRR results for varying char ratio	148

PART 1: RESEARCH OUTLINE

This part provides the context and motivation for this master thesis. Based on the sketched context, the research definition is given. Hereby formulating the research goal, research questions and methodology.

- CHAPTER 1: INTRODUCTION

- CHAPTER 2: RESEARCH DEFINITION
 - Chapter 2.1: Research goal
 - Chapter 2.2: Research questions
 - Chapter 2.3: Relevance of the work
 - Chapter 2.4: Methodology
 - Chapter 2.5: Report outline
 - Chapter 2.6: Scope limitations

1 INTRODUCTION

The Great Fire of London in 1666 is the largest and most influential fire of the last centuries. It was a devastating fire that burned down a substantial part of the city. Fuelled by the large number of timber-framed buildings and narrow streets, it consumed over 13000 homes leaving tens of thousands of people homeless.

This catastrophic event marked a turning point in architectural history. It led to more strict building codes, emphasising the use of brick and stone over timber, ultimately transforming construction practices. This tragic event has had a lasting influence on urban planning and the gradual shift away from combustible construction materials, like timber, towards non-combustible materials.



Figure 1: *The Great Fire of London* (Museum of Fine Arts, Budapest, n.d.)

Today, an ongoing trend can be seen in the construction industry in the resurgence of timber's popularity as a construction material. This trend is mainly driven by the increasing importance of sustainability and facilitated by the development of excellent engineered wood products. Timber's mechanical properties, aesthetical appeal and low carbon footprint have opened the eyes of architects and structural engineers.

Engineered wood products, especially cross-laminated timber (CLT), are being applied more often. CLT has gained popularity because of its good mechanical properties due to the crosswise layup of the CLT panels. Additionally, CLT panels allow for fast on-site construction due to its prefabricated nature. Apart from all these benefits, the combustible nature of timber remains, which raises questions regarding fire safety.

In recent decades fire safety of CLT elements has been assured by protecting the timber with fire-resistant products. An often-applied protective measure is gypsum plasterboard. In recent years experiments have been performed to investigate the fire behaviour of CLT in case the panels are left exposed, thus without protective measures. In the Netherlands, an ongoing trend can be observed in leaving CLT elements exposed in structures. The reason for this is the valuation of the aesthetical quality of timber. Yet, leaving CLT elements exposed comes with an inherent fire risk which should be dealt with carefully based on current knowledge and to provide a balance between architectural beauty and fire safety.

Fire safety guidelines are focused on the concept of compartmentation. Compartmentation aims to confine a fire within one compartment for the prescribed fire resistance duration, simultaneously preventing the fire from spreading to adjacent compartments. Current guidelines are based on compartments where the fire is fuelled solely by the interior furniture, and not the construction itself. This framework applies to concrete and steel structures, but when dealing with CLT elements, a notable shift occurs. Compartments consisting of CLT walls, floors and/or ceilings show different fire behaviour compared to traditional compartments due to the additional fuel load. Consequently, gaining a deeper understanding of the compartment fire dynamics and the influence of exposed CLT panels is essential to facilitate the translation of this knowledge into design guidelines. This way architects and structural engineers can make fast and decisive choices regarding CLT compartment configurations in multi-storey residential buildings, where CLT panels are most commonly applied.

Current research on CLT compartment fire behaviour is focused on real-life experimental testing. Testing large compartments is time consuming and expensive to setup. As with many other disciplines in the engineering industry, it would be beneficial to develop computational tools to accelerate research in the timber fire safety engineering (FSE) industry. These tools will allow for quick parametric studies to gain useful insights into the fire behaviour within a timber structure, focussing on CLT compartments for this thesis. The development of these tools is still in the early stages for this specific application. Therefore, it is of great importance to contribute to the existing modelling knowledge. In the long run, knowledge gained from adequate computational models can be implemented in building regulations regarding safe amounts of exposed CLT in compartment fires.

This thesis aims to help set the stage for the future of fire-safe sustainable construction.

2 RESEARCH DEFINITION

Based on the aforementioned problem description in Chapter 1, the research scope for this master thesis can be defined. First, the research goal and coherent questions are addressed. Subsequently, the research methodology is described with the relevant scope limitations to set the boundaries within which the research is conducted.

2.1 RESEARCH GOAL

The goal of this research is to enhance the understanding of the computational modelling of the burning behaviour of wood, hereby contributing to the important ambitions for thriving towards a more sustainable building industry. After completion of this master thesis, the following research goal will be obtained in the best way possible:

“Develop a computational modelling tool applicable for simulating the fire dynamics within a Cross-Laminated Timber (CLT) compartment using chemical reactions, specifically examining the impact of exposed CLT surfaces on compartment fire dynamics.”

2.2 RESEARCH QUESTIONS

For ultimately accomplishing the overarching research objective of this thesis, the main research question is formulated for clearly defining the research scope:

“Under what conditions can a computational model be developed which accurately assesses the influence of exposed CLT surfaces on compartment fire dynamics using chemical reactions?”

Due to the wide scope of the above-mentioned question, the main research question can be divided into multiple sub-questions which contribute to finding a conclusive answer to the main question of this master thesis. The subquestions are used to structure the report, hereby highlighting the contribution of each part of the thesis for attaining the research goal.

The sub-questions are listed below, with the relevant chapter for each question listed between brackets. A more elaborate description of the implemented approach for this master thesis is presented in Chapter 2.4.

- **Subquestion 1:** What currently restricts the use of exposed CLT in the building industry? (CH5)
- **Subquestion 2:** To what extent does the orientation of exposed CLT surfaces limit the configuration of a CLT compartment? (CH6)
- **Subquestion 3:** To what extent does the ventilation factor influence the fire dynamics within a CLT compartment? (CH6)
- **Subquestion 4:** What are current limitations in computational software for modelling the burning behaviour of wood? (CH7)
- **Subquestion 5:** In what way can CFD software provide a solution in practical engineering situations? (CH11)

2.3 RELEVANCE OF THE WORK

The building industry is aiming for a sustainable circular economy in which the use of engineered wood products like CLT plays a key role. The design guidelines for timber structures as specified in the current NEN-EN 1995-1-2 do not include the use of CLT specifically. The recently proposed prEN 1995-1-2 makes a big step in including CLT on element level. However, on compartment level the required knowledge is missing regarding fire safety. Extension of this knowledge has the potential to allow for designing full-scale partially exposed CLT compartments in a fire-safe manner.

This thesis utilises computational fluid dynamics (CFD) software to analyse various exposed CLT configurations within a compartment to reach a better understanding of the fire dynamics in a combustibile compartment. The capability of modelling the distinct burning behaviour of wood through the chemical reactions occurring in fire-exposed timber elements is a big step forward in the research field of CFD modelling. Additionally, analysing the impact of various input parameters on CFD simulation results gives a better understanding of the applicability of this type of software to timber structures, hereby focusing on CLT compartments.

An adequate CFD model can open the path for analysing the fire safety of timber structures in a new manner. The main relevance of this thesis is therefore found in assessing the possibilities and limitations of modelling CLT compartment fires with CFD software.

2.4 METHODOLOGY

Part 1: Research outline

First, an introduction is given focussing on the increasing popularity of CLT as a construction material and the associated fire concerns. This presents the necessity of this thesis in a comprehensive way. Subsequently, the research goal and coherent research questions are formulated. The research outline is presented, and the relevant scope limitations are mentioned.

Part 2: Theoretical framework

The theoretical framework consists of multiple chapters focussing on various relevant topics for assessing CLT compartment fires. CLT as a construction material is discussed, followed by a general description of fire dynamics, giving special attention to CLT compartments. The concept of fire safety and its implementation in the Dutch building decree is explained, presenting the relevant regulatory gap in the application of exposed CLT elements. Additionally, an overview is given of the existing experimental research into the fire behaviour of CLT compartments and its potential for self-extinguishment. Lastly, the state of the art of computational modelling in the field of timber fire safety engineering is presented.

This part presents the theoretical basis for setting up a representative computational model in Part 3.

Part 3: Computational testing

This part covers the setup, simulation and analysis of a Computational Fluid Dynamics (CFD) model. The goal is to assess the fire behaviour within a CLT compartment, specifically aiming to gain a better understanding of the influence of exposed CLT surfaces and other influencing factors on the fire dynamics. The setup of the model, specifically focussing on modelling the burning behaviour of wood, is presented extensively. Representative existing experimental results and empirical data are used to validate the computational model. Fire Dynamics Simulator (FDS) is used as software due to the large

possibilities associated with this CFD software. The comparison between experimental and simulation results aims to assess the possibilities and limitations of FDS for modelling CLT compartment fires.

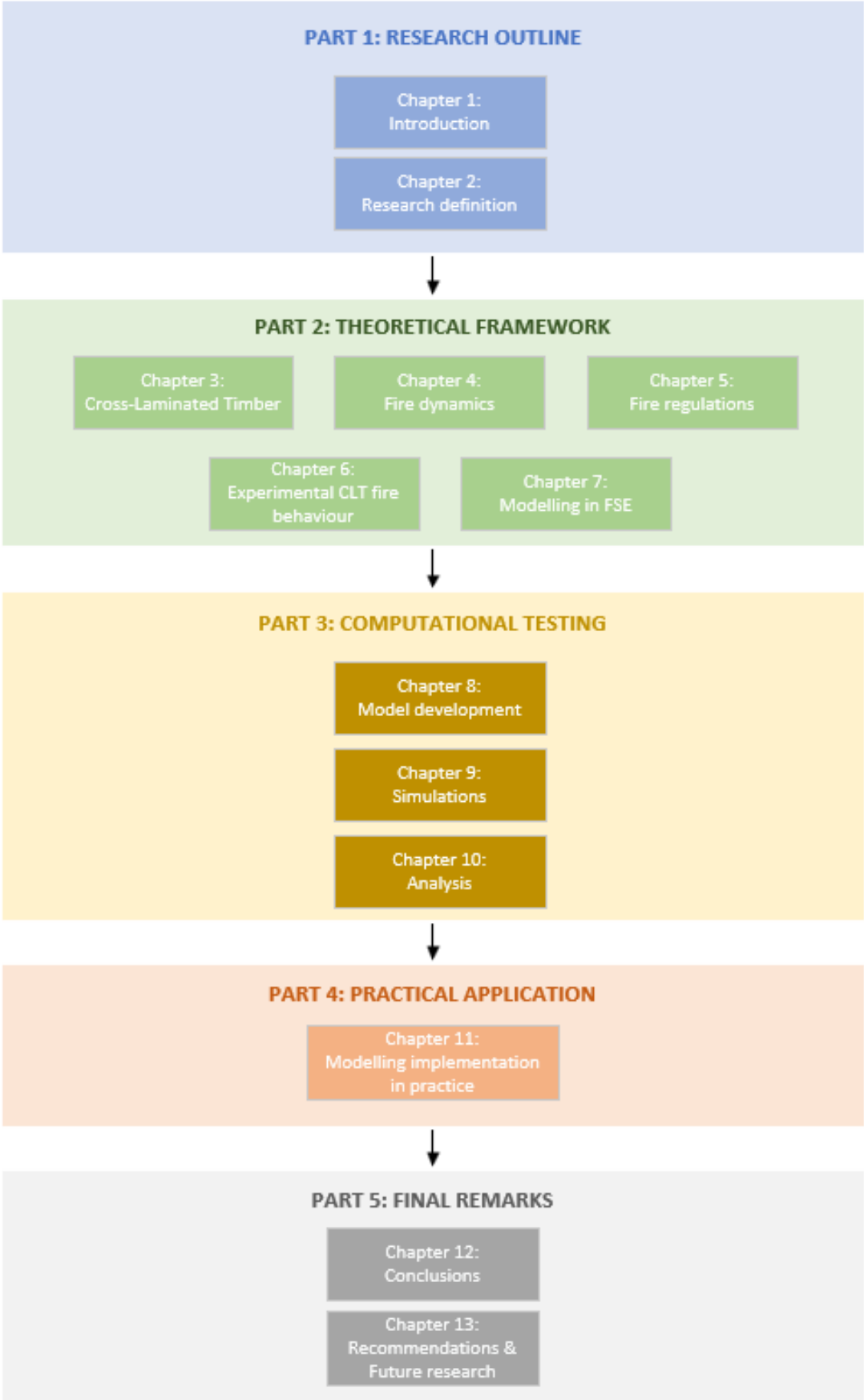
Part 4: Practical application

Based on the results of the FDS simulations, the application possibilities of FDS as a modelling tool in practice are explored. First, the simulated local gas temperatures are used to determine the charring development of exposed CLT surfaces in a small-scale compartment. Subsequently, the FDS model is extrapolated to a full-scale compartment to assess the influence of the geometry size on the functionality of the model. Conclusively, it is discussed to what extent computational software like FDS provides a useful tool for engineers to apply in practice when designing CLT structures.

Part 5: Final remarks

The final part of this master thesis provides adequate answers to the main research question and the corresponding sub-questions based on the presented theoretical framework and the simulation results. Additionally, recommendations are given based on a critical view of the performed research methodology. Topics for future research are presented to increase the knowledge in CLT fire safety engineering and explore the possibilities and limitations of CFD software for timber structures.

2.5 REPORT OUTLINE



2.6 SCOPE LIMITATIONS

- The validation of the FDS model is solely focused on the simulated HRR and gas temperatures. Other characteristic quantities are not considered and may not be accurately approximated.
- Validation of the simulated results in FDS is only considered in the heating phase, because of the poor approximation without an external heat source in the form of a gas burner.
- Validation of the FDS model is based on one specific set of experiments as conducted by Olivier (2019). The influence of deviations in the experimental results therefore directly impacts the accuracy of the model validation.
- The influence of the size of the simulated compartment is only investigated to a small extent by simulating one full-scale compartment corresponding to the experiment by McGregor (2013).
- The FDS model is simulated for one specific wood species, which is pine wood. Therefore, the influence of varying wood material properties like density and porosity is not considered.
- The influence of a char layer on the burning behaviour of wood is not considered due to the exclusion of a physical char layer from the FDS model based on an extensive sensitivity analysis.
- Delamination of CLT lamellae is not included in the FDS model due to the highly complex and unpredictable nature of this phenomenon. Therefore, non-delaminating CLT is assumed and an experimental series is used for validation where delamination is limited.
- The simulated CLT surfaces are exposed and untreated, therefore excluding the potential benefits of fire-protective cladding and impregnation.
- Practical applications of the computational model are only explored to the extent that the focus matches the remainder of the research.
- No active fire protection systems are considered because the research goal is to focus solely on modelling the burning behaviour of exposed CLT panels. Active fire protection systems, like sprinklers, can be modelled in FDS and its impact on reducing the fire intensity can be an interesting topic for future research. This way integral fire safety strategies can be explored in FDS simulations.
- Other CFD software are not considered for simulating the fire dynamics in a CLT compartment due to the known functionalities of FDS.

PART 2: THEORETICAL FRAMEWORK

This part provides the theoretical framework required for understanding the background of this master thesis. A wide range of topics is discussed, varying from CLT fire dynamics to computational modelling in timber fire safety engineering.

- CHAPTER 3: CROSS-LAMINATED TIMBER
 - Chapter 3.1: CLT elements
 - Chapter 3.2: Mechanical properties
 - Chapter 3.3: Fire risk

- CHAPTER 4: FIRE DYNAMICS
 - Chapter 4.1: Fundamentals of wood combustion
 - Chapter 4.2: Heat release
 - Chapter 4.3: Heat transfer
 - Chapter 4.4: Effects of fire exposure on mechanical properties of timber
 - Chapter 4.5: Compartment fires

- CHAPTER 5: FIRE REGULATIONS
 - Chapter 5.1: Fire safety
 - Chapter 5.2: Fire resistance
 - Chapter 5.3: Regulatory gap
 - Chapter 5.4: Conclusion

- CHAPTER 6: EXPERIMENTAL CLT FIRE BEHAVIOUR
 - Chapter 6.1: Existing CLT experiments
 - Chapter 6.2: Conclusion

- CHAPTER 7: MODELLING IN FIRE SAFETY ENGINEERING
 - Chapter 7.1: Relevance
 - Chapter 7.2: Existing software
 - Chapter 7.3: Research on CFD modelling of wood combustion
 - Chapter 7.4: Conclusion

3 CROSS-LAMINATED TIMBER

This chapter provides a comprehensive overview of Cross-Laminated Timber (CLT). The increasing range of applications is discussed with the required mechanical properties and the fire risk that is associated with CLT structures. This provides the basis for understanding CLT as a construction material and the challenges that engineers face regarding fire safety.

3.1 CLT ELEMENTS

CLT panels are large-sized plate-like structural elements which are usually composed of 3, 5 or 7 layers. Each layer constitutes of lamellas which are placed side by side and finger-jointed in the longitudinal direction to produce the required dimensions of the CLT panel (Falk et al., 2016). In Europe, it is common to use Norway spruce for CLT panels.

The European product standard for CLT, EN 16351, allows the layer thickness to range between 6 mm and 45 mm. The width of a single lamella can range between 40 mm and 300 mm. The layers are subsequently glued together in a crosswise pattern by means of an adhesive using either vacuum or hydraulic pressing (SWEDISH WOOD, 2019).

The production process allows for large-sized CLT panels. However, commonly used maximum dimensions by manufacturer Stora Enso are 16,5m in length and 3,5m in height, which are restricted by transportation possibilities and onsite storage of the panels (Brandner et al., 2016). Openings for doors and windows can be easily positioned during the production process. The high degree of prefabrication allows for fast onsite construction, compared to concrete structures.

The standardisation of the use of CLT has been an ongoing topic in Europe for the last two decades. It has resulted in reference test conditions for CLT elements, as stated in NEN-EN 408. CLT elements should preferably be tested at an ambient temperature of 20°C and an equilibrium moisture content of 12%. In the year 2021, the norm NEN-EN 16351 was released, presenting an extensive overview of the requirement for CLT elements.

As part of the standardisation process, CLT products must be approved through a product certification. Stora Enso is a large-scale CLT manufacturer in Europe. Its products comply with the European Technical Assessment ETA-14/0349. This ETA contains all the required dimensional limitations, material properties and fire-related characteristics for the application of CLT products by Stora Enso. Other CLT manufacturers have slightly adjusted ETA certifications, but the layout is similar. For the scope of this thesis, the ETA-14/0349 is regarded because of the extensive use of CLT products by Stora Enso in Europe.

3.2 MECHANICAL PROPERTIES

The gaining popularity of CLT as a construction material is largely due to its structural possibilities. CLT panels can carry loads both in and out of plane. The crosswise layering of the CLT layers enables high dimensional stability. CLT panels are therefore highly suitable for stabilising a multi-storey building (Brandner et al., 2016).

Timber inherently shows a large variability in mechanical properties due to its natural origin, even within one element. CLT panels can lower that variability due to the interaction in the laminar structure of CLT where homogenization of strength properties and density takes place within and between individual layers (Falk et al., 2016).

Often used strength classes are CL24h and CL28h which indicate the bending strength out-of-plane for the CLT panel. It is common in practice to apply wood of a higher strength in the surface layer of the panel and in the main direction of the load, where the applied stresses are maximal. It is important to consider the reduction of timber strength over time, depending on the intensity and duration of the applied stresses on the CLT panel. In NEN-EN-1995 this is dealt with by applying a modification factor to the timber strength.

For the scope of this thesis, the understanding of the structural behaviour of CLT is essential in determining the structural integrity of a compartment exposed to a fire.

3.3 FIRE RISK

The use of combustible CLT panels, in combination with the increasing trend of leaving CLT exposed, results in other fire risks than commonly associated with steel and concrete structures as described in the literature study by Brandon et al. (2022). The influence of combustible construction is further discussed in Chapter 4.5.3 with the related impact on fire safety being discussed in Chapter 5.

The structural performance of a fire exposed CLT panel is highly dependent on the thermal properties of the adhesive layer, bonding the CLT layers. In general, the thermal conductivity and thermal capacity of a CLT panel are similar to the properties of solid timber which indicates that a CLT panel can behave like solid timber if failure of the adhesive, referred to as delamination, is prevented (SWEDISH WOOD, 2019). A more detailed description of the adhesive influence on CLT panels exposed to fire, with the risk of delamination, is given in Chapter 4.1.3.2.

In practice, the design of a CLT element is commonly governed by serviceability limit state (SLS) conditions, instead of fire conditions. However, it is highly important to consider the additional risks that come within a fire exposed CLT compartment with exposed CLT panels to determine the structural integrity of the structure and the safety of the building occupants.

4 FIRE DYNAMICS

This chapter covers a wide range of topics related to fire dynamics, relevant for assessing compartment fires. First, the fundamentals of wood combustion are discussed. Consequently, the heat release and associated heat transfer modes are presented. Lastly, the compartment fire behaviour is discussed, giving special attention to CLT compartments and the impact of fire exposure on wood properties. Ultimately, the fire dynamics fundamentals are utilised in setting up the computational model in Chapter 8.

4.1 FUNDAMENTALS OF WOOD COMBUSTION

4.1.1 Combustion

Wood is a cellulose-based material. The constituents of wood can function as fuel during a fire by reacting with oxygen after being ignited by a heat source. This is the so-called fire triangle, as depicted in Figure 2, which presents the three required elements for establishing a fire.

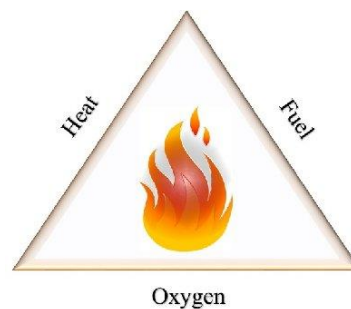
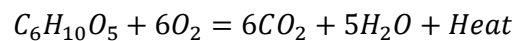


Figure 2: Fire triangle (Bahrani, 2015)

The chemical reaction leading to the occurrence of a fire is called the combustion reaction. For cellulose based materials, the fire triangle translates to the following combustion reaction:



(1)

The wood constituents (lignin, hemicellulose and cellulose) decompose at different temperatures thereby releasing gaseous pyrolysis products, as described in Chapter 4.1.2. Ignition of the solid fuel source can occur by two distinct mechanisms: piloted ignition and spontaneous ignition. This section is based on the work of Drysdale (2011).

Piloted ignition occurs at the point when the pyrolysis process releases sufficient combustible gases to form a flammable gas mixture near the surface of the fuel source. At this point, ignition of the gas mixture by a flame or spark results in a flame. This is referred to as the flashpoint. The pyrolysis rate enables a sufficient production of combustible gases to sustain the flame.

In case there is no flame or spark to ignite the fuel source, the fuel will continue heating. At a certain point, the heat flux has reached a sufficiently high value at which the released combustible gases will spontaneously ignite. This is accompanied with a higher surface temperature of the fuel, compared to piloted ignition.

After ignition, the fuel source can go either in flaming combustion or smouldering combustion. For the scope of this thesis, both are relevant in determining the process towards self-extinguishment of a CLT compartment. This is discussed in the following sections.

4.1.1.1 Flaming combustion

Flaming combustion is a dynamic and visible process, characterized by the presence of a visible flame. This phenomenon occurs when a fuel undergoes rapid oxidation in the presence of oxygen from the ambient air. The combustion reaction releases heat, light, and various combustion by-products. During flaming combustion, the fuel vaporizes, and the vapour combines with oxygen in the air to produce a combustion zone. In this combustion zone visible flaming is observed. The flame results from the incandescence of hot gases and particles produced in the combustion process (Drysdale, 2011).

4.1.1.2 Smouldering combustion

Smouldering combustion occurs in materials which are porous and form a solid carbonaceous char layer, which corresponds to wood. Smouldering is a slow, low-temperature form of combustion which often results in no visible flaming. In the context of wood, smouldering combustion involves the slow and incomplete oxidation of the material, usually taking place in the absence of sufficient oxygen. During smouldering, wood undergoes pyrolysis, further discussed in Chapter 4.1.2. The smouldering process is characterized by a glowing or hot surface, and it can continue for extended periods. Unlike flaming combustion, which relies on rapid oxidation and the presence of flames, smouldering combustion is a more self-sustaining process.

Although smouldering combustion generates only a fraction of the heat compared to flaming combustion, it poses different challenges. Smouldering fires can go unnoticed for extended periods, leading to the gradual release of combustible toxic gases and the generation of heat. If conditions within the compartment change, such as increased oxygen availability, smouldering combustion can transition to a more intense flaming combustion.

4.1.2 Pyrolysis

Pyrolysis of wood is an endothermic process by which materials decompose upon exposure to heat. The pyrolysis process involves both chemical and physical changes to the base material (Browne, 1958). For wood to burn, its polymers first need to be decomposed into smaller molecules which can exist in the gaseous phase at ambient conditions. These gaseous products, also referred to as volatiles, can escape the wood surface and burn above this surface if mixed in the right conditions with oxygen (Crielaard, 2015).

To create a self-sustaining burning reaction of wood, the combustion of the released gases must generate sufficient heat to continue the production of volatiles. Wood is a heterogeneous material, constituting of various polymers. These polymers decompose at different temperatures, hereby releasing volatiles. Typically, wood undergoes three main stages of pyrolysis, which is discussed below based on the work of A. I. Bartlett et al. (2018):

1. Free water begins to evaporate when temperatures within a wood element approach 100°C. Part of the water vapour migrates deeper into the wood element, consequently recondensing as temperatures decrease and increasing the local moisture content. In this phase, three zones can be identified. A dry zone closest to the exposed surface, where the pyrolysis takes place. One layer deeper, the dehydration zone is found, and the deepest layer is the wet zone. The temperature rise within the wood element propagates slowly as a significant amount of energy is used for the evaporation of free water.
2. Onwards from temperatures of 200°C within the wood element, mainly non-combustible volatiles are released from the fire-exposed surface such as carbon dioxide, formic acids and

acetic acids. Prolonged heating at these temperatures causes hemicellulose and lignin to convert into a carbonaceous char layer. The cellulose remains unaffected.

3. Between 300°C and 500°C the pyrolysis rate increases significantly in combination with additional exothermic reactions. Consequently, the temperature rises rapidly. At these temperatures cellulose is decomposed, hereby releasing combustible gases. These gases are ignited due to the high wood surface temperature, resulting in flaming combustion of the wood element. The 300°C isotherm is often taken as the position of the char layer (Hadden et al., 2017). The charring process is discussed elaborately in Chapter 4.1.3.

The transition between wood and char is visualised in Figure 3. This supports the assumption that wood is transformed into char around the 300°C isotherm. The pyrolysis process forms the basis of understanding the fire dynamics within a CLT compartment.

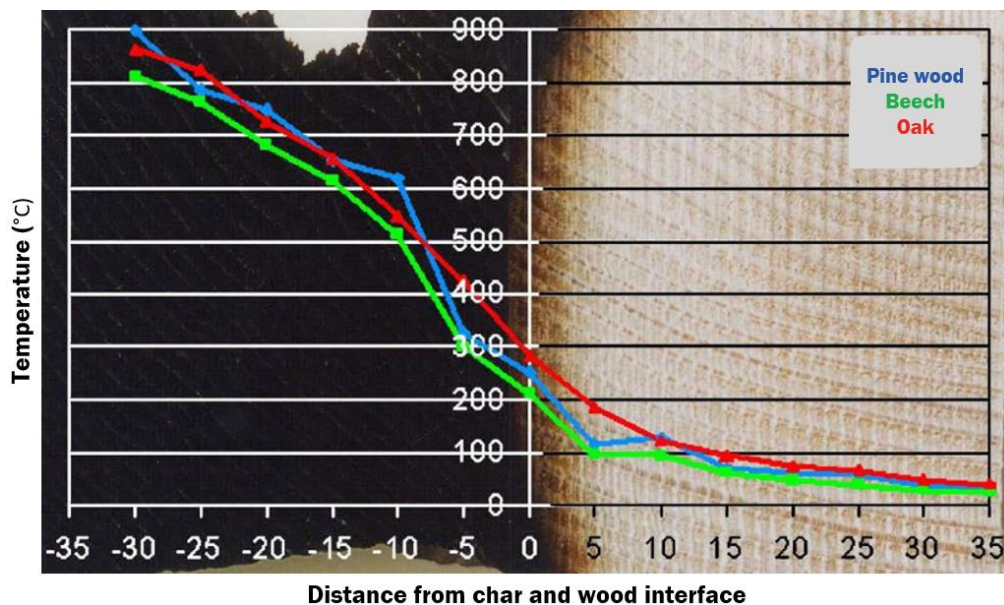


Figure 3: Temperature development through various wood species (TU München, 2023)

4.1.3 Charring

The combustion process, as described in Chapter 4.1.1, is not a fully efficient process which is referred to as incomplete combustion. As such not all wood polymers are used as fuel, hereby leaving some residue behind. For wood this residue is called char, which is a carbon-rich porous solid (Crielaard, 2015). This chapter discusses the fundamentals of charring behaviour, its influence on wood properties and the relevance for CLT panels.

When wood is burning in ambient conditions, approximately 20% of the original mass remains as char. Due to the low density and high porosity of the char layer, it forms a natural insulating barrier for the unaffected wood under the char layer. The pyrolysis process continues below the char layer, but the release of combustible volatiles is reduced due to the char layer. Hereby, the supply of fuel gases to the combustion zone is reduced, effectively limiting the fire growth (Drysdale, 2011).

Compared to wood, the mechanical properties of the char layer can be disregarded in determining the residual strength of a timber element during and after a fire. As such the charring rate is of great importance in assessing the structural integrity of a timber structure.

4.1.3.1 Factors influencing the charring rate

The charring rate depends on various factors which are discussed below, mainly based on the work of A. I. Bartlett et al. (2018).

The density of wood is affecting the charring rate significantly. Research has shown a general trend that a higher density corresponds to a lower charring rate as depicted in Figure 4. This is due to the larger mass that needs to be pyrolyzed, which requires more energy to keep the endothermic pyrolysis process going. Additionally, Friquin (2010) relates this to the lower lignin content in hardwoods which has shown a correlation with lower charring rates.

However, it can reasonably be assumed that this has no significant impact on the design of a timber structure. Usually in construction, softwoods are used which have limited spread in density, resulting in a limited spread in charring rates.

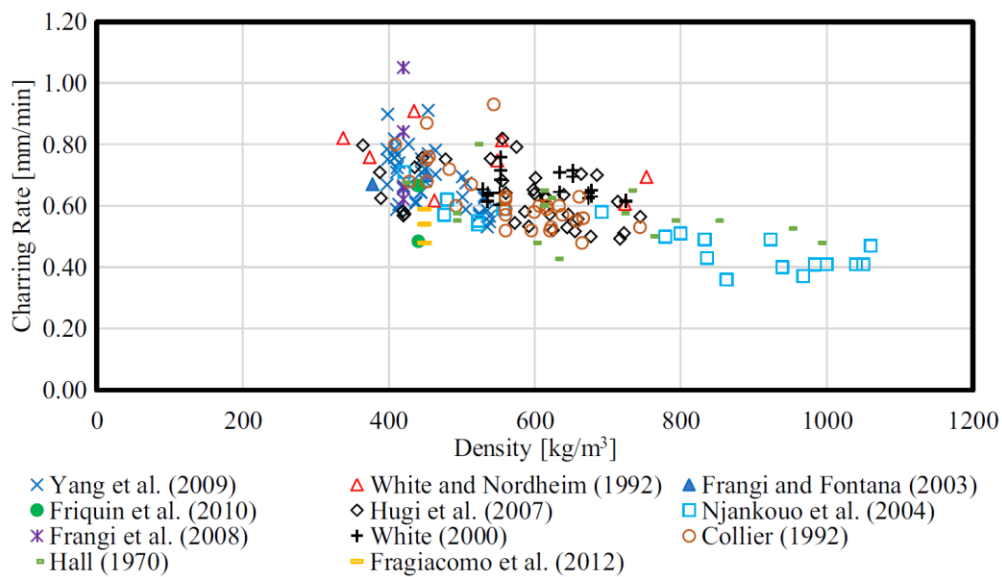


Figure 4: Charring rate versus density (A. I. Bartlett et al., 2018)

Moisture content is a notable factor in retarding the pyrolysis process as depicted in Figure 5. This is due to the required energy to evaporate the water within the wood element, which leaves less energy for the pyrolysis process. However, experimental research resulted in poor agreement on quantifying the impact of moisture content on the charring rate. In practice, the moisture content will not be a governing factor as it is a material property which will be determined by the climate in which the structure is placed depending on the ambient temperature and relative humidity.

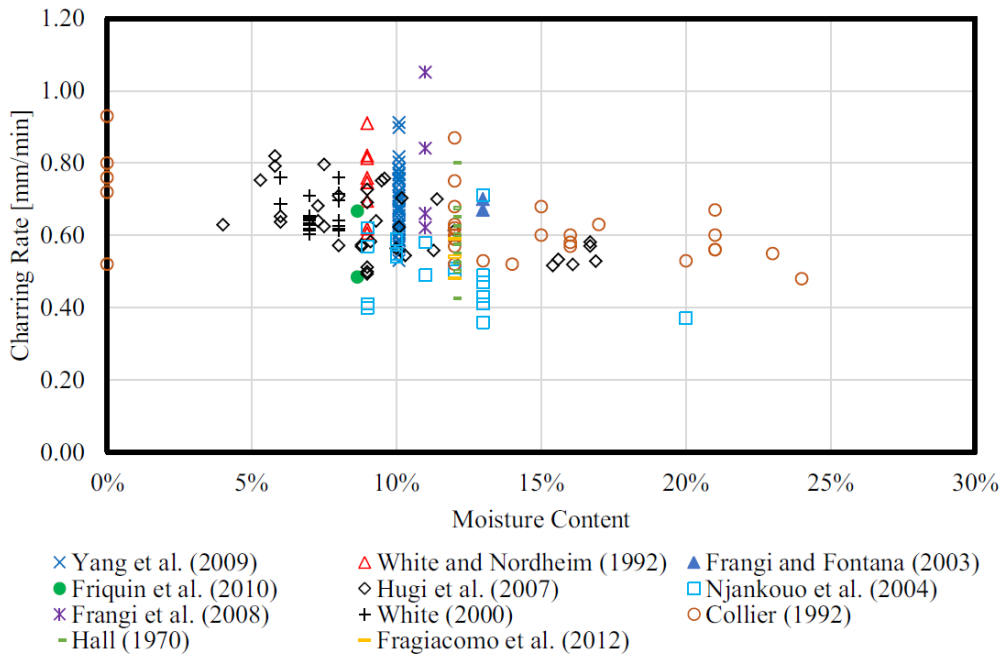


Figure 5: Charring rate versus moisture content (A. I. Bartlett et al., 2018)

System properties such as sample orientation (horizontal or vertical) and grain direction (parallel or perpendicular) have shown little influence on the charring behaviour of a wood sample. This was contradictory to the expectations because higher charring rates were expected parallel to the grain due to a higher permeability in this direction.

The influence of encapsulation of timber elements has been investigated by applying varying amounts of gypsum plasterboard. It was concluded that gypsum plasterboard delays the ignition of the underlying timber. However, once the gypsum layer falls off the charring rate increases significantly due to the lack of an insulating char layer, as depicted in Figure 6.

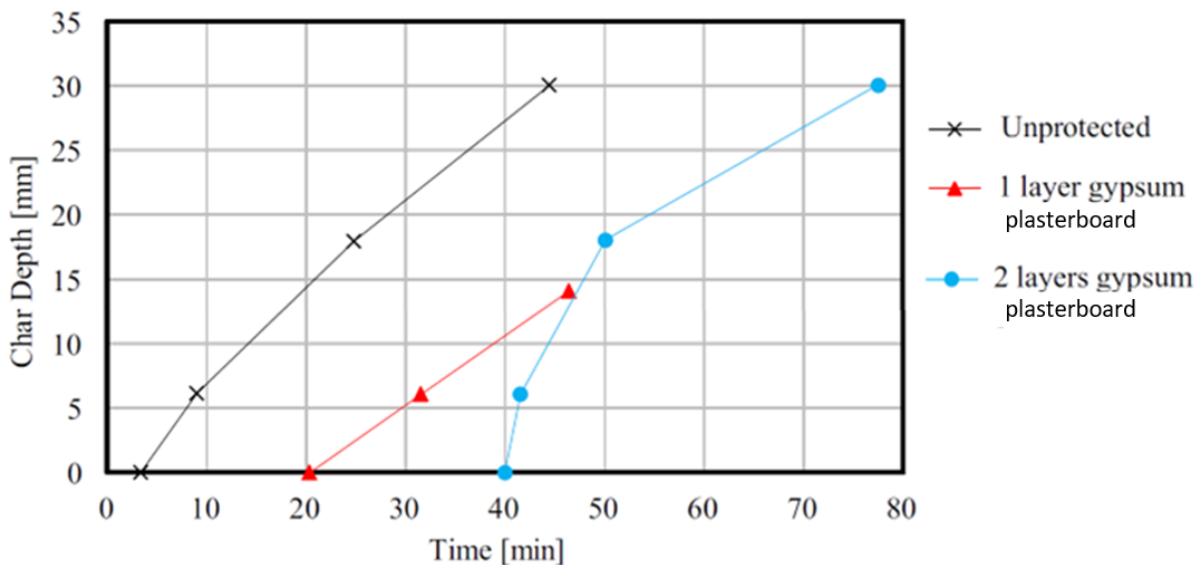


Figure 6: Influence of encapsulation on the char depth (Hakkarainen, 2002)

4.1.3.2 Delamination

For the scope of this thesis, the relevance of charring for CLT panels is discussed, including the associated issue of delamination. Delamination is defined as a phenomenon in which the fire-exposed outer lamella (partially) detaches from the rest of the timber element (Wade, 2019). This is relevant to CLT due to its layered build-up. The cause of delamination is specifically the failure of the adhesive, bonding the lamellas together. Therefore, the thermal resistance of the used adhesive is crucial during a fire in preventing delamination. Often used adhesives are polyurethane (PU) or melamine-urea-formaldehyde (MUF) which have shown different charring behaviour. The influence of the adhesive type and the CLT configuration is depicted in Figure 7.

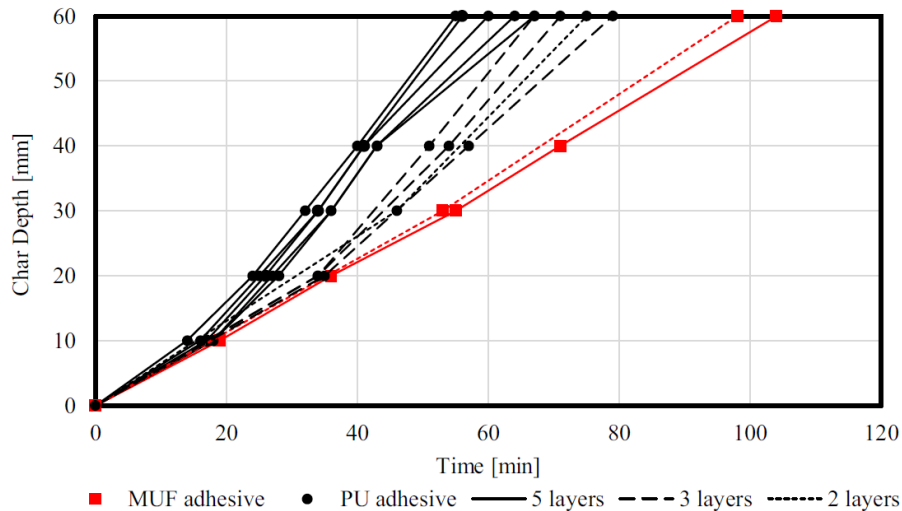


Figure 7: Influence of adhesive and CLT configuration on char depth (Frangi et al., 2009)

The conditions under which delamination occurs are currently difficult to determine. A theoretical approach is to assume that delamination occurs once the 300-degree isotherm, which is often taken as the position of the char-line in timber members, reaches the adhesive layer. In practice, it is not as straightforward because of the inherent material variability of wood and the complexity of fire dynamics, especially within a CLT compartment.

Delamination of lamella exposes the underlying layer of unaffected timber. As temperatures are commonly very high at this stage, the newly exposed timber goes into flaming combustion with a high charring rate as a result because no insulating char layer is present yet after delamination. Compared to a solid timber element, delamination can lead to sustained burning, while for solid timber the char layer propagates steadily hereby forming a natural insulation layer. Ideally, a CLT panel can resemble a solid timber panel if delamination is prevented. The experiments discussed in Chapter 6 show the issue of delamination in CLT compartment fires.

4.1.3.3 Charring rates in prEN 1995-1-2

After having presented various factors affecting the charring rate, it is important to analyse the charring rate for CLT elements as described in the prEN 1995-1-2.

For a solid wood panel with multiple layers like CLT, a basic design charring rate of $\beta_0 = 0,9$ mm/min is determined. This is considerably higher than the value for solid wood of 0,65 mm/min. For initially unprotected CLT panels, the charring rate is depicted in Figure 8. To account for delamination of the individual layers, the charring rate of each subsequent layer is doubled for the first 25 mm. This assumes that delamination only occurs once the charring front reaches the adhesive layer.

As explained in previous Chapter 4.1.3.2, delamination is difficult to predict. Therefore, the method as presented in prEN 1995-1-2 could underestimate the actual charring rate.

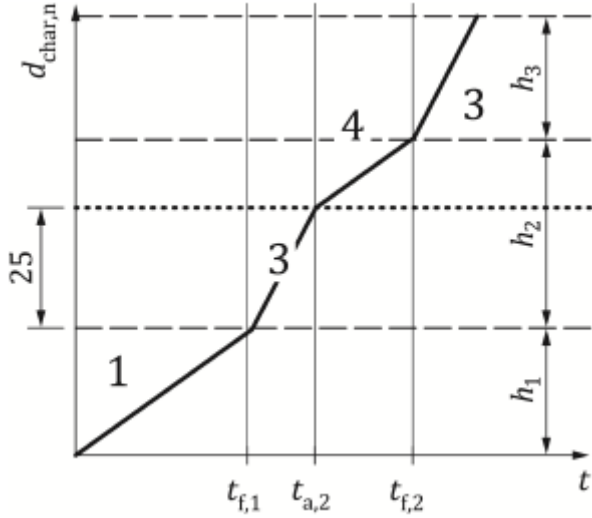


Figure 8: Charring rate initially unprotected CLT element (NEN, 2023)

For initially protected CLT panels, employing a fire-retardant gypsum board, the onset of the charring process is theoretically delayed until the protective layer falls off. Consequently, charring starts at a double rate due to the sudden exposure of unaffected CLT. This is depicted in Figure 9. The prEN 1995-1-2 presents calculation methods for determining the failure time of various types of gypsum protective layers. The effectiveness of protective gypsum layers is described based on experimental results in Chapter 6.1.

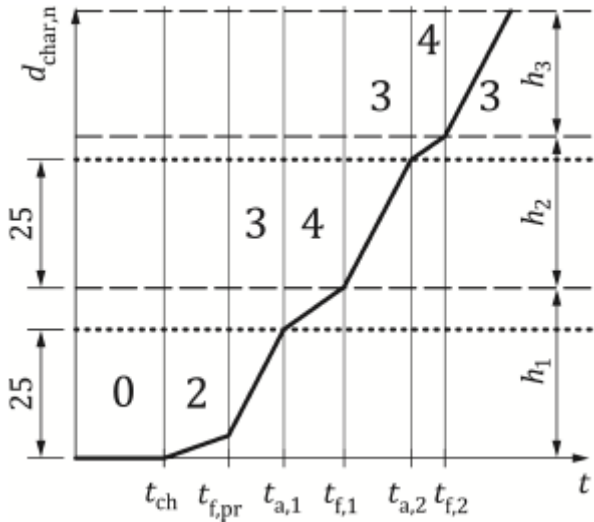


Figure 9: Charring rate initially protected CLT element (NEN, 2023)

In prEN 1995-1-2:2023 Annex A an alternative method is described for determining the one-dimensional charring depth. It is based on the work of Werther (2015) stating that the design charring depth of unprotected timber members is directly related to the compartment gas temperature, as given in Equation (2):

$$d_{char} = \left(\frac{\int_0^t T^2 dt}{1,35 * 10^5} \right)^{\frac{1}{1,6}} \quad (2)$$

Hereby the compartment gas temperature is given in Kelvin, the time in minutes and consequently the charring depth in millimetres. Equation (2) allows for a detailed assessment of the charring development of a timber element, depending on the temperature distribution within the compartment. In Chapter 11.1, the applicability of Equation (2) is extensively analysed.

4.1.3.4 Charring rates in ETA-14/0349

As explained in Chapter 3.1 the CLT products by Stora Enso must comply with the European Technical Assessment ETA-14/0349. This certification includes a brief overview of charring rates as prescribed by Stora Enso. An overview is given in Table 1.

It is interesting to note the substantial difference in charring behaviour for subsequent layers between floors and walls. While the charring of the outer layer is similar for floors and walls, the effect of delamination seems to play a more significant role for horizontally oriented CLT panels. It is noted by A. I. Bartlett et al. (2018) that in vertically oriented CLT panels the buoyancy will drive convection upwards parallel to the sample. While for horizontally oriented panels, the convective heat flux hits the panel perpendicular. This is a likely reason for assuming a higher charring rate in floors.

Table 1: CLT charring rates in ETA-14/0349

Charring rate	Floor/Roof	Wall
Charring of the outer fire-exposed layer	0,65 mm/min	0,63 mm/min
Charring of subsequent layers behind the outer layer	1,3 mm/min	0,86 mm/min

4.2 HEAT RELEASE

The rate at which energy is released during a fire, also referred to as heat release rate (HRR), is an important characteristic for determining the severity of a compartment fire.

In the context of compartment fires, HRR is usually measured in kilowatts [kW] or megawatts [MW]. The fire development within a compartment is commonly characterised by the HRR versus time. Engineers use a design fire, with a given relation between HRR and time, to assess the impact of the fire on the construction. The design fire provides essential information required for estimating the flame height, the production of smoke, the compartment temperature and the time to flashover (Karlsson & Quintiere, 1999). The HRR depends mainly on the type of fuel source and its orientation within a compartment, like proximity to openings. Additionally, the compartment geometry and presence of ventilation openings can have an impact on the severity of the fire.

The HRR of a burning item can be expressed in terms of the burning rate, which is the mass loss rate per unit area in kg/m²/s. This method applies to single-burning items. However, for full-scale compartments with multiple burning items, the oxygen consumption calorimetry test is commonly preferred. The oxygen consumption calorimetry test is based on extensive experimental research that has shown that for most gases, liquids and solids a constant amount of energy is released per unit mass of oxygen consumption, which is 13,1 kJ per kg consumed oxygen. Therefore, by measuring the oxygen consumption during a fire, an accurate estimate of the HRR is given (Drysdale, 2011).

On top of the burning interior items, the exposed CLT panels in the compartment add to the total fuel load thereby contributing to the HRR. This energy contribution depends on the heat of combustion of the wood material. The heat of combustion is defined as the amount of energy that is released when a unit mass is fully oxidised, which assumes a fully effective combustion process. The heat of combustion of wood ranges between 16-20 MJ/kg depending on the wood composition (MacLeod et al., 2023). The quantification of the contribution to the HRR due to the burning CLT elements is presented in Chapter 6.1.

For this thesis a design fire needs to be specified to simulate a CLT compartment fire and give representative results corresponding with experimental data as presented in Chapter 6.1. The fire load input for the computational model is discussed in Chapter 8.

4.3 HEAT TRANSFER

For sustained combustion to occur, there are three distinct heat transfer modes for spreading thermal energy. Each mode contributes in its own way to the fire development. The following is based on the work of Rego et al. (2021) and Drysdale (2011).

Radiation is the heat transfer through the air to other items. It occurs when energy is transferred from a hot molecule to a cold molecule through the air via electromagnetic waves. Thermal radiation does not require a material medium for energy transfer, as such it can travel through a vacuum such as a liquid or gas like air. Radiation is the dominant mode for heat transfer during a fire, especially during the growth phase when the fire source radiates energy towards other objects. In CLT compartment fires, radiation between burning CLT surfaces is of interest and requires further research.

Conduction is the heat transfer between solids that are in contact with each other. For the burning of wood, conduction mainly plays a role in the pre-ignition stage when heat transfer occurs within the wood element from the reaction zone towards the pyrolysis zone. Within a CLT compartment fire, conduction has no significant impact on the fire development. However, it can be useful in determining the temperature gradient through a CLT panel. Joseph Fourier found that the heat transfer through a material is directly proportional to the temperature difference and inversely proportional to the distance travelled.

Convection is the heat transfer between a gas or liquid and a solid. The convective heat flux between an object with a given temperature and a fluid at a certain temperature depends on the temperature difference and the heat transfer coefficient. With convection, movement of the fluid medium occurs. Convection is mainly important near the fire source in the early stages of a CLT compartment fire.

4.4 EFFECTS OF FIRE EXPOSURE ON MECHANICAL PROPERTIES OF TIMBER

To assess the structural integrity of a timber structure, it is crucial to understand the decrease in mechanical properties when exposed to elevated temperatures. Strength properties like bending, compression and tension all decrease rapidly with increasing temperatures, as depicted in Figure 10.

The decrease in strength is caused by a decreasing moisture content and chemical changes within the wood structure. When exposed to elevated temperatures, water evaporates from the timber thereby decreasing the moisture content. Wood is a hygroscopic material and consequently, its mechanical properties are influenced by the presence of water, associated with a decrease in the structural integrity of the wood.

Additionally, at elevated temperatures thermal degradation of the wood constituents occurs. Cellulose, hemicellulose and lignin are decomposed resulting in the weakening of the wood structure. The decrease in lignin mainly affects the compressive strength, while the decrease in cellulose affects the tensile strength. An increase in temperature leads to a more or less linear decrease in tensile strength and modulus of elasticity up to 200°C. Beyond this temperature, there is a more rapid decline due to the thermal softening of wood (Östman, 1985).

When temperatures have reached 300°C, charring is assumed to have taken place. Therefore, the residual mechanical properties can be disregarded because the char layer has no meaningful strength left, as described in Chapter 4.1.3. It is important to have a good understanding of the decrease in mechanical properties for determining the residual strength of a timber structure, e.g. a CLT compartment.

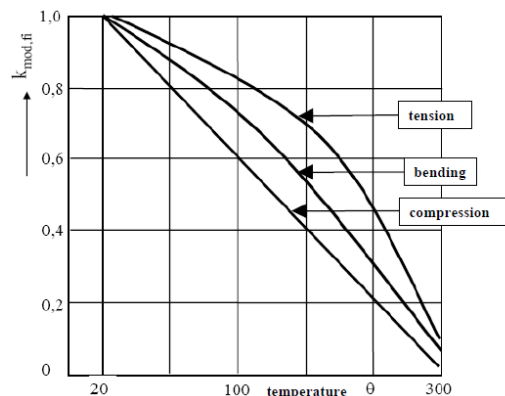


Figure 10: Reduction in mechanical properties of wood due to elevated temperatures (Östman, 1985)

4.5 COMPARTMENT FIRES

In this chapter, an elaboration is given on the fire behaviour within a compartment. In the Dutch building code, a compartment is defined as a part of the building designated as the maximum expansion area of a fire for a specified period based on the typology of the building. The various fire stages and compartment conditions are discussed for compartments with traditional building materials. Lastly, the influence of combustible construction materials is discussed, focussing on CLT compartments.

4.5.1 Fire development

There are two distinct ways of describing the fire development within a compartment. The most used method is in terms of temperature development within the compartment, while the other method utilises the mass flows in and out of the compartment. Analysing both methods gives a complete understanding of the processes during a compartment fire. This section is mainly based on the work of Karlsson and Quintiere (1999).

4.5.1.1 Temperature method

This method describes the development of a compartment fire in terms of compartment gas temperatures. A typical graph depicting this development is given in Figure 11.

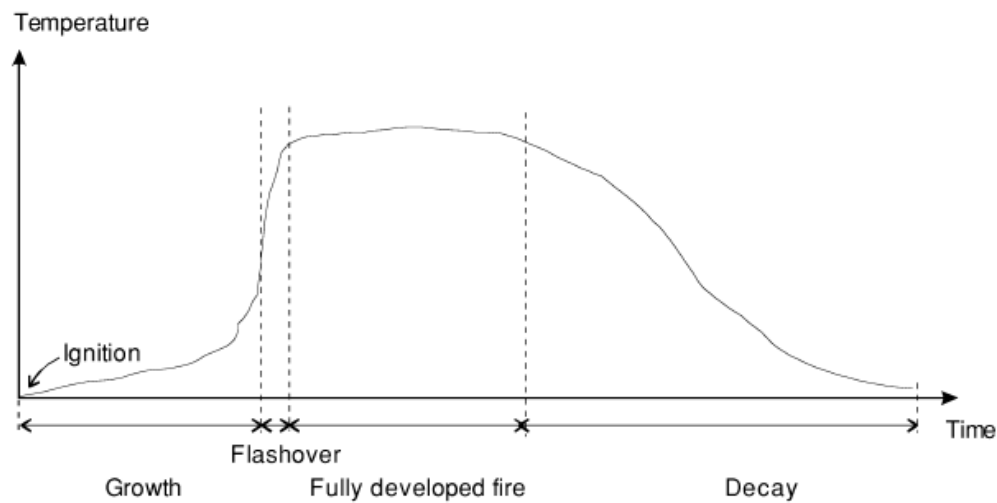


Figure 11: Temperature development for a compartment fire (Karlsson & Quintiere, 1999)

Ignition:

The fire starts with the piloted or spontaneous ignition of a fuel source. Ignition can be characterised as a process resulting in an exothermic reaction which increases the temperature within a compartment. The ignited fuel source can go either in flaming combustion or smouldering combustion, for further explanation read Chapter 4.1.1.

Growth:

Subsequently, the fire enters the growth phase where compartment temperatures keep rising. The growth phase of the fire is highly dependent on the type of combustion, the type of fuel, the compartment geometry and the access to oxygen. If the ignited fuel source goes into smouldering combustion, toxic combustion gases are produced but energy release rates are low. This results in a slow fire development, which may even extinguish before reaching further fire stages.

For a fuel source in flaming combustion the opposite holds, resulting in a rapid-fire growth where the flame spreads fast over the surface of the ignited fuel source. With flaming combustion, the heat produced by the fuel source can be sufficiently large to ignite nearby combustible items. During the fire growth phase, it is often assumed that the compartment consists of a hot upper layer and a cold lower layer. This is due to the accumulation of hot smoke at the ceiling of a compartment. The fire growth is usually limited by the fuel load in the compartment because there is sufficient oxygen available for the ongoing combustion process.

Flashover:

The flashover point marks the transition from the growth phase to a fully developed fire. After flashover, all combustible items in the compartment are in flaming combustion, thus contributing to the generated heat. The flashover point is characterised by a steep increase in compartment temperatures where the previously mentioned hot and cold zones are mixed in one hot zone.

The exact flashover point is difficult to determine. In general, flashover is estimated to occur once compartment temperatures reach 500-600°C or when the heat flux from the upper hot layer towards the floor is above 15-20 kW/m² (Drysdale, 2011).

Flashover marks an important switch in fire safety strategies. In the pre-flashover phase, the emphasis is on evacuating building occupants and ensuring the safety of people. In the post-flashover phase, the emphasis shifts towards ensuring the structural stability of the construction, thereby protecting the firefighters. Fire safety strategies and building regulations are discussed extensively in Chapter 5.

Fully developed fire:

After the flashover, the fire is fully developed with maximum compartment temperatures and energy release rates. Temperatures in non-combustible compartments can typically reach up to 1200°C. The influence of using combustible building materials on temperature development is presented theoretically in Chapter 4.5.3 and experimentally in Chapter 6.1. During the fully developed stage the combustion process, and coherent energy release, are often limited by the availability of oxygen within the compartment. Therefore, the fire at this moment can be described as ventilation controlled. In this stage, external flaming outside the compartment is often observed due to hot combustible gases escaping the compartment through ventilation openings. These combustible gases cannot ignite in the compartment due to the limited amount of oxygen, but outside the compartment there is oxygen in abundance, resulting in severe flaming.

Decay:

Finally, once all compartment fuel is consumed the energy release within the compartment diminishes and the temperatures start decreasing. The shift from flaming combustion to smouldering combustion is inherent to this stage. Additionally, the fire development now depends on the amount of fuel left because oxygen is sufficiently available. This stage is thus a fuel-controlled fire.

4.5.1.2 Mass flow method

This method describes a compartment fire development based on the pressure difference between the inside and outside of a compartment, and the coherent mass flow. A visualisation of the pressure development and the in and outflow of gases is given in Figure 12.

The first phase (A) describes the early stages of a fire. The pressure in the upper hot smoke layer of the compartment is larger than the outside air due to the expansion of hot gases. As the hot gases have a larger volume than the lower cold layer, cold gases are forced out of the compartment.

The second phase (B) is very limited in duration. The hot smoke layer increases in volume and once it reaches the compartment opening, hot gases flow out of the compartment. For a very short period, the pressure inside is still larger than outside, resulting in a net mass outflow.

In the third phase (C) hot gases continue to exit the compartment. The mass balance requires an equal mass of cold gases to enter the compartment, which is driven by the lower pressure inside compared to outside in the lower layer of the compartment. This phase continues until the compartment is fully filled with smoke or until flashover occurs, which can take a considerable amount of time.

The above-described phases A, B and C are associated with the growth phase of the fire. Usually in between phase C and the fourth phase (D), flashover occurs. Therefore, in phase D it is assumed that the compartment is fully filled with smoke with a single average temperature for the entire compartment as described in Chapter 4.5.1.1

Once all compartment fuel load is consumed the hot smoke will start dissipating and the pressure within the compartment will start levelling out with the ambient pressure.

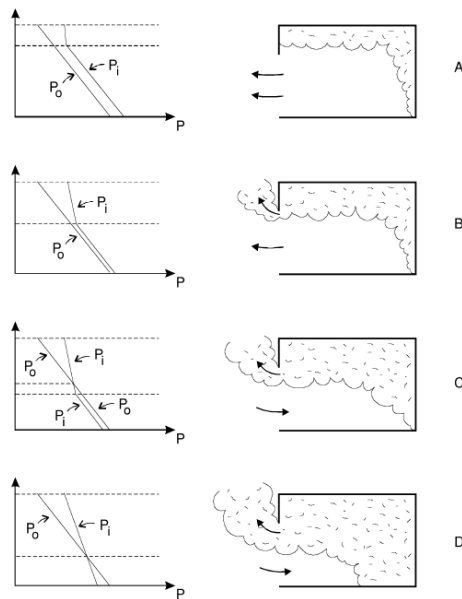


Figure 12: Pressure development in and outside the compartment (Karlsson & Quintiere, 1999)

4.5.2 Influencing factors

The fire development within a compartment as described in Chapter 4.5.1 is a generalisation of the fire dynamics. In reality, compartment fire characteristics like fire duration and maximum temperature depend on various factors such as the ignition source, the compartment geometry and the ventilation openings. The following is based on the work of Karlsson and Quintiere (1999).

A higher fuel load in the compartment does not necessarily result in a more severe fire development. Heavy fuel sources which are slow to catch fire, will result in a slow fire development. While lightweight plastic-based materials will ignite rapidly.

The location of the ignition source relative to the walls is important in determining the flame spread in the compartment. A burning item near a wall will result in a vertical upward flame spread along the surface of the wall. This vertical spread propagates more rapidly than flame spread along a horizontally oriented surface, like a floor.

Along with the ignition source, the compartment dimensions impact the way a fire spreads through the compartment. The burning of the interior fuel load is driven by the radiation from the hot smoke layer. In a compartment with a low ceiling, the radiation towards the floor will be more pronounced, resulting in a more severe fire development. Additionally, flames from the ground may reach the ceiling, which can lead to horizontal flame spread along the ceiling.

Lastly, compartment openings can have a significant influence on the fire development. In compartments with no ventilation openings, the fire will self-extinguish or continue burning at a very slow rate due to the lack of oxygen, which is called oxygen starvation. A slow-burning fire produces combustible gases which can ignite once exposed to sufficient oxygen. Accidents in the past have happened in this scenario, where the accumulated combustion gases suddenly ignite, producing large amounts of heat and flames. This phenomenon is called 'backdraft.'

In compartments with significant openings, the burning rate of the fuel load depends on the ventilation factor. In the fully developed phase, the fire is often ventilation controlled. Therefore, the inflow of

oxygen directly determines the fire development. At a certain ventilation factor, the fire switches to fuel-controlled due to the availability of sufficient oxygen. At that point, the impact of the ventilation factor is not directly linked to the fire development.

Conclusively, it can be noted that the proximity of walls, ceilings and ventilation openings impacts the fire development in a compartment.

4.5.3 Influence of combustible construction

The fire development within a traditional compartment assumes non-combustible surface materials. However, using combustible CLT panels as the structural elements of the compartment poses questions regarding the validity of traditional fire development curves. This section provides the theoretical framework for combustible compartments and Chapter 6.1 presents experimental results of CLT compartment fires.

Current fire safety design methods are based on the fire dynamics within a non-combustible compartment. Gaining a better understanding of fire exposed CLT compartments is crucial for engineers in predicting the time to flashover, the fire growth rate, the maximum compartment temperatures, the fire duration and the risk of external flaming (Hadden et al., 2017).

A more rapid-fire growth, compared to traditional compartments, has consequences for the safety of building occupants as this directly impacts the available safe evacuation time. Additionally, the use of cellulose-based materials like CLT most likely results in a more rapid smoke development, leading to more difficult evacuation conditions (Brandon et al., 2022).

As described in Chapter 4.5.1, a fully developed compartment fire is often ventilation controlled. The use of combustible CLT panels increases the fuel load within the compartment, while the available oxygen remains the same (Hadden et al., 2017). This has consequences for the amount of combustible gases that escape from the compartment and ignite outside of the compartment, resulting in more severe external flaming compared to non-combustible compartments. Hereby, the safety of firefighters is affected while attempting to extinguish the fire. Additionally, external flaming can result in fire spread via the exterior façade and lead to significant damage to adjacent buildings.

It is hypothesised that the additional fuel load from the CLT panels results in a longer fire duration, caused by the radiation between burning CLT panels while all the interior compartment fuel is already consumed. This is checked with existing experimental research in Chapter 6.1.

Fire safety strategies require the fire to remain and extinguish within one compartment. It needs to be verified under what circumstances this can be achieved for CLT compartments, without the fire spreading to adjacent compartments. This is currently one of the most relevant topics in CLT structures. Chapter 5 will elaborate on the concept of fire safety and the related building regulations for compartmentation.

Delamination, as explained in Chapter 4.1.3.2, exposes unaffected CLT layers which instantly get involved in the fire. Due to the additional fire load, the compartment temperature rises again with a risk of a second flashover. If delamination is not prevented, the CLT panels keep burning due to the lamellas falling off, eventually resulting in the structural failure of the compartment. The prevention of delamination is therefore essential in guaranteeing the concept of compartmentation. If the charring can be limited to the outer lamella or if failure of the adhesive can be prevented, the self-extinguishment of a CLT panel is possible. Research on the conditions for self-extinguishment and the influence of the adhesive type on delamination has been conducted by Crielaard (2015) and Olivier (2019), presented in Chapters 6.1.3 and 6.1.8.

5 FIRE REGULATIONS

In the previous chapters the theoretical basis for CLT and fire dynamics is presented. The practical application of this knowledge by engineers in the building industry is discussed in this chapter. Chapter 5.1 first explains the concept of fire safety and how it is determined. Chapter 5.2 presents the calculation methods in Eurocode for determining the fire resistance of timber structures. Lastly, Chapter 5.3 discusses the current regulatory gap in the Dutch building decree regarding the use of exposed timber as a structural element.

5.1 FIRE SAFETY

Fire safety is governed by national legislation. The Dutch building decree identifies two goals regarding fire safety. The first goal is assuring personal safety of the building users and fire service during a fire which focuses on evacuation and suppression strategies. The second goal is to protect neighbouring plots and adjacent buildings. Therefore, it is no explicit requirement to preserve the building where the fire originates. However, when a building is divided into compartments, as explained in Chapter 4.5, there are specific requirements regarding fire resistance. This is further discussed in Chapter 5.2.

Fire safety can be assured by two design approaches: prescriptive design and performance-based design. Most countries adopt the prescriptive based design method. This method aims to meet the same level of fire safety in different buildings based on the building height, largest compartment size and type of occupancy. Prescriptive regulations are based on exposing a structural element to the standard fire curve (ISO 834). This curve simplifies the fire development as it starts at the flashover point which limits the approach as it does not represent a real fire.

Following the prescriptive requirements results in a clear uniform way of achieving a fire safe structure which can be implemented across the building industry (Pettersson, 2020). However, this method limits the design freedom as unconventional designs often do not match with the predefined prescriptive requirements.

To enhance design freedom in achieving a fire safe structure, the performance-based design method can be utilised. This is an engineering approach in which fire safety is assured by performing calculations to assess the building response to a fire. Computational models are often applied as calculation tool. The goal is to achieve the same level of fire safety as intended with prescriptive regulations. Engineers need to prove that their alternative design solution matches with the fire safety requirements (Su et al., 2018).

Timber structures are often limited by prescriptive regulations regarding building height and exposing timber elements (Östman, 2021). Newly developed performance-based design methods, like computational models for fires in timber structures, can be an important tool in broadening the design possibilities of timber structures.

5.2 FIRE RESISTANCE

Fire safety of a building can be achieved by ensuring adequate fire resistance of the structure. In general, fire resistance is based on three main criteria: load bearing capacity and stability (R), integrity of the structure (E) and insulation ability (I). Fire resistance is therefore a structural property which is expressed in terms of minutes, depending on the specific requirements for the building.

The fire resistance of structural elements is determined by exposing the element to the standard fire curve (ISO 834) as shown in Figure 13. For non-combustible building materials this proves to be an

adequate tool. However, the applicability to timber elements is being questioned because of the additional heat that is released due to the burning of timber.

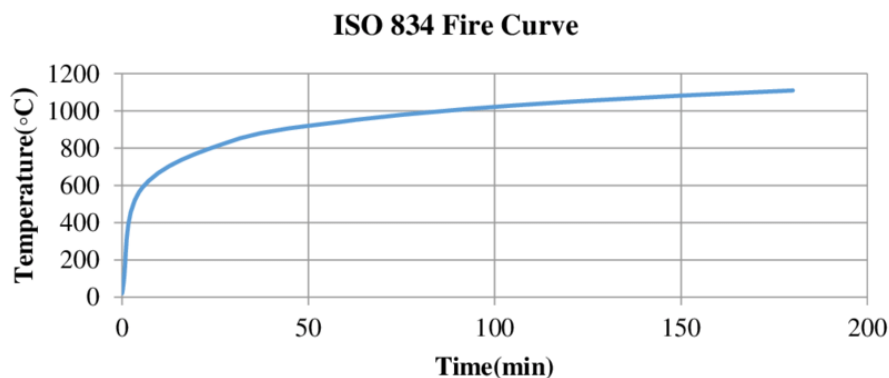


Figure 13: Standard fire curve (International Organisation for Standardization, 2014)

The fire resistance requirements are listed in the Dutch building decree. The requirements depend on the function of the building and the height of the highest floor level. Therefore, the requirements are material independent. For a multi-storey residential building, a fire separation of 60 minutes is required between compartments. Fire separation concerns fire penetration through the wall and fire spread through the open air. Additionally, for these types of buildings the structural integrity needs to be maintained for at least 120 minutes according to the Dutch building decree.

To assess the structural integrity, the remaining structural capacity of the load bearing elements needs to be calculated. For timber elements the reduced cross section method is used which depends on the charring process, as described in Chapter 4.1.3. The method first calculates the remaining cross-section based on the notional charring rate. Additionally, a zero-strength layer is subtracted from the cross-section. This layer takes the heated timber zone beneath the char layer in consideration. According to the prEN 1995-1-2, the thickness of the zero-strength layer can be calculated as follows for plane timber members like CLT: $d_0 = 9 + \frac{h}{20}$ (with 'h' being the depth of the initial cross-section).

The prEN 1995-1-2 provides a complete overview of designing timber structures on element level. However, little attention is given to the fire behaviour on compartment level.

5.3 REGULATORY GAP

The applicability of current fire safety regulations to the increasing number of timber structures is being questioned. Initiated by the Dutch government, a literature study is performed by the Research Institute of Sweden (RISE) to assess what changes are required in the building regulations to allow for fire safe timber constructions. This study by Brandon et al. (2022) links the available research with the building regulations from the Dutch building decree: 'Besluit Bouwwerken en Leefomgeving' (BBL). The most important identified problems are listed below:

- Delamination of CLT can result in longer sustained burning and potentially a second flashover.
- Current fire safety regulations from the BBL are not always adequate for timber structures.
- Performance requirements from the BBL do not sufficiently include the additional risks associated with combustible timber:
 - Timber elements add to the total fuel load, resulting in a longer and more intense fire.

- Burn through of the load bearing system, leading to structural failure.
- Burn through of fire separation walls.
- Flame spread due to external flaming.
- Classifying fire resistance based on the standard fire curve is not always representative of a real fire in a timber structure.
- The amount of timber that can be left exposed strongly depends on the ventilation conditions.
- Leaving timber exposed enlarges the risk for flashover and the time to flashover.

Based on this literature study, Brandon et al. (2022) recommend the following design approach to limit the additional fuel load that comes with CLT structures:

- Use non-delaminating CLT.
- Only use exposed timber for the ceiling.
- Protect the walls with two layers of 15,9 mm fire resistant gypsum board.

5.4 CONCLUSION

This chapter explained the concept of fire safety in the Netherlands and the assessment tools for determining the fire resistance of structural elements. Subsequently, the regulatory gap for fire safety in timber structures is discussed.

Answer subquestion 1

Based on the presented literature study in the previous chapters, subquestion 1 can be answered to the best extent.

SUBQUESTION 1: "WHAT CURRENTLY RESTRICTS THE USE OF EXPOSED CLT IN THE BUILDING INDUSTRY?"

It can be concluded that the calculation methods as presented in prEN 1995-1-2 are focused on calculating fire resistance on element level. However, compartment fire dynamics are not dealt with. The fire behaviour of a CLT panel is different on element level compared to its fire behaviour when applied in a full-scale compartment due to the additional imposed radiation from other CLT panels. Therefore, the possibilities of using exposed CLT within a compartment are restricted by the lack of appropriate calculation methods. Additionally, the Dutch building decree is not suited for fire safety in CLT buildings where the additional risks of building with CLT are greatly underestimated. Gaining a better understanding of the fire dynamics within a CLT compartment can bridge the current gap in the Eurocode and the Dutch building decree.

6 EXPERIMENTAL CLT FIRE BEHAVIOUR

This chapter presents an overview of the existing experiments researching the fire behaviour of CLT compartments. The experiments are listed in chronological order to display the scientific progress that is made over time. Attention is given to the contribution of exposed CLT to the fire development regarding e.g. temperature, HRR, fire duration and charring rates. An overview of the conclusions of the presented research is given in Appendix D.

6.1 EXISTING CLT EXPERIMENTS

6.1.1 McGregor (2013): Contribution of CLT panels to a room fire

The goal of the experiments conducted by McGregor (2013) was to assess the contribution of CLT panels to the development, duration and intensity of compartment fires. Five experiments were conducted with propane or furniture as fuel load. In three of the test compartments, all CLT panels were protected by gypsum board. In the remaining two test compartments all CLT panels were left exposed. The floor in each compartment was protected by a gypsum board with a cement board on top. The test compartment dimensions were 4,5 m x 3,5 m x 2,5 m (LxWxH) with 105 mm thick 3-ply CLT panels. Additionally, a ventilation opening was used with dimensions 1,07 m x 2,0 m (WxH). An average design fire load of 534 MJ/m² was used which represents a standard bedroom.

From the protected compartment tests, it followed that the gypsum board prevented the involvement of CLT in the fire. The protected CLT thus did not contribute to the fire development, duration and intensity. In the protected compartments with propane as fuel, localised failure of the gypsum board did occur which led to the involvement of CLT in the fire. The newly exposed CLT extinguished before delamination occurred. It was concluded that a propane burner as fuel gives less accurate results for real-life compartment fires compared to furniture as fuel. This is due to the relatively intense fire development induced by the propane burner.

From the exposed compartment tests, it followed that the exposed CLT panels contributed significantly to the fire. It was observed that compared to a fully protected compartment the HRR was approximately doubled in a fully exposed compartment. Additionally, the peak HRR was notably higher than the ventilation-controlled peak, which indicates that combustion was taking place outside the compartment. This has major consequences for adjacent buildings and firefighters.

In the exposed compartments, delamination of CLT lamellas occurred which led to regrowth of the fire. The compartments had to be manually extinguished to prevent structural collapse. Related to delamination, an average charring rate of 0,85 mm/min was found which is notably higher than the 0,65 mm/min as mentioned in the Eurocode.

It was concluded that fully protected compartments will self-extinguish without affecting the CLT panels. For fully exposed compartments no indication of self-extinguishment was observed, thus requiring manual extinguishment.

6.1.2 Medina Hevia (2014): Fire resistance of partially protected CLT

The experiments conducted by Hevia and Ramón (2018) followed up on the experiments from McGregor (2013). The same compartment dimensions were used. The goal was to assess the fire behaviour of partially exposed CLT compartments to find an optimal configuration that provides maximal exposed CLT surfaces with minimal contribution of the CLT panels to the fire. To replicate a realistic fire development, furniture was used as a fuel source as recommended by McGregor (2013).

Three experiments were performed with varying amounts of exposed CLT. Test 1 had an exposed back wall and side wall. Test 2 had two exposed side walls. Test 3 had one exposed side wall.

Experimental results showed that two opposing exposed walls resulted in a higher HRR compared to two adjacent walls. This is attributed to the greater radiation between two opposing walls due to a higher configuration or view factor. However, in a fully developed fire, the compartment will be filled with a thick layer of smoke. This smoke layer is impenetrable to infrared radiation, thus questions can be asked about the validity of this conclusion for practical applications. The experiment setup may have allowed smoke to dissipate sufficiently for radiation between CLT walls to play a role. It was also observed that the compartment with one exposed wall had a very similar HRR compared to a fully protected compartment as investigated by McGregor (2013).

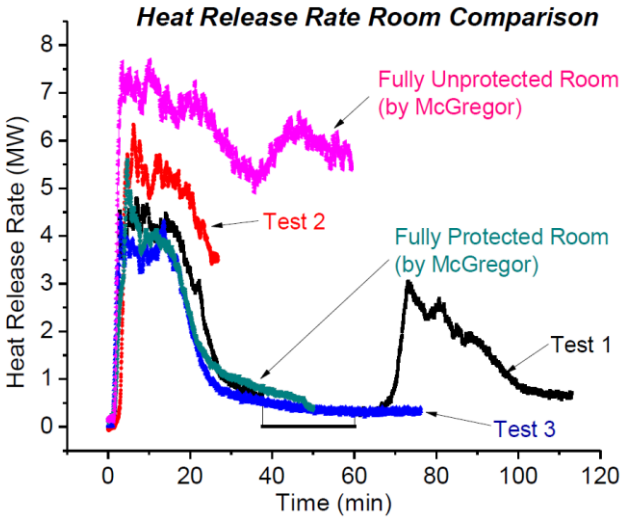


Figure 14: HRR comparison of fully protected, partially protected and fully exposed (Hevia & Ramón, 2018)

In Figure 15 the influence of exposed CLT on compartment temperatures is given. It was observed that compartment temperatures at the initial stages of the fire were comparable for all test setups. However, in the decay phase temperatures decreased slower in compartments with more exposed CLT which can again potentially be attributed to the cross-radiation between CLT surfaces.

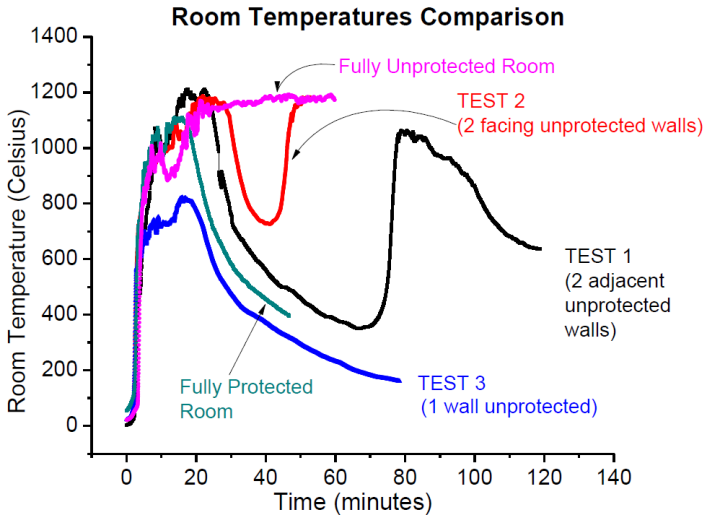


Figure 15: Comparison of compartment temperatures (Hevia & Ramón, 2018)

Delamination of CLT lamellas occurred in both compartments with two exposed CLT walls, which led to a second flashover. That can be seen in Figure 14 and Figure 15 with a second peak in HRR and temperatures. The graphs show that exposed CLT walls in partially exposed compartments did not have a major contribution to the fire except when delamination occurred which led to a significant regrowth of the fire. It was concluded that delamination should not be a concern if sprinklers are installed, which would be able to control the fire well before flashover.

Slightly higher charring rates were observed than the typically assumed 0,65 mm/min. Charring rates increased with an increasing amount of exposed CLT which can be linked to the higher HRR. As the charring progressed the charring rate decreased linearly with the increasing thickness of the char layer. Lastly, the CLT panels protected by gypsum board showed very little charring which shows the effectiveness of the gypsum board as fire protection.

It was concluded that self-extinguishment occurred in the compartment with one exposed CLT wall, which showed comparable behaviour to a fully protected compartment regarding fire intensity, growth rate and duration. For compartments with two exposed CLT walls, no indication of self-extinguishment was observed and manual extinguishment was required.

6.1.3 Crielaard (2015): Self-extinguishment of CLT

The goal of the experiments conducted by Crielaard (2015) was to formulate conditions under which there is a potential for self-extinguishment of a CLT compartment. One test series used small CLT compartments (0,5 m x 0,5 m x 0,5 m) as a test setup with varying amounts of exposed CLT. Each compartment was built up from 5 polyurethane bonded lamella, each 20 mm thick. An opening was added being 0,18 m in width and 0,5 m in height. The non-exposed walls are constructed from a non-combustible material to prevent involvement in the fire. The different test configurations are as follows:

- Test 1: one exposed back wall
- Test 2: one exposed back wall and two exposed side walls
- Test 3+4: two exposed side walls (executed twice for validation)
- Test 5: two exposed side walls (with 40 mm thick lamella at the fire-exposed side)

The compartments are exposed to a simple propane-induced design fire with a constant HRR of 41 kW and subsequently a decay phase. The initial fire is stopped when the exposed CLT is charred to a representative degree of 20 mm. After this, the involvement of the exposed CLT will determine the fire development over time, as visualised in Figure 16.

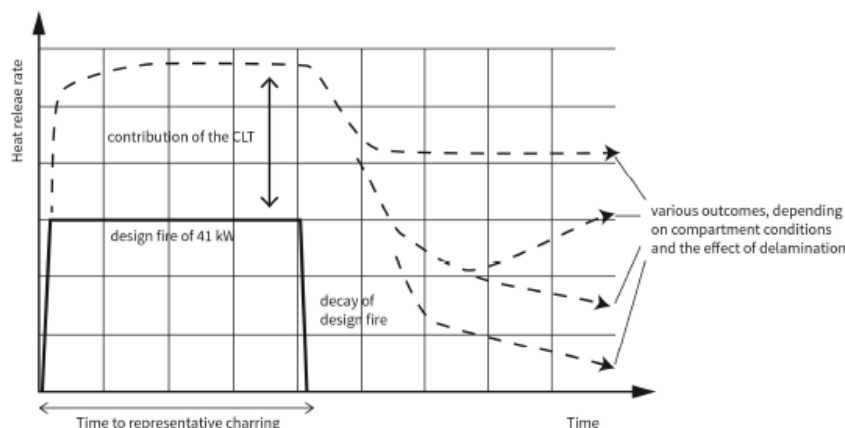


Figure 16: Hypothesis of fire development due to involved CLT (Crielaard, 2015)

Tests 2 and 3 experienced delamination while heat fluxes were high, resulting in a second flashover and eventually burning through. It was observed that test 4 did self-extinguish, which can be attributed to the fact that delamination occurred when temperatures and heat fluxes were sufficiently low. Following this, it can be concluded that the unpredictable nature of delamination makes it difficult to rely solely on self-extinguishment in practice.

Tests 1 and 5 both self-extinguished as well, showing the importance of the amount of exposed CLT and the influence of a thicker outer lamella in preventing delamination.

On average a charring rate of 0,76 mm/min was observed with average individual test values ranging between 0,52 – 0,96 mm/min. An increasing amount of exposed CLT seems to result in higher charring rates, which was observed as well by McGregor (2013).

It was observed that delamination could occur safely, without resulting in regrowth of the fire, when compartment temperatures were below 250°C and heat fluxes on the wall were limited to 4 kW/m². The prevention of delamination is crucial in reaching self-extinguishment, which can reasonably be achieved by increasing the thickness of the outer lamella. This way the first adhesive layer will not reach critical temperatures.

Furthermore, the influence of the airflow speed over the surface of the exposed CLT was investigated with a test series consisting of small CLT samples. The conclusion was drawn that it can be reasonably assumed that burning CLT samples result in self-extinguishment if heat fluxes are below 6 kW/m² and airflow speed is below 0,5 m/s. This is slightly higher than the critical heat flux found for CLT compartments.

6.1.4 Emberley et al. (2017): Description of small and large-scale CLT fire tests

The experiment conducted by Emberley et al. (2017) analysed the conditions for self-extinguishment within a CLT compartment with an exposed wall and ceiling. Compartment dimensions were 3,5 m x 3,5 m x 2,7 m (LxWxH) with an opening of 0,85 m x 2,10 m (WxH). Each CLT panel was 150 mm thick with the following build-up: 45x20x20x20x45. Two 40 kg wood cribs were used as fuel which corresponded to 100 MJ/m² to reach flashover.

Self-extinguishment of the compartment was observed after 30 minutes during the decay phase of the wood cribs. This occurred at approximately the same moment for the exposed ceiling as the wall. It was noticed that extinguishment started at the base of the exposed surface and progressed to the ceiling. From experimental results it followed that self-extinguishment occurred when the incident heat flux on the exposed CLT panels was below 45 kW/m², which is significantly higher than the value found by Crielaard (2015).

No delamination was observed, which can be attributed to the relatively late flashover which led to a shorter period of the fully developed fire limiting the charring process. During the experiment a maximum compartment temperature of 1125°C was measured.

It was concluded that self-extinguishment can be achieved during the steady state burning phase of CLT if uncertainties associated with delamination are minimised.

6.1.5 Hadden et al. (2017): Effects of exposed CLT on compartment fire dynamics

The experiments conducted by Hadden et al. (2017) aimed to assess the influence of exposed CLT surfaces on the fire dynamics within a compartment. The compartment dimensions were

2,72 m x 2,72 m x 2,77 m (LxWxH) with a door opening 0,76 m x 1,84 m (WxH). Three experiments were performed with varying amounts of exposed CLT. Test alpha had an exposed back wall and side wall. Test beta had an exposed back wall and ceiling. Test gamma had an exposed back wall, ceiling and side wall. Wooden cribs were used as fuel load to reach flashover conditions, corresponding to 132 MJ/m².

It was observed that the orientation of the exposed CLT surfaces influenced the combustion rate of the wood cribs. An exposed ceiling compared to an exposed wall resulted in a faster combustion of the wood cribs and thus a shorter burning duration. This can be attributed to the improved radiative view factor to the wood cribs due to the ignition of the ceiling. Increasing the area of exposed CLT led to an even further decrease in the burning duration of the wood cribs. The fire behaviour of the exposed ceiling also differed from exposed walls regarding charring rate. A lower charring depth was observed at the ceiling which can most likely be attributed to the lower oxygen concentration near the ceiling which results in a lower pyrolysis rate.

For test setup gamma the measured thermal penetration time of the exposed CLT panels was much longer than the duration of the wood cribs burning, suggesting that in this case the sustained burning is due to the radiative exchange between the exposed CLT surfaces.

For all test setups, the measured peak compartment temperatures were not substantially different from those predicted by existing correlations, suggesting that exposed CLT has only a small influence on the compartment temperature. This is in accordance with the results found by Hevia and Ramón (2018).

It was concluded that self-extinguishment is possible in compartments with two exposed CLT surfaces, under the condition that delamination is prevented. In compartments with three exposed CLT surfaces no indication of self-extinguishment has been observed.

6.1.6 Su et al. (2018): CLT compartment fire tests

The goal of the experiments conducted by Su et al. (2018) was to quantify the contribution of exposed CLT to compartment fires, assess the influence of the ventilation factor and characterise the effectiveness of gypsum board in delaying the involvement of CLT in the fire.

Six compartments with dimensions 9,1 m x 4,6 m x 2,7 m (LxWxH) have been tested in which 4 tests had an opening to the ambient air of 1,8 m x 2,0 m (WxH) and 2 tests had an opening of 3,6 m x 2,0 m (WxH). Furniture was used as fuel with a movable fire load density of 550 MJ/m². An equally vertically distributed load is applied to the ceiling of 0,95 kN/m². The test setups are as follows (numbering as indicated in the report):

- Small opening:
 - Test 1: fully protected
 - Test 4: exposed ceiling
 - Test 5: exposed long wall
 - Test 6: exposed long wall and ceiling
- Large opening
 - Test 2: fully protected
 - Test 3: exposed long wall

In Figure 17 the HRR development for each test is graphed. It was observed that a smaller opening resulted in a longer duration of the fully developed fire phase due to the limited ventilation. This led to

the increased involvement of exposed CLT surfaces in the fire. On the other hand, a larger opening resulted in a higher overall peak HRR but for a shorter duration. This notably increased the exterior fire exposure which has implications for the exterior fire spread towards adjacent buildings.

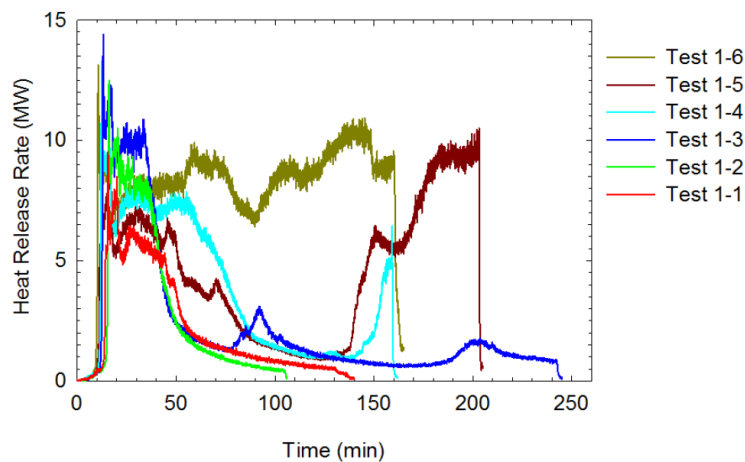


Figure 17: Comparison of HRR between 6 test setups (Su et al., 2018)

In all the tests with exposed CLT, flashover occurred earlier than in the baseline (fully protected) tests. For all tests, the peak compartment temperatures were similar to the baseline, which is in accordance with the experiments conducted by Hadden et al. (2017) and Hevia and Ramón (2018). However, the HRR was significantly higher for compartments with exposed CLT. Other than test 3, which showed a general trend of decay, all compartments with exposed CLT either had a second flashover or a continuously intense fire without decay. This can be attributed to the delamination of CLT lamellas which led to regrowth of the fire.

It was observed from the protected compartments that a gypsum board is an effective way to delay and/or prevent ignition and involvement of exposed CLT. Additionally, active fire protection like sprinklers would prevent flashover by controlling the fire well before that point.

6.1.7 Just et al. (2018): CLT compartment fire

The goal of the experiment conducted by Just et al. (2018) was to demonstrate self-extinguishment of CLT and investigate the fire spread through the façade and joints. A full-scale two-storey house was used as a test setup consisting of two compartments. All surfaces were 130 mm thick CLT with the following build-up seen from the fire-exposed side: 40-30-20-20-20.

In each compartment two walls were protected by gypsum board and two walls were left exposed. Furthermore, the ceiling and floor were protected with gypsum board and cement board, respectively. The compartments both had two windows (1,4 m x 1,5 m) and one door (0,95 m x 2,1 m). A furniture fuel load was used, corresponding to 600 MJ/m².

The test failed to demonstrate self-extinguishment of the CLT elements because a second flashover was observed. This happened 73 minutes after the first flashover, from which it can be concluded that a sufficiently long time was provided for firefighters to intervene.

On average delamination of the char layer of the exposed CLT wall was only observed after 117 minutes from the start of the test. For one wall this occurred while temperatures were below 300°C, while for another wall it occurred with temperatures above 300°C. It is therefore difficult to predict if the

adhesive will keep the CLT panels bonded at the critical charring temperature, which is frequently assumed as 300°C. The relatively long time until delamination can be related to the observed charring rates which were approximately 0,50 mm/min. This is lower than the assumed charring rate of 0,65 mm/min in the Eurocode and conflicts with the values found in other experiments which were often higher than 0,65 mm/min. Within the compartment a peak temperature of 1250°C was observed.

Lastly, it was concluded that two layers of gypsum board provide adequate protection for the underlying CLT panel during a fire. Temperatures below the gypsum layer only just reached 300°C with minimal charring as a result. This is in accordance with the results found by McGregor (2013), Hevia and Ramón (2018) and Su et al. (2018).

6.1.8 Olivier (2019): Fire performance of CLT

The goal of the experiments conducted by Olivier (2019) was to investigate the fire behaviour of a CLT compartment with melamine-urea-formaldehyde (MUF) used as the adhesive. The experiments are a continuation of the research by Crielaard (2015) to compare the performance of MUF and polyurethane as adhesives exposed to a fire. The same test setup was used as described by Crielaard (2015) to allow for an accurate comparison of the results. Small adjustments in the configuration of exposed CLT have been made to obtain a better understanding of the influence of an exposed ceiling within a CLT compartment, as described below:

- Configuration 1: exposed CLT back wall
- Configuration 2: two exposed CLT side walls
- Configuration 3: one exposed CLT side wall
- Configuration 4: exposed CLT ceiling
- Configuration 5: exposed CLT back wall and ceiling

First, it was observed that MUF-bonded CLT panels showed a better capability in preventing delamination compared to the results of Crielaard (2015) for polyurethane-bonded panels. As self-extinguishment is heavily dependent on preventing delamination, MUF-bonded panels are recommended. Additionally, lower charring rates and HRR were observed in the MUF bonded compartments, resulting in an overall better fire safety performance. Comparable charring rates were observed to the assumed value of 0,65 mm/min in the Eurocode.

The orientation of the exposed CLT panels greatly influenced the time to self-extinguishment. It was observed that compartments with 2 adjacent walls self-extinguished approximately 3 times faster than compartments with 2 opposing walls. It is therefore recommended to avoid CLT compartments with 2 exposed opposing walls.

Exposed CLT ceilings resulted in the most beneficial fire behaviour regarding time to self-extinguishment and additional heat release due to burning CLT. This can potentially be attributed to the lack of oxygen near the ceiling hereby limiting the combustion process, as hypothesised by Hadden et al. (2017).

Lastly, it was observed that delamination during the decay phase resulted in faster self-extinguishment, while delamination during the fully developed phase resulted in more sustained burning of the exposed CLT. The unpredictable behaviour of delamination and its influence remains a point of attention.

6.1.9 Mindeguia et al. (2020): Thermo-mechanical behaviour of CLT slabs

The primary objective of the experiments conducted by Mindeguia et al. (2020) was to investigate the mechanical response of exposed CLT slabs when subjected to natural fire exposures. These CLT slabs were comprised of five lamellas, each with a thickness of 33 mm, resulting in a total thickness of 165 mm. The experiments were conducted within a compartment measuring 6 meters in length, 4 meters in width, and 2.52 meters in height, which was exposed to a natural fire. The focus of the study by Mindeguia et al. (2020) was to examine how varying ventilation conditions within the compartment influenced the behaviour of the CLT slabs. To achieve this, three distinct test scenarios were established, each characterized by different opening factors: 0,14 m^{0,5} (scenario 1), 0,05 m^{0,5} (scenario 2) and 0,03 m^{0,5} (scenario 3). Wood cribs were used as fuel with a fuel load density of 891 MJ/m².

In comparison to commonly used standard fire tests, the natural fire tests resulted in a higher heating rate. Nevertheless, this elevated heating rate did not result in significantly different maximum temperatures. In both types of tests, the temperatures reached approximately 1200°C.

To assess the impact of varying ventilation conditions, the charring rate and associated delamination were employed as measurement tools. The results of the study revealed that in scenario 1, characterized by a larger opening factor, the fire exhibited a more rapid progression and earlier decay. This minimised the influence of delamination of the first lamella on the fire behaviour of the CLT slab. In scenarios 2 and 3, it was observed that a reducing opening factor corresponded to a later onset of delamination. This observation can be attributed to the slower fire development associated with a decreasing opening factor. Consequently, as the opening factor decreased, the intensity of the fire decreased as well, resulting in the lowest charring rates observed in scenario 3. However, it is important to note that the fire duration in scenario 3 was longer compared to the other test setups. This extended duration led to a greater charring depth and a more pronounced impact of delamination on the structural integrity of the CLT slab.

For scenario 1 an average charring rate of 1,43 mm/min was observed which was limited to the first lamella due to the rapid decay phase. For scenario 2 a value of 1,19 mm/min was observed for the first lamella and 0,80 mm/min for the second lamella. For scenario 3 a value of 0,85 mm/min was observed for the first lamella and 0,92 mm/min for the second lamella. Higher charring rates can be attributed to the more intense fire due to a larger opening factor.

For the remaining structural capacity of the slab following exposure to a natural fire, the study's findings indicate that a larger opening factor offers a more favourable outcome in terms of preserving the required load-bearing capacity and preventing structural collapse.

6.2 CONCLUSION

This chapter provides an elaborate overview of the existing experimental research into the fire behaviour of CLT compartments. Hereby, an adequate understanding is provided for setting up the computational model, as presented in Chapter 8.

For a complete comprehensive overview with the conclusions of each individual research, Appendix D can be consulted. The most important conclusions from the discussed research are listed below:

- The heat release rate (HRR) within a compartment increases significantly with an increasing amount of exposed CLT surfaces.
- Exposed CLT surfaces do not notably influence the peak compartment gas temperatures, but an increased amount of exposed CLT does result in a slower decay period of the fire.
- The orientation of exposed CLT surfaces influences the potential for self-extinguishment. Two opposing exposed CLT walls have a higher risk of sustained burning, while two perpendicular exposed CLT walls show more potential for self-extinguishment.
- Delamination of CLT lamellas is highly unpredictable and prevention is crucial in reaching self-extinguishment.
- A larger ventilation factor results in a more severe fire with a shorter duration compared to a fire in a compartment with a smaller ventilation factor.
- Gypsum board is an effective means to delay or prevent ignition and involvement of underlying CLT during a fire.

Answer subquestion 2 and 3

Based on the aforementioned presented literature study, subquestion 2 and 3 can be answered to the best extent.

SUBQUESTION 2: “TO WHAT EXTENT DOES THE ORIENTATION OF EXPOSED CLT SURFACES
LIMIT THE CONFIGURATION OF A CLT COMPARTMENT?”

Literature shows that the HRR increases significantly with an increasing amount of exposed CLT. It is concluded that the orientation of exposed CLT panels affects the decay phase of a compartment fire. It is advised to place two exposed CLT walls adjacent instead of opposed to each other. Additionally, an exposed CLT ceiling shows a lower contribution to the HRR, compared to an equal sized exposed CLT wall, and is therefore advised to leave exposed instead of walls.

SUBQUESTION 3: “TO WHAT EXTENT DOES THE VENTILATION FACTOR INFLUENCE
THE FIRE DYNAMICS WITHIN A CLT COMPARTMENT?”

Literature shows that the ventilation factor strongly affects the fire dynamics within a compartment. A lower ventilation factor commonly results in a ventilation-controlled fire, where combustion of exposed CLT is limited by the availability of oxygen. This results in a longer fire duration, with a lower HRR compared to a fuel-controlled fire which is the result of a larger ventilation factor. Therefore, the ventilation factor directly affects the development of a fire within a CLT compartment regarding e.g. time to flashover, maximum temperatures and length of the decay phase.

7 MODELLING IN FIRE SAFETY ENGINEERING

This chapter first presents the relevance of computational modelling in the field of fire safety engineering in Chapter 7.1. Subsequently, various software are discussed in Chapter 7.2 with their distinct possibilities and limitations for modelling CLT compartment fires. Lastly, existing research on computational modelling of the burning behaviour of wood is discussed in Chapter 7.3.

7.1 RELEVANCE

7.1.1 Integration in the building industry

The integration of computational modelling tools in the analysis of CLT compartment fires opens doors to a range of insightful analyses. It enables engineers to investigate complex fire behaviour scenarios that are otherwise challenging to replicate in real-world experiments. This saves both a considerable amount of money and time. By adjusting various parameters within the model, engineers can explore the effects of different fuel loads, compartment geometries, ventilation conditions, and fire suppression strategies. This can significantly enhance the understanding of CLT compartment fires and hereby optimise fire safety measures in CLT constructions.

From a regulatory perspective, the ability of computational modelling allows for fast checking of proposed design rules. Computational modelling tools can be an accessible way of creating consistent regulations, without there being the need for multiple large-scale experiments. Ideally, computational modelling will speed up the process of new design rules being implemented in the Eurocode.

As part of this master thesis, the aim is to contribute to the ongoing questions regarding fire safety in CLT compartments by developing a comprehensive and validated computational model. By doing so, a link can be made between scientific research and subsequent practical applications.

The strength of the computational modelling approach, which can be used in FSE performance based design, is to explore new methods for obtaining fire-safe constructions which would be restricted by the current prescriptive approach as explained in Chapter 5.1.

7.1.2 Challenges and limitations

Computational modelling tools do come with challenges and limitations inherent to numerical methods. The most common challenge in implementing computational models is the computational complexity of especially large-scale problems. As the size of the simulated geometry increases, the number of calculations and required memory on a computer or server increases drastically. This has consequences for both the computing time required for the simulation as well as the costs of running the simulation.

The second concern of computational models is the numerical stability. The numerical stability of a model refers to the ability of a model to produce accurate results while small errors are present in the input data of the model. If a model is numerically unstable, a small error in the model will amplify exponentially over time, eventually causing the model to stop working (Smith & Brebbia, 1977). Mesh grid resolution, thermal boundary conditions and gas species concentrations are common causes for numerical instabilities in computational models (McGrattan et al., 2023).

The last important concern to be covered is the validation of the computational model. Large-scale problems often have complex or unknown solutions. Therefore, checking the accuracy of the produced results by the computational model is difficult. It is of importance to check the validity of the model by comparing the simulated results with experimental results and empirical data (Carley, 2017) Once the model is validated, extrapolation possibilities of the model to other geometries can be explored.

7.2 EXISTING SOFTWARE

In the field of FSE two types of modelling tools are commonly used: Two-zone models and computational fluid dynamics (CFD) models. Two-zone models are characterized by the assumption that the compartment is split in a lower cold gas layer and an upper hot gas layer. For each of these layers a uniform temperature and chemical composition is assumed. Two-zone models can be used for quickly calculating a rough temperature and smoke development within a compartment. However, the application of two-zone models is usually limited to fires in small sized compartments. The reason for this is that two-zone models can only give accurate results in strongly stratified conditions, meaning that the hot and cold gas layer have a uniform temperature and composition throughout the entire compartment (Johansson, 2020).

Therefore, two-zone models are not that widely used because small compartments can often be engineered by prescriptive building regulations, while for larger compartments specific performance-based methods are required.

CFD models are based on the concept of dividing a compartment in 3-dimensional meshes consisting of small cells and subsequently utilising the Navier-Stokes equations for solving the gas flows within the compartment. Because of the fine computational grid, CFD models allow for calculating detailed temperature developments and gas concentrations throughout a larger compartment like industrial buildings and offices. The downside of CFD models is that they require more computational power and knowledge in setting up the model and running the simulations.

Current applications of both CFD and two-zone models in FSE are restricted to non-combustible construction materials. The fire is assumed to be fuelled solely by the interior fuel load, therefore not considering surface materials. With the increasing application of CLT compartments, the additional fuel load due to the burning exposed CLT surfaces needs to be considered in the modelling software.

This thesis attempts to enhance the modelling capabilities of fires within CLT compartments, driven by the increasing need for a better understanding of fire safety in timber buildings. In the following subsections three well known modelling software in FSE are discussed, each with their advantages and disadvantages for the scope of this thesis.

7.2.1 Ozone

OZone is a two-zone model developed by the University of Liège. It is an accessible modelling tool which allows for quick simulations of compartment fires to gain insights into the fire behaviour. The key aspects of Ozone are listed below:

Fire modelling:

In OZone the standard fuel load is defined as the design fire described in EN 1991-1-2. Furthermore, a user-defined fire can be inserted with a time depended HRR, mass loss rate and fire area. The location of the fire source can be specified by inputting localised fires within the compartment. This could be of particular interest for analysing the influence of ventilation openings on localised fires.

Compartment specifications:

Compartment dimensions and openings can quickly be modelled. Surface materials can be chosen from a preselected list, or self-defined properties can be given as input.

Output files:

OZone provides graphs for the development of the pyrolysis rate, HRR and the temperature of the hot and cold layers. Additionally, the development of the two-zone interface height, floor pressure, fire area and oxygen mass are given. These graphs provide an overall representation of the compartment fire dynamics.

Usability:

The interface of OZone is relatively easy to use, and the simulations can run fast. Therefore, it is an ideal software to gain quick insights into the parameters affecting the fire behaviour within a compartment.

Relevant limitation:

OZone is a simplified modelling tool which is not capable of considering the chemical processes of pyrolysis and combustion of wood surfaces and the coherent charring process. The temperature output is an average value for each of the two zones within the compartment, which does not allow for a local analysis within the compartment.

Conclusion

OZone is a quick accessible modelling tool to gain a better understanding of compartment fire dynamics. However, due to the simplified nature of two-zone models, it is not capable of accurately modelling CLT compartments, hereby considering the distinct burning behaviour of wood. Additionally, OZone only outputs graphs with average temperatures, not taking into account local differences.

7.2.2 CFAST

CFAST (Consolidated Fire and Smoke Transport) is a two-zone fire model developed by the National Institute of Standards and Technology (NIST) in the United States. CFAST is designed for the analysis and simulation of fire dynamics and smoke movement within compartmentalised structures. It provides engineers, architects, and fire safety specialists with a simplified tool for assessing fire scenarios and their impact on structures and occupants. The key aspects of CFAST are listed below:

Fire modelling:

CFAST utilises simplified mass and energy conservation equations to calculate the fire development, combustion and smoke development. Fire sources can be specified via a time dependent HRR function, which specifies the fire growth and decay over time. The specified heat of combustion is used to calculate the mass loss rate (MLR) of the fuel, from which the production rate of combustion products can be calculated using specified product yields.

Compartment specifications:

Compartment dimensions and openings for doors or windows can be easily modelled within CFAST. Additionally, the thermal material properties of surfaces can be specified like conductivity, specific heat capacity, density, thickness and emissivity. If required CFAST allows for modelling multiple compartments at a time with multiple simultaneous fires within the construction. Active fire protection equipment like smoke detectors and sprinklers can be implemented in the model.

Output files:

CFAST generates various output files including temperatures of the upper and lower gas layers, the surface temperatures and the visible smoke and gas species concentrations for each gas layer. Additionally, a quick visualisation of the fire and smoke development can be generated using Smokeview.

Relevant limitation:

CFAST is a simplified two-zone fire model that does not have the capability to directly model the chemical processes for pyrolysis and combustion of timber in a detailed manner. Therefore, including the additional energy release due to burning timber is not possible. It is not designed for simulating the specific thermal degradation and combustion behaviour of solid materials like CLT.

Conclusion:

While CFAST enables a large design freedom when modelling compartment fires, it is not suited for accurately modelling CLT compartment fires due to the lacking capability of modelling the distinct burning behaviour of fire-exposed wood.

7.2.3 FDS

FDS (Fire Dynamics Simulator) is a computational fluid dynamics (CFD) software developed by the National Institute of Standards and Technology (NIST) for simulating fire and smoke behaviour in complex, three-dimensional environments. The key aspects of FDS are listed below:

Fire modelling:

FDS allows for the modelling of fires in complex and large-scale compartments. It uses a CFD approach to simulate the fluid flow, heat transfer, combustion and the transport of species within a three-dimensional compartment.

Combustion modelling:

FDS allows users to define the thermal properties, combustion characteristics, and chemical reactions of materials. This is essential for accurately modelling various fuels, including solid materials like wood. The thermal properties of wood can be specified with the associated pyrolysis and combustion processes. Therefore, the additional energy release due to the burning of timber can be modelled.

Species transport:

Within the compartment, FDS calculates the movement of species like gases and smoke. This can be used to gain important insights into the fire development and its impact on the safety of the occupants during the required evacuation time.

Computing power:

Running FDS simulations requires a significant amount of computational power. Therefore, frequently adjusting the model and running the simulation is time-consuming.

Output:

FDS allows for detailed temperature developments within the three-dimensional compartment. In the input file, specific locations can be identified where the temperature-time data is requested. This enables a more accurate representation of a compartment fire, compared to two-zone models. Additionally, a visualisation of the fire development can be generated using Smokeview.

Relevant limitation:

In case multiple modelling factors are still relatively uncertain and need to be adjusted in the model by trial-and-error, it is not recommended to use FDS because of the time required to run simulations. FDS is a complex software, which requires quite some understanding in the early stages of a project.

Conclusion:

While FDS is a relatively complex and time-consuming software to run simulations, the benefit of being able to model the distinct burning behaviour of wood is crucial to accurately model CLT compartment fires for the scope of this master thesis.

7.2.4 Conclusion

For ultimately reaching the goal of this thesis to accurately model the fire behaviour of a CLT compartment, only FDS as CFD software is suitable. Two-zone models are too limited for the purpose of this thesis.

There are more CFD programs available. However, FDS is well known, widely used, free of charge and specifically designed for fire simulations. Because FDS is a free software, future follow-up research is better repeatable.

FDS will be used mainly due to its capability of modelling the pyrolysis and combustion process and the underlying chemical reactions. Subsequently, the additional energy release within the compartment is crucial in realistically modelling CLT compartment fires. Additionally, FDS provides a large design freedom to investigate the influence of various parameters within a CLT compartment.

7.3 RESEARCH ON CFD MODELLING OF WOOD COMBUSTION

In this section the state of the art is given regarding the CFD modelling of the burning behaviour of wood, required for accurately modelling the fire dynamics within a CLT compartment. The presented existing research is used as scientific reference for setting up the model in the FDS software in Chapter 8. Table 2 gives an overview of the presented research in this section.

Table 2: Overview research on CFD modelling

Section	Test setup	Goal
7.3.1	Wood sample with radiation panel	Find input data for the modelling of the burning behaviour of wood in CFD software.
7.3.2	Tunnel	Setup a CFD model that simulates the fire spread on wood cribs and to introduce a correction for the mesh dependency of the fuel surface area.
7.3.3	Compartment	Assess the influence of exposed timber and the size of the ventilation opening on compartment fire dynamics.
7.3.4	Wood cribs with radiation panel	Model the fire spread over wood cribs in full-scale tests in FDS.
7.3.5	Compartment	Develop an FDS model that simulates a fire within a mid-scale CLT compartment which can be integrated with 4D BIM software to assess fire safety in the early stages of a construction project.
7.3.6	Wood sample with radiation panel	Model the burning behaviour of softwoods and hardwoods by implementing a two-step combustion model in FDS.
7.3.7	Compartment	Assess the fire safety performance of a multi-storey CLT building by setting up a model in FDS.

7.3.1 Hejtmánek et al. (2017): Input data of burning wood for CFD modelling

The goal of this paper by Hejtmánek et al. (2017) is to find input data for the modelling of the burning behaviour of wood which can be implemented in CFD software. The implemented approach consists of setting up a model in the FDS software, and subsequently comparing the simulation results with experimental data.

For the FDS model a simplified cone calorimeter is modelled and a gas burner output of 35 kW/m². The sample size is 10 cm x 10 cm with a thickness of 1 cm. All boundaries of the geometry are modelled as open, meaning that an infinite amount of oxygen can enter the volume. A fine mesh is chosen with cubical cells of 10 mm near the sample and the burner, with a coarser mesh in between.

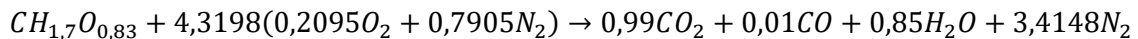
For the burning behaviour of wood, a pyrolysis model is defined. Based on a thermogravimetric analysis, the composition of the wood sample and the pyrolysis gases is documented. The chemical formula for pine wood is given as $CH_{1,7}O_{0,83}$. The sample has a moisture content of 7,8%. The used material properties in the FDS model are given in Table 3.

Table 3: Material properties FDS model (Hejtmánek et al., 2017)

	Density [kg/m ³]	Specific heat capacity [kJ/(kg*K)]	Thermal conductivity [W/(m*K)]
Water	1000	4,18	0,6
Pine wood	520	2,5	0,2
Char layer	200	1,6	1

In the FDS model first the pine wood material changes in 84,7% pyrolysis gases and 15,3% char. This pyrolysis reaction peaks at a reference temperature of 350°C with a range between 250°C and 450°C. The energy required for this reaction is specified as the heat of reaction, being 1047 kJ/kg. Subsequently, the pyrolysis gases will combust in access of oxygen. This reaction releases energy as stated in the effective heat of combustion, being 11405 kJ/kg. The effective heat of combustion accounts for unused energy due to incomplete combustion.

Based on the thermogravimetric analysis, the ratio between the combustion products is determined. The corresponding combustion reaction can be stated as the following, where the first term represents the pyrolysis gases that react with air to form combustion products:



When comparing the experimentally obtained HRR with the FDS model, results match relatively well in the early stages of the experiment. This is visualised in Figure 18 where model 1 simulates the net heat of combustion and model 2 simulates the effective heat of combustion. It is concluded that using the effective heat of combustion resembles reality in the best way. Using the net heat of combustion leads to an overestimation of the HRR released during the fire. Once large parts of the sample are charred, the model does not match with the real experiment. In the model the flame moves randomly over the sample surface, while in the experiment the flame spreads gradually over the surface.

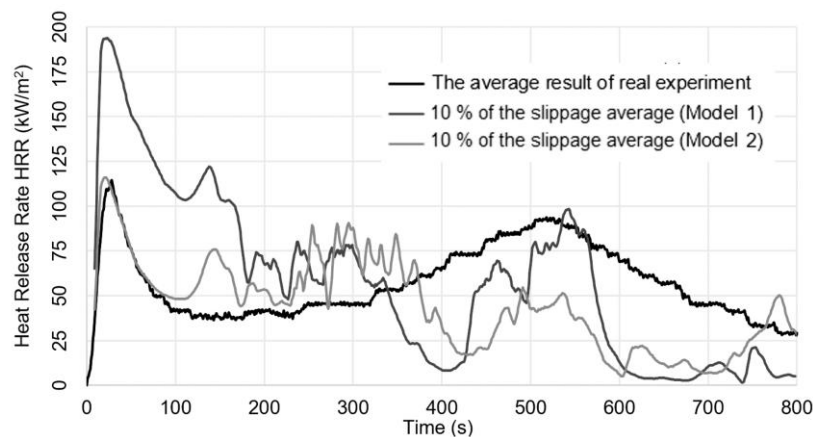


Figure 18: Comparison of results (Hejtmánek et al., 2017)

The paper recommends improving the modelling of the fire spread on the pine wood surface. Additionally, more wood components could be added to the model to get a more realistic representation of the chemical processes in the sample. However, this would increase the complexity of the model and therefore increase the required computational time to calculate the results.

Therefore, the main limitation of the FDS model is the complexity of taking into account the influence of the char layer on the fire spread over the wood surface.

Conclusively, the FDS model is able to simulate the burning behaviour of a small-size wood sample in the early stages where no large charred parts are present. The paper provides an adequate method for modelling the chemical reactions of wood pyrolysis and combustion.

7.3.2 Janardhan and Hostikka (2019): CFD simulation of fire spread on wood cribs

The goal of the paper by Janardhan and Hostikka (2019) is to setup a CFD model that simulates the fire spread on wood cribs and to introduce a correction for the mesh dependency of the fuel surface area. The approach consists of validation of the model with a fire in a laboratory tunnel. Subsequently, the model is applied to a compartment fire to check the extrapolation possibilities.

The simulated tunnel had the following dimensions: 10,9 m x 0,6 m x 0,4 m (x, y, z). The used mesh consists of cells with dimensions of 20 mm x 20 mm x 18 mm in x, y and z direction respectively.

The FDS software is used where an ignition temperature is set to 300°C for the wood cribs which simplifies the pyrolysis process of wood. The chemical formula for the pine wood is specified as $C_{3,4}H_{6,2}O_{2,5}$. Once ignited, the wood cribs have a constant HRR of 260 kW/m². The burnout time of the wood cribs is calculated based on the bulk density parameters.

Table 4: Input data FDS model by Janardhan and Hostikka (2019)

Parameter	Quantity
Test dimensions	10,9 m x 0,6 m x 0,4 m (X, Y, Z)
Mesh cell size	20 mm x 20 mm x 18 mm (X, Y, Z)
Ignition temperature	300°C
Heat flux on wood surface in flaming combustion	260 kW/m ²
Heat of combustion	18,1 MJ/kg
Fuel load	Wood cribs ($C_{3,4}H_{6,2}O_{2,5}$)

Simulations took between 2 and 3 days to run and showed good agreement on the experimentally measured HRR as shown in Figure 19. However, the decay phase underpredicts the HRR which is attributed to the complexity of modelling char retention and smouldering in a realistic manner.

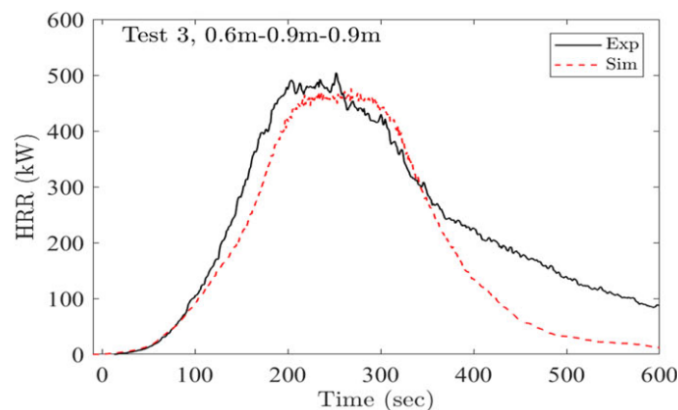


Figure 19: Comparison of results (Janardhan & Hostikka, 2019)

When applying the FDS model to a compartment fire, the predicted fire spread depended heavily on the mesh size and the size of the prescribed fire source. Due to the long computing time of the fine mesh simulation, the area adjusted parameter was introduced. This parameter accounts for the reduced surface area of the fire source in simulations with a coarse mesh. Applying this parameter brought the coarse mesh results closer to the fine mesh simulations, while at the same time reducing the computation time with a factor four.

Conclusively, the FDS model is able to predict the fire spread on wood cribs in an adequate way. However, the limitation of the applied ignition temperature method is the inability to adjust the burning rate when the material cools down below the pyrolysis temperature. The formation of a char

layer is also not considered in the model. This way the burning behaviour of wood is simplified, without considering the chemical reactions that occur within burning wood.

7.3.3 Brunkhorst and Zehfuß (2020): Compartment fires with immobile fire load

The paper by Brunkhorst and Zehfuß (2020) examines an experimental test series according to ISO 9705-1 to assess the influence of exposed timber and the ventilation opening on compartment fire dynamics. Following upon this test series, a CFD model is developed in the FDS software to compare with the experimental results and to assess the methods for including the contribution of exposed timber to compartment fire dynamics.

The dimensions of the simulated compartment are 2,4 m x 3,6 m x 2,4 m (x, y, z) with a ventilation opening of 0,8 m x 2,0 m (x, z). The fuel load consists of a 50 kg wooden crib. The main challenges of the modelling in FDS are identified as the HRR development and the post-combustion behaviour.

Two separate methods for modelling the additional HRR of exposed timber in FDS are presented. Method 1 uses a predefined time dependent HRR as input based on experimental results of a compartment fire with an exposed timber ceiling.

Method 2 models a simple one-step pyrolysis reaction, transforming wood into char. In this method no predefined HRR is used, but the rate of the chemical reaction is defined by the pre-exponential factor ($A_l = 1,89E10 \text{ s}^{-1}$) and the activation energy ($E_l = 1,51E5 \text{ J/mol}$). Transforming the reactants into products costs energy, specified by the heat of reaction ($\Delta H_R = 430 \text{ kJ/kg}$). On the other hand, energy is produced with the combustion of the reactants, specified by the heat of combustion ($\Delta H_C = 14500 \text{ kJ/kg}$).

Table 5: Input data FDS model by Brunkhorst and Zehfuß (2020)

Parameter	Quantity
Test dimensions	2,4 m x 3,6 m x 2,4 m (x, y, z) (0,8 m x 2,0 m (x, z) ventilation opening)
Mesh cell size	<i>Not mentioned</i>
Pre-exponential factor (pyrolysis)	$A_l = 1,89E10 \text{ s}^{-1}$
Activation energy	$E_l = 1,51E5 \text{ J/mol}$
Heat of combustion	14,5 MJ/kg
Fuel load	50 kg wood cribs

Results show in Figure 20 that method 1 exhibits a reasonable agreement in temperature and HRR with the experimentally tested compartment. This is in line with expectations because the predefined HRR was based on the experimental compartment that was used for validation.

However, method 2 shows no additional HRR due to the exposed timber, meaning that the timber is not ignited in the model. Further refinement of the listed reaction parameters is therefore required for accurately modelling the contribution of exposed timber to compartment fire dynamics.

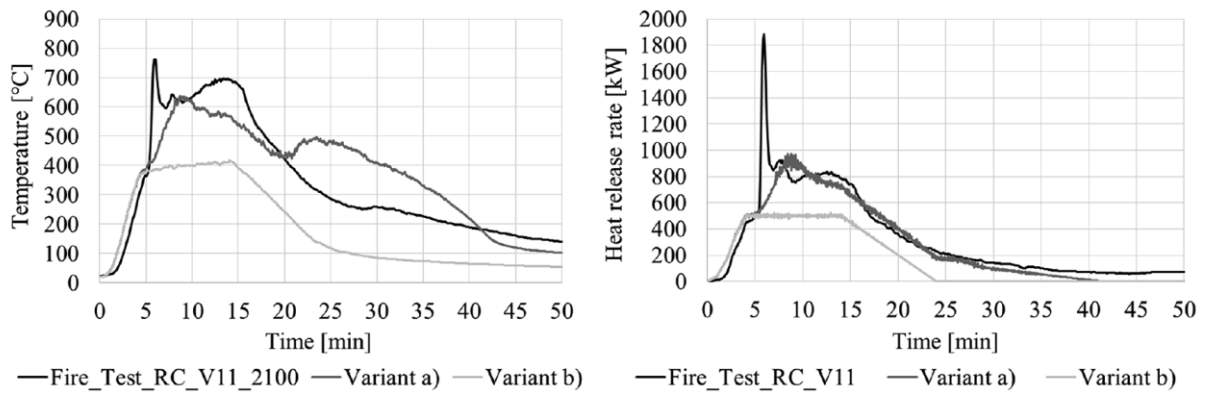


Figure 20: Comparison of results (Brunkhorst & Zehfuß, 2020)

7.3.4 Dai et al. (2022): Engineering CFD model for fire spread on wood cribs

The paper by Dai et al. (2022) aims to model the fire spread over wood cribs in full-scale tests in the FDS software. The following parameters are used for validation: HRR, fire spread, burn-away rate, flame height, gas and solid phase temperatures and the radiant heat flux.

The experimental setup consists of a wood crib which resembles the fuel load in an office building, being 511 MJ/m². The wood crib is built up from wood sticks with cross-section dimensions of 30 mm x 35 mm. In the FDS model a mesh cell size is defined as 15 mm x 15 mm x 17,5 mm in the wood crib. In the horizontal surroundings of the wood crib the cell size was increased by a factor 2. Above the wood surface, the cell size was increased again with a factor of 2. A finer mesh size near the fire source is important for accurately solving the heat flow between cells.

In the FDS model the ignition temperature method is used. This means that once the wood reaches this temperature (310°C), it is ignited and will subsequently burn with a self-defined time dependent HRR. The HRR peak is specified at 240 kW/m² in flaming combustion. In the decay phase a HRR of 60 kW/m² is assigned to the wood cribs which should resemble smouldering combustion.

The chemical formula used for the spruce wood is $CH_{3,584}O_{1,55}$. Based on experiments an average net heat of combustion is applied, being 10,84 MJ/kg. The thermal conductivity and specific heat of wood were defined as temperature dependent in FDS in accordance with Appendix C.

Table 6: Input data FDS model by Dai et al. (2022)

Parameter	Quantity
Test dimensions	4,4 m x 4,4 m x 2,2 m (X, Y, Z)
Mesh cell size	15 mm x 15 mm x 17,5 mm (X, Y, Z)
Ignition temperature	310°C
Heat flux on wood surface in flaming combustion	240 kW/m ²
Heat of combustion	10,84 MJ/kg
Fuel load	511 MJ/m ²

Results show in Figure 21 that the FDS model matches reasonably well on various important fire parameters like HRR, fire spread, burn-away and flame temperature. All parameters are strongly coupled. Therefore, this study is unique in the sense that all parameters match simultaneously.

Sensitivity analyses are performed for all relevant parameters. The following parameters have a high sensitivity regarding simulation results: heat of combustion, ignition temperature, thermal inertia, self-specified HRR of the wood crib and the fuel load density. On the other hand, soot yield, moisture content and ceiling height have very limited effect on the simulation results.

Based on the simulation results, it can be stated that the FDS model is capable of simulating the fire spread on wood cribs and the released energy. However, by applying the ignition temperature method the burning behaviour of wood is simplified, hereby not considering the charring behaviour. Additionally, the sensitivity analysis shows that extrapolating this model to other test setups should be performed carefully.

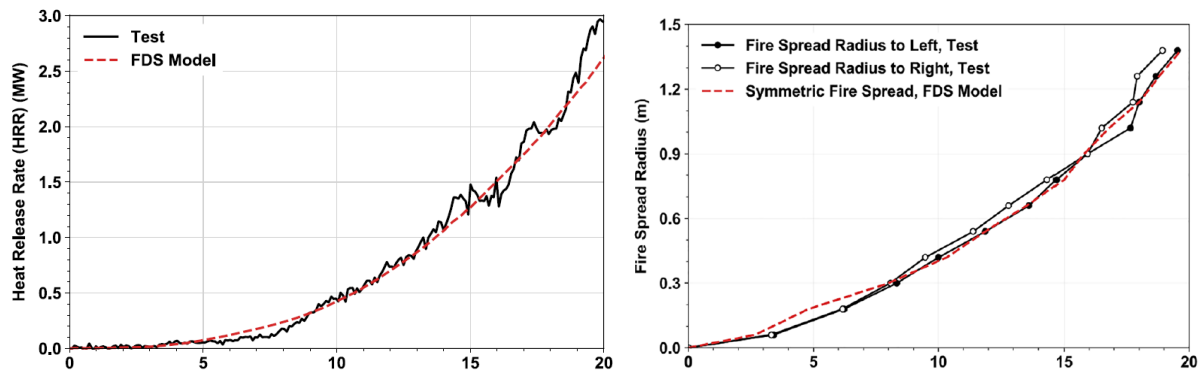


Figure 21: Comparison HRR and fire spread results (Dai et al., 2022)

7.3.5 Sun et al. (2022): BIM and FDS framework for simulation of CLT compartments

The paper by Sun et al. (2022) aims to develop an FDS model that simulates the fire dynamics within a mid-scale CLT compartment. A real-scale test is used for validating the model. The goal is to integrate the 4D BIM model with the FDS model to assess fire safety in the early stages of a construction project.

It is recognised that the high variability of the combustion process and input data for material properties in FDS requires the model to be validated with a real-life experiment. This could allow for the extrapolation of the model to other geometries. The compartment geometry consists of a box with dimensions 0,8 m x 0,5 m x 0,6 m (X, Y, Z) with a door opening for oxygen supply. The mesh is divided into cubical cells with dimensions 10 mm.

The burning behaviour of the CLT panels is modelled according to the ignition temperature method with a heat of combustion assigned to the wood material, respectively 364°C and 17,9 MJ/kg. A predefined burn rate of 1,5 mm/min is assigned to the CLT surfaces. The fire source within the compartment is a kerosene pool fire with a HRR of 64,5 kW/m².

Table 7: Input data FDS model by Sun et al. (2022)

Parameter	Quantity
Test dimensions	0,8 m x 0,5 m x 0,6 m (X, Y, Z)
Mesh cell size	10 mm (cubical)
Ignition temperature	364°C
Heat of combustion	17,9 MJ/kg
Fuel load	64,5 kW/m ²

Results show in Figure 22 that the HRR can be accurately modelled both within and outside the compartment. The energy contribution of the exposed CLT is approximated adequately. The flow velocities have also been measured in the door opening as a function of the amount of exposed CLT. More exposed CLT results in a larger mass flow due to the burning CLT panels. This also corresponds well with the experimental results. Lastly, gas phase temperatures and cross-section temperatures show good correspondence with the experiments.

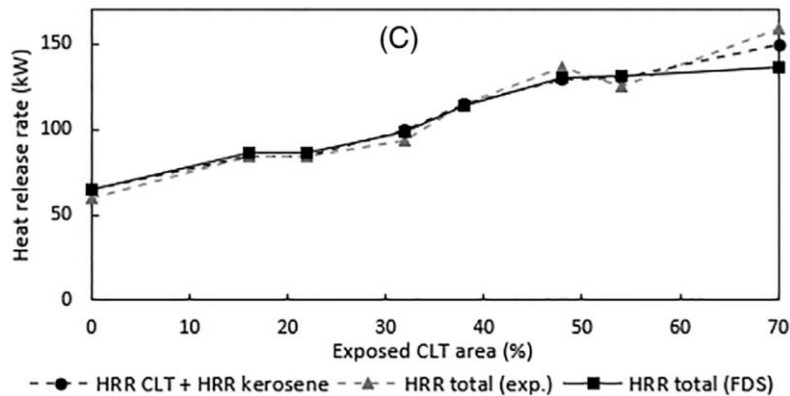


Figure 22: Comparison of results (Sun et al., 2022)

Conclusively, the FDS model is capable of simulating the fire dynamics within the specified compartment. However, it is recognized that extrapolation of the model geometry should be done with care as the compartment size has a direct impact on the internal air flow. Therefore, results heavily depend on the size of the assessed CLT structure. The formation of a char layer is also not considered in the FDS model, instead a constant burning rate is used as input.

7.3.6 Nakrani et al. (2023): Characterization of wood combustion through simulations

The paper by Nakrani et al. (2023) proposes a two-step combustion model in FDS for soft and hard woods based on the physical characterization of various wood samples.

In FDS the wood samples are modelled as 100 mm x 100 mm x 10 mm (X, Y, Z) obstructions in a larger computational domain that is open to ambient conditions on all boundaries. The mesh is divided into cubical cells with dimensions of 5 mm. The mesh size choice follows from an extensive mesh sensitivity analysis. This study showed that cubical cells of 10 mm resulted in a higher HRR, while reducing the cell size even further than 5 mm did not result in large changes in the HRR.

The common one-step combustion model transforms wood into pyrolysis gases and char. The proposed two-step combustion model divides the wood material into a cellulose and hemicellulose component. Both constituents show their own distinct thermal decomposition when heated. Therefore, for more accurately modelling the burning behaviour of wood this approach is chosen. Both constituents are transformed into pyrolysis gases and char once the appropriate material temperature has been reached.

A thermogravimetric analysis has been performed to determine the material properties of the wood samples. It was found that mass loss rates peak between 350°C and 380°C for both softwoods and hardwoods. Additionally, the activation energy and pre-exponential factor are determined to use as input parameters for the combustion model in FDS.

For modelling softwood in FDS a heat of combustion of 12,21 MJ/kg is assumed. Additionally, the thermal conductivity and specific heat are temperature dependent as listed in Appendix C. A cone calorimetry setup is used with a maximum output of 75 kW/m² for the radiation panel.

Table 8: Input data FDS model by Nakrani et al. (2023)

Parameter	Quantity
Test dimensions	100 mm x 100 mm x 10 mm (X, Y, Z) wood sample
Mesh cell size	5 mm (cubical)
Reference temperature for pyrolysis reaction	350-380°C
Heat of combustion	12,21 MJ/kg
Fuel load	75 kW/m ² (radiation panel)

The FDS model is validated on the HRR development over time. Results show in Figure 23 that the FDS simulation with the two-step combustion model shows better agreement with experimental results compared to the one-step combustion model. The tail in the experimentally obtained HRR represents the glowing oxidation of the char layer. The char layer is not included in the model and therefore validation in the decay phase is poor.

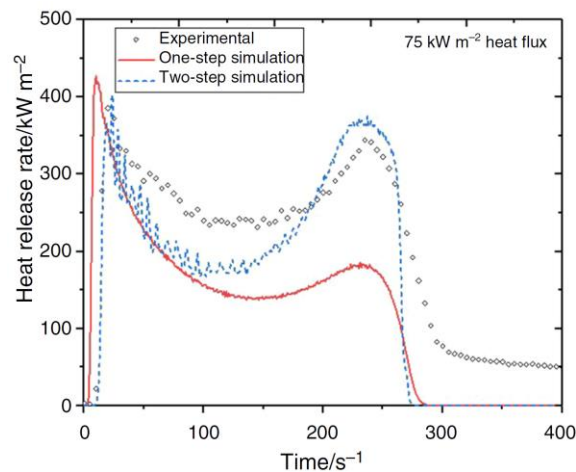


Figure 23: Comparison of results (Nakrani et al., 2023)

7.3.7 Hayajneh and Naser (2023): CFD study of fire spread in multi-storey timber building

The goal of the paper by Hayajneh and Naser (2023) is to assess the fire safety performance of a multi-storey timber building by setting up a model in the FDS software.

Five full-scale compartment fire tests in a two-storey CLT building, as performed by Zelinka et al. (2018), are used for the validation of the FDS model. The validation study focuses on temperatures, HRR and gas concentrations. The total fuel load of 570 MJ/m² represents a residential function. The FDS model represents a ten-storey CLT building with a floor plan of 11,2 m x 14,5 m.

The building is divided into meshes with a cubical cell size of 150 mm as shown in Figure 24. The mesh resolution has been optimised until further effects of the mesh size on the simulation results were eliminated. Additionally, the mesh is extended beyond the boundaries of the building to simulate a realistic fire spread through the windows.



Figure 24: FDS model multi-storey CLT building (Hayajneh & Naser, 2023)

The furniture and the wood cribs within the building can burn via the simple pyrolysis model as specified with kinetic and thermal properties. Every surface is assigned a self-specified HRR output which is based on experimental data. The wood material is converted into 82% pyrolysis gases and 18% char according to the pyrolysis model in FDS. The HRR as specified on the CLT surface determines the mass loss rate of the CLT in combination with the ventilation conditions.

Results show reasonable agreement of temperatures between the experimental data and the simulations. Additionally, the HRR in Figure 25 corresponds very well with experimental results. Therefore, the FDS model showed good potential for assessing fire scenarios within a multi-storey CLT building.

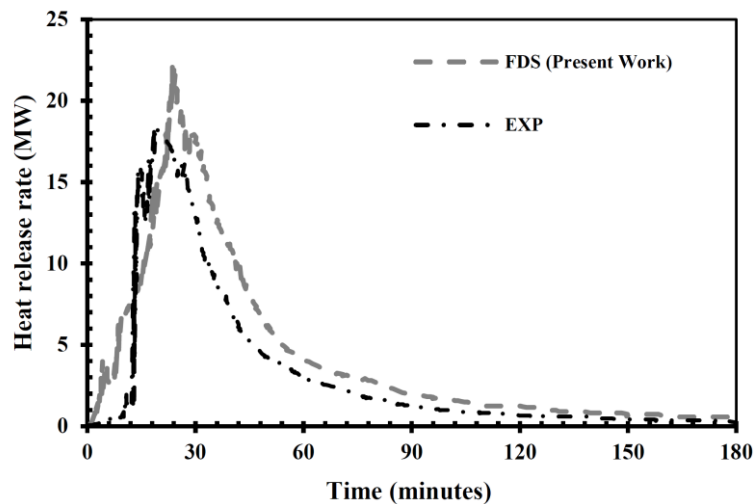


Figure 25: Comparison of results (Hayajneh & Naser, 2023)

7.4 CONCLUSION

This chapter presented the state of the art on computational modelling in FSE. The use of modelling tools allows for quick insights into the fire dynamics within both simple and complex geometries. This saves a considerable amount of time and money compared to real-life experimental research.

FDS is the preferred computational modelling tool. With the capabilities of CFD software, FDS allows for a detailed assessment of the fire dynamics within a CLT compartment with the possibility of localised analyses. Two-zone models have too limited functionalities to include the burning behaviour of wood.

The existing research on CFD modelling of burning wood is limited but shows potential for replicating real-life experimental results. Most existing research utilises the ignition temperature method for simplifying the burning behaviour of wood which disregards the chemical processes in the fire-exposed wood like pyrolysis and charring. Simulating the burning behaviour of wood by modelling the chemical processes of pyrolysis and combustion is of special interest due to the limited available knowledge for this approach.

It is shown that CFD models, which simulate the burning behaviour of wood, are highly sensitive to the mesh cell size and the heat of combustion of wood. On the other hand, moisture content of wood has limited influence on the simulation results. It is concluded that extrapolation of CFD models to larger geometries and other test configurations should be performed carefully due to the mesh dependency.

Answer subquestion 4

Based on the literature presented in Chapter 7, subquestion 4 can be answered to the best extent.

SUBQUESTION 4: "WHAT ARE CURRENT LIMITATIONS IN COMPUTATIONAL SOFTWARE FOR
MODELLING THE BURNING BEHAVIOUR OF WOOD?"

Modelling the pyrolysis process and the char formation is the primary challenge in computational software due to the natural origin of wood with its high inherent material variability. The high material variability makes it difficult to present uniform material properties for the modelled wood. The formation of the char layer and its impact on reducing the release of pyrolysis gases is a complex phenomenon which is difficult to translate to a computational model. Delamination of the char layer is highly unpredictable and therefore very challenging to include in modelling software. This affects the decay phase of the fire, which is often underestimated in computational software due to the complexity of modelling char retention and smouldering combustion of wood.

Additionally, the inherent complexity of CFD modelling poses uncertainties regarding boundary conditions and input parameters. Simulation results can be highly sensitive to specific input parameters and the gas flow at the boundaries of the computational domain. The numerical stability of computational models can also be heavily affected by small changes in input parameters.

Conclusively, simulated results with CFD software need to be benchmarked with representative experimental test results. This way the validity of the computational model can be verified. Only then the computational model can be used, while extrapolation of the model should still be done carefully.

PART 3: COMPUTATIONAL TESTING

This part presents the development of the FDS model based on reference experiments by Olivier (2019) and empirical data. Subsequently, the simulations are presented hereby simulating various exposed CLT compartment configurations and comparing these to the reference experimental results. Lastly, the results of the simulations are analysed, explaining similarities and differences between the simulations and experiments.

- CHAPTER 8: MODEL DEVELOPMENT
 - Chapter 8.1: Structure FDS file
 - Chapter 8.2: Model geometry
 - Chapter 8.3: Modelling burning behaviour of wood
 - Chapter 8.4: Fire modelling
 - Chapter 8.5: Output
 - Chapter 8.6: PyroSim post processing
 - Chapter 8.7: Conclusion

- CHAPTER 9: SIMULATIONS
 - Chapter 9.1: Simulation 1: left side wall exposed
 - Chapter 9.2: Simulation 2: 2 side walls exposed
 - Chapter 9.3: Simulation 3: ceiling exposed

- CHAPTER 10: ANALYSIS
 - Chapter 10.1: Comparison simulations and experiments
 - Chapter 10.2: Sensitivity analysis

8 MODEL DEVELOPMENT

Following upon the conclusion of Chapter 7, this chapter presents the development of an FDS model which simulates the fire dynamics within a CLT compartment. The underlying theoretical background and the order of the FDS model are discussed with relevant input parameters being explained. The complete FDS model can be found in Appendix A. This chapter is largely based on the knowledge gained from the FDS user guide by McGrattan et al. (2023). FDS version 6.8 is used for this thesis.

8.1 STRUCTURE FDS FILE

An FDS file consists of lines of textual code. The parameters in the input file are specified by using namelist formatted records. Every namelist record line in the FDS code starts with the ‘&’ sign, followed by the name of the namelist group. Subsequently, on the same line the input parameters linked with this namelist group are listed. An example of this code format for specifying the mesh size is listed below:

```
&MESH ID='mesh1', IJK=15, 6, 15, XB=0.0, 0.5, 0.0, 0.20, 0.0, 0.5, /
```

These namelist records vary from geometrical input to defining pyrolysis reactions. The order of the namelist records in the FDS code does not influence the simulation. However, because FDS files can be very extensive, it is suggested to group the various namelist records within the code to increase readability and identify potential modelling mistakes. This chapter elaborates on specific input parameters. For a full overview of the used namelist records and input parameters, Appendix B can be consulted.

8.2 MODEL GEOMETRY

8.2.1 Multiple meshes

In FDS the computational space is divided into three-dimensional meshes. Each mesh consists of a particular grid of cells with a self-defined cell size in X, Y and Z direction. It is recommended that the cells have a cubical shape, meaning that they have an equal length in X, Y and Z direction. The cubical shape contributes to the numerical stability of the simulation and result in more accurate numerical solutions.

FDS allows for using multiple computer cores simultaneously to decrease simulation times. For this thesis, FDS is running by means of Message Passing Interface (MPI). MPI requires the computational domain to be divided into multiple meshes, depending on the amount of available computer cores. Subsequently, the flow field within each mesh can be calculated in parallel. The simulation time is limited by the mesh with the largest number of cells. Therefore, it is preferred for all meshes to have a similar number of cells to reduce the required simulation time.

The simulations are performed on the servers of OneSimulations, which is part of Sweco where the thesis is conducted. The servers allow for a significant amount of meshes to be simulated with MPI. The FDS model in this thesis consists of 20 meshes, while a regular laptop is limited to running 6 meshes at the same time. Therefore, using the servers of OneSimulations significantly enhances the computational efficiency.

In FDS the interface between adjacent meshes is important for assuring numerically stable simulations and accurate resolvment of the gas flow between cells. The ideal alignment between multiple meshes in FDS is depicted in Figure 26. In some cases, it is preferred to have a finer mesh near the fire source and combustible surfaces to accurately resolve the heat transfer. In that case it is of importance that the cell size is reduced to a cell size that is a multitude of the original cell size, as is visualised in

Figure 27. Otherwise, the alignment between meshes would not be adequate and result in numerical instabilities, as is visualised in Figure 28.

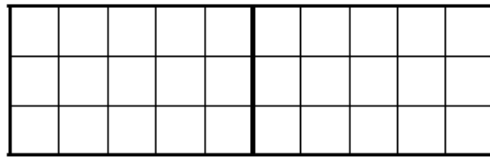


Figure 26: Ideal FDS mesh alignment

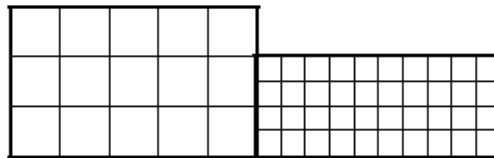


Figure 27: FDS alignment 2 mesh sizes

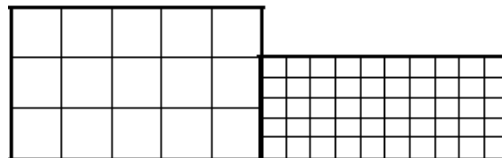


Figure 28: Incorrect FDS mesh alignment

Reducing the cell size in X, Y and Z direction by a factor of two will increase the simulation time by a factor of roughly 16. This is caused by an increase in number of cells with a factor 8 and an adjusted time step in the simulation. An increase in number of cells results in more accurately solving the Navier Stokes equations for the heat transfer between adjacent cells. Therefore, reducing the mesh cell size can influence the simulation results. The goal is to find a fitting mesh size such that reducing the mesh size even further does not notably influence the simulation results. The influence of the mesh size is assessed in a sensitivity analysis in Chapter 10.2.1. Based on this sensitivity analysis, it was decided to use 20 mm cubical cells for all meshes in the computational domain.

8.2.2 Thermal boundary conditions

In FDS the outer boundaries of the computational domain are by default solid boundaries which are maintained at the ambient temperature. To create a three-dimensional compartment geometry in FDS, obstructions need to be added with appropriate surface properties. The default setting for surfaces is labelled as 'INERT' which resembles a smooth wall with a fixed surface temperature corresponding to the ambient temperature of 20°C.

For this thesis, a pine wood surface is constructed representing a CLT panel. The front side of the pine wood surface is exposed to the fire within the compartment, while the back side is exposed to the surrounding ambient temperature. First, the material properties of pine wood are required as input. Values for thermal properties like specific heat and thermal conductivity are temperature dependent in the model, in accordance with data from prEN 1995-1-2. The input values for these parameters are listed in Appendix C.

The density of pine wood is taken as a constant value of 520 kg/m³ because this property cannot be temperature dependent in FDS, otherwise resulting in numerical instability of the model. The pine surface has a specified thickness and moisture content based on the reference experiments as presented in Chapter 8.2.3. The moisture is used to cool down the model and slow down the

temperature increase within the pine wood surface. Furthermore, the surface has a heat transfer coefficient of $0,13 \text{ W}/(\text{m}^2 \cdot \text{K})$.

The other (non-timber) surfaces within the compartment are non-combustible. In the modelling process, three distinct variants are analysed: INERT, ADIABATIC and PromatectH. PromatectH is a non-combustible calcium-silicate material with adequate thermal properties to withstand fire induced loads. PromatectH is used for non-combustible surfaces in the reference experiments as presented in Chapter 8.2.3. After analysing the implications of each non-combustible surface on the simulation results, PromatectH is chosen as the best method for modelling as it approximates the experimental setup (Chapter 8.2.3) in the most realistic way. The extensive comparison between simulations with INERT, ADIABATIC and PromatectH surfaces is presented in Appendix F.

Modelling an exterior volume outside the compartment is required to simulate realistic gas flows in and out of the compartment openings, like oxygen inflow and heat dissipation. The boundaries outside the compartment are modelled as OPEN in FDS, meaning that the computational domain is connected to the ambient environment. This allows for the inflow of oxygen to prevent oxygen depletion within the simulated computational domain.

If the exterior volume is not included in the model, the temperatures remain at ambient conditions at the compartment openings, thus not including external heat release outside the compartment. Therefore, extending the computational space in X, Y and Z direction outside the compartment openings is crucial for the validity of the model.

Modelling limitation

It is important to note that in the FDS model the CLT surface is constructed of one pine wood layer. Therefore, delamination is not considered in the modelling process. Due to the unpredictability and complexity of the delaminating behaviour, it is not included within the scope of the FDS model.

8.2.3 Reference experiments

Validation of the FDS model by comparing simulation results with experimental results is crucial for checking the functionality of the model. The choice is made to validate the model with the small-scale experimental setup as performed by both Crielaard (2015) and Olivier (2019). These experimental series are discussed in Chapter 6.1.3 and 6.1.8 respectively.

The choice for this experimental setup is motivated by the easy burner setup. This way the HRR of the gas burner can be modelled in a simple way, as opposed to larger experiments which use furniture as fuel load. Due to the easy quantification of the burner HRR, the contribution of the exposed CLT panels to the HRR can be calculated by subtracting the burner output from the total HRR.

The goal of the validation study is to exactly replicate the test conditions. This includes the time until the burner is turned off for each test. In the experiments the burner is turned off once all exposed CLT panels reach a charring depth of 20 mm in the middle of the panel. It was hypothesized by Crielaard (2015) that after the formation of this char layer, the initial interior fuel load is consumed. The exact burner output for each test configuration is copied in the simulations.

For the scope of this thesis, delamination is not included in the modelling process. Therefore, the tests by Olivier (2019) are preferred because a non-delaminating adhesive is used. This resembles better with the developed FDS model compared to the unpredictable delamination behaviour in the tests by Crielaard (2015).

The test setup of Olivier (2019), depicted in Figure 29, consists of a small-scale cubical compartment with dimensions 0,5 m x 0,5 m x 0,5 m. The used CLT panels consist of 5 layers of 20 mm plywood, bonded by a melamine-based adhesive, resulting in a 100 mm wall thickness. For the non-CLT surfaces, the material PromatectH is used which is a non-combustible calcium-silicate. The relevant material properties of PromatectH and an overview of the test setup is given in Table 9.



Figure 29: Experimental setup (Olivier, 2019)

A ventilation opening is added in the middle of the front wall to allow for the inflow of oxygen, hereby preventing possible oxygen depletion within the compartment. The ventilation opening is 0,18 m x 0,5 m (x, z) corresponding to an opening factor of 0,042 m^{0,5}.

In the experiments by Olivier (2019), the oxygen consumption calorimetry method is used to calculate the produced HRR during the fire. Further elaboration on this method can be found in Chapter 4.2.

The various compartment configurations regarding exposed CLT in the experiments by Olivier (2019) are listed in Table 9 with corresponding abbreviations.

Table 9: Overview test setup (Olivier, 2019)

	Quantity
Compartment dimensions	- 0,5 m x 0,5 m x 0,5 m (x, y, z)
Ventilation opening	- 0,18 m x 0,5 m (x, z)
CLT surfaces	- 5 plies of 20 mm thick = 100 mm total thickness - Melamine based adhesive
PromatectH surfaces	- Thickness = 20 mm - Density = 870 kg/m ³ - Thermal conductivity = 0,18 W/(m*K) - Specific heat capacity = 0,92 kJ/(kg*K)
Gas burner output during heating	- 41 kW
Test configurations	<ul style="list-style-type: none"> • Configuration 1: back wall exposed (BW) • Configuration 2: 2 side walls exposed (2SW) • Configuration 3: left side wall exposed (LSW) • Configuration 4: ceiling exposed (C) • Configuration 5: back wall and ceiling exposed (BW+C)

8.3 MODELLING BURNING BEHAVIOUR OF WOOD

One of the most challenging and innovative aspects of this thesis, is the modelling of the burning behaviour of wood. For achieving this, the distinction is made between the pyrolysis and combustion process. The modelling approach in FDS for both chemical processes is discussed in this section.

8.3.1 Pyrolysis

In FDS materials can undergo several reactions that can occur at different temperatures. The pyrolysis process as presented in Chapter 4.1.2 shows a wide temperature range during which pyrolysis gases are being released. FDS can take this range into account by specifying a reference temperature at which the pyrolysis reaction has the highest mass loss rate, and an associated pyrolysis range. The reference temperature and pyrolysis range are set to 300°C and 100°C respectively, in accordance with the thermogravimetric analysis as performed by Hejtmánek et al. (2017). This means that between 200-400°C the pyrolysis reaction occurs within the pine wood with the reaction speed peaking at 300°C. This pyrolysis range is supported by the findings in Figure 30 by Nakrani et al. (2023) which shows that the mass of pine wood decreases the most between these temperatures. This graph shows various heating rates plotted versus each other. The value 5 K/min is the default value in FDS, which is used in the model for this thesis.

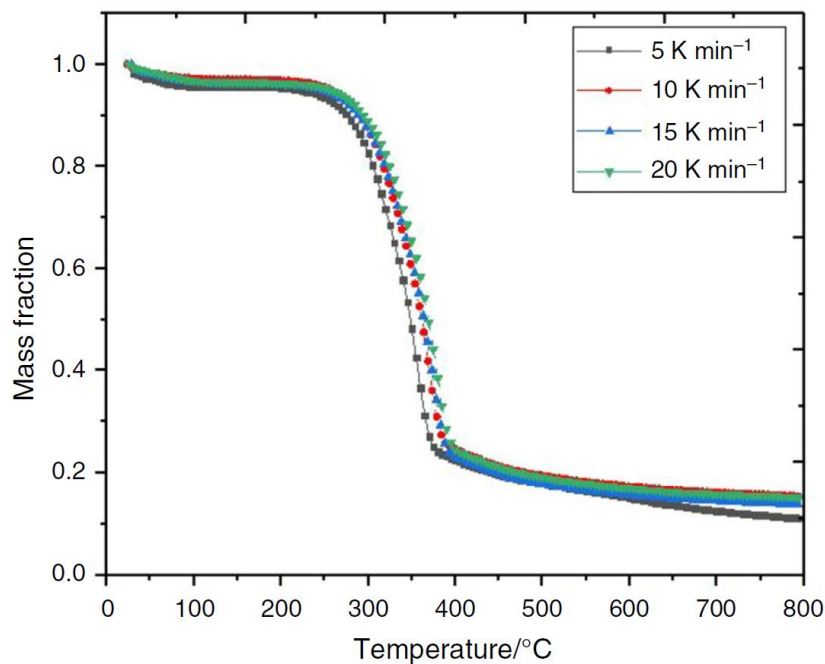


Figure 30: Thermal degradation of pine wood (Nakrani et al., 2023)

In physical experiments the pyrolysis reaction of pine wood results in the formation of pyrolysis gases and a char layer. Initially, in the FDS model a ratio between the pyrolysis gases and the char layer of 84,7% and 15,3% respectively was assumed in accordance with the thermogravimetric analysis by Hejtmánek et al. (2017). The pyrolysis gases are then released into the compartment and can subsequently combust.

However, after an extensive analysis of the results in the simulations with the formation of a physical char layer, it was decided to exclude the char layer from the FDS model due to the highly fluctuating HRR development. Therefore, a fully efficient pyrolysis process is assumed with 100% of the pine wood being transformed into pyrolysis gases. To consider the incomplete combustion, from which the char layer is the result, an effective heat of combustion value is assigned to the pine wood. Chapter 8.3.2

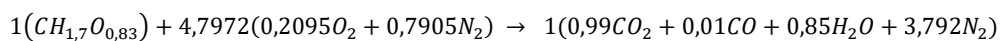
elaborates further on the combustion process. The extensive analysis of the impact of the formation of a physical char layer in the FDS model on the simulation results can be found in Appendix G.

In real-life, the char layer most notably influences the decay phase of burning wood. Due to the formation of an insulating char layer at the surface, the underlying timber can sustain smouldering combustion. Therefore, the char layer has an impact on the length of the decay phase. Excluding the char layer from the FDS model has consequences for simulating the burning behaviour in the decay phase. Conclusively, considering that including a char layer is a more advanced and realistic method for modelling the burning behaviour of wood, this research still chose to exclude the char layer to obtain a more realistic burning behaviour. Further research into modelling the char layer is required.

8.3.2 Combustion

The next step in the FDS model is for the pyrolysis gases to combust and release energy into the compartment. This part is mostly based on the work by Hejtmánek et al. (2017), as presented in Chapter 7.3.1, who conducted experiments to find input data for CFD modelling of burning wood.

Below, the chemical reaction describing the combustion process is presented. The first term of the reactants is the pyrolysis gas, also referred to as pyrolyzate, which is the product of the pyrolysis reaction. This pyrolyzate reacts with air to form the gaseous products CO₂, CO, H₂O and N₂. The ratio of the combustion products is determined by a thermogravimetric analysis. By default, in FDS the reaction of fuel and oxygen is infinitely fast and only controlled by mixing of the reactants (mixing-controlled).



The combustion of the pyrolyzate releases energy into the compartment, which is specified by the heat of combustion. The input value in the FDS model for the heat of combustion of wood is 10 MJ/kg. This follows from an extensive sensitivity analysis in Chapter 10.2.2 to find an appropriate value.

Additionally, a soot yield is specified for the combustion reaction to visualise the smoke formation within the compartment. A value of 0,02 is assigned to the soot yield based on the work by Robbins and Wade (2007).

8.4 FIRE MODELLING

In FDS there are two ways of modelling the ignition source for a fire. The first method is to model a simple gas burner with a specified HRR output. The second method, which is more complicated, models combustible furniture with appropriate thermal properties in the compartment. Subsequently, one item is ignited and the fire will spread through the room via the burning furniture.

For the goal of clearly identifying the contribution of the burning CLT walls, the simple burner method is applied in accordance with the experimental setup by Olivier (2019). The burner is modelled over the entire compartment floor area and the burner output over time corresponds to the experiments.

The time at which the burner is turned off is identical to the experimental setup. The method for determining this moment is explained in Chapter 8.2.3. In the FDS model the input for the gas burner output is given as 164 kW/m², which corresponds to the burner output of 41 kW over the 0,25 m² floor area in the reference experiments by Olivier (2019).

8.5 OUTPUT

In FDS, self-defining the desired output quantities is an important modelling aspect for being able to extract the required information for extensively analysing the simulated compartment fire dynamics. For validating the FDS model with the reference experiments, measurement devices (abbreviation DEVC in FDS) are placed in the model at the same locations as in the experiments. This section gives an overview of the measured quantities in the experiments by Olivier (2019) and their implementation in the FDS model. Additionally, some output tools of FDS are discussed that broaden the understanding of the fire dynamics within the simulated compartment. Full elaboration on the FDS input is given in Appendix B

A complete overview of all measured output quantities in the FDS model is given in Table 10.

Table 10: FDS model output quantities

Quantity	Unit	Location
Gas temperature	°C	<ul style="list-style-type: none"> - 0,2 and 0,4 m height in middle of compartment - Right above the middle of each exposed CLT surface - 2D slices for visualisation of local differences - 3D visualisation of distribution in the computational domain
Cross section temperature	°C	Thermocouples at 5, 10, 20, 30, 40, 50 and 60 mm depth in the middle of each exposed CLT surface
Heat release rate	kW	Total compartment
Oxygen fraction	•	2D slices
Burn rate	kg/(m ² *s)	2D slices at all compartment boundaries
Flow velocity	m/s	3D visualisation of the gas flow speed in the computational domain

By default, FDS calculates the HRR development over time in the compartment. The other output quantities have to be implemented manually, all in accordance with the experimental setup by Olivier (2019).

Gas phase temperatures are measured in the middle of the compartment at 0,2 m and 0,4 m height from the floor. Thermocouples are placed in the middle of each exposed CLT surface at depths of 20, 30, 40, 50 and 60 mm. Additionally to the measured output by Olivier (2019), to get a more broad understanding of the fire behaviour within the CLT element, the FDS model also calculates the CLT surface temperature and in depth cross section temperatures at 5 mm and 10 mm. Lastly, the FDS model calculates the gas phase temperature right above the exposed CLT surface. This allows for the implementation of Equation (2) as presented in Chapter 4.1.3.3, which requires the gas phase temperature as input value to calculate the charring depth over time of the fire exposed CLT element.

FDS allows for the visualisation of specific output quantities over a 2-dimensional plane. These 2D slices are placed at multiple locations, measuring temperatures and oxygen concentration. Oxygen concentration is measured to obtain quick insights in the combustion conditions for the exposed CLT.

The flow speed of gases within the computational domain is visualised in 3D, as depicted in Figure 31.

Lastly, a boundary quantity can be measured in FDS which provides a visualisation of this quantity for each surface within the compartment. The burn rate is specified as boundary quantity which measures the rate at which surfaces burn away in kg/(m²*s). This is depicted in Figure 31 where the left side wall

of the compartment is burning. This quantity provides an easy visual tool for assessing if exposed timber surfaces are ignited, in flaming combustion or already extinguished.

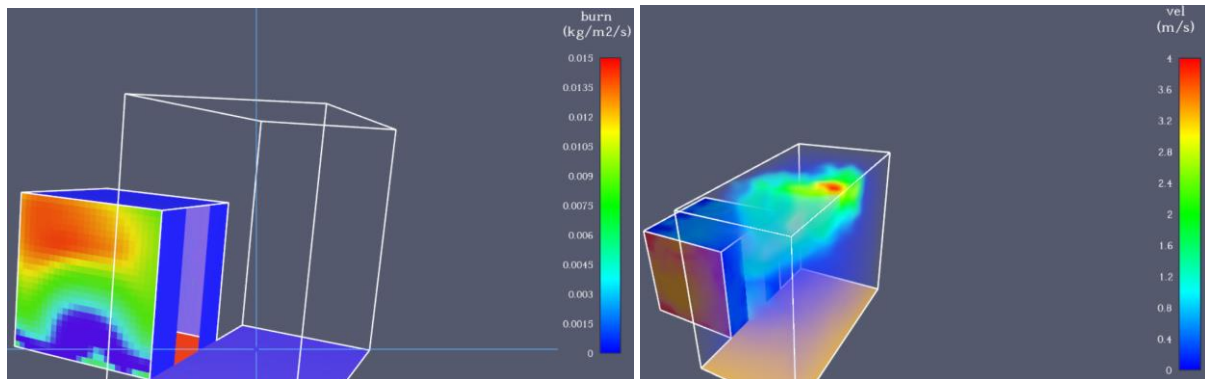


Figure 31: Example visualisation FDS model output

8.6 PYROSIM POST PROCESSING

This section presents an overview of how simulations are performed by using the PyroSim software. PyroSim is developed to complement the FDS software. FDS files can be imported into PyroSim, where the textual FDS model is visualised. This is shown in Figure 32 where the modelled compartment and outside environment can be seen. The red surface represents a CLT surface, while the other surfaces are non-combustible. This visualization allows for an easy way of checking your model geometry. Additionally, PyroSim indicates where problems might arise in the model which can then be resolved before running the simulation.

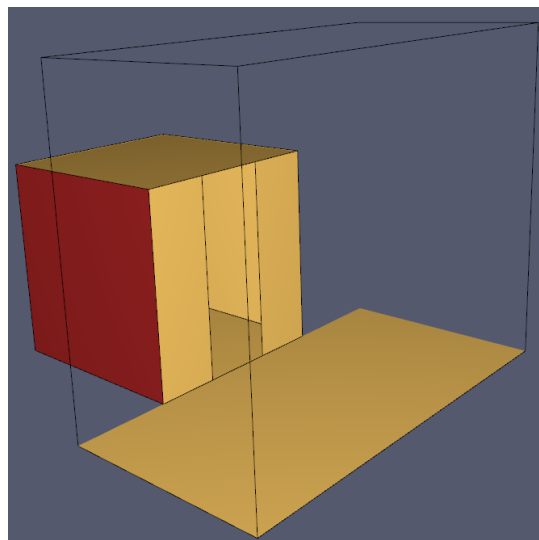


Figure 32: Visualisation FDS model in PyroSim

PyroSim is used for running the simulations, which allows for efficient use of computational power by means of parallel simulation running with multiple meshes on the servers of OneSimulations as explained in Chapter 8.2.1. The default simulation mode 'VLES' (Very Large Eddy Simulation) is used.

Once the simulation is finished, the results are stored in CSV files. PyroSim allows for the visualization of flames, smoke and specified output quantities inside the compartment, as can be seen in Figure 33. Conclusively, PyroSim provides a user-friendly tool to visualise, run and process FDS models.

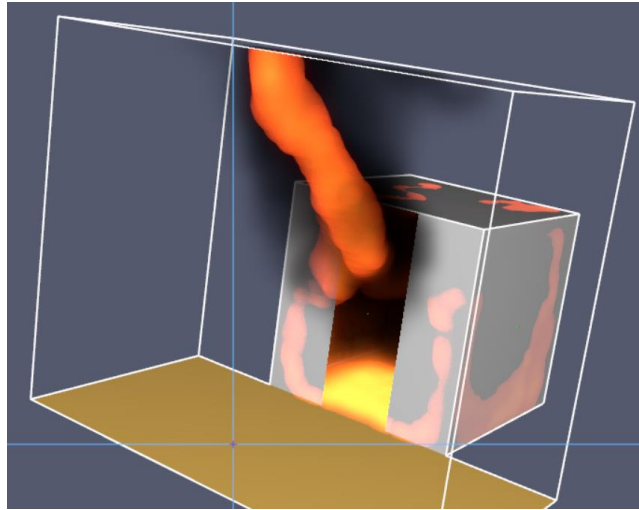


Figure 33: PyroSim fire and smoke visualisation

8.7 CONCLUSION

Chapter 8 presents the development of the FDS model which is used in upcoming chapters for simulating the fire dynamics in a CLT compartment. The most important take-aways are listed below:

- The computational domain is divided into 20 meshes to allow for MPI processing that reduces the computing time of the simulation.
- The burning behaviour of wood is modelled through chemical reactions for the pyrolysis and combustion process.
- No physical char formation is included in the pyrolysis process. Incomplete combustion is considered by specifying an effective heat of combustion value.
- The non-combustible surfaces are modelled as the calcium-silicate material PromatectH.
- The experimental test series by Olivier (2019) is used for validating the FDS model, using a small-scale compartment of 0,5 m x 0,5 m x 0,5 m.
- Post-processing of the simulated results is done with the PyroSim software.

In the following chapters, the presented FDS model is used to assess its applicability to CLT compartment fires. Hereby, the simulation results from the FDS model are compared with experimental results and the impact of various input parameters of the model is analysed.

9 SIMULATIONS

This chapter presents an overview of the performed simulations in FDS. Three compartment configurations with varying exposed CLT surfaces are simulated, corresponding to the experimental setup by Olivier (2019). The simulated results are compared with the experimentally obtained results to check the validity of the FDS model for CLT compartment fires. Chapter 10 dives deeper into the analysis of the simulation results and the most important factors of the FDS model, combining the observations of Chapter 9.

For the setup of the FDS model, used for the simulations, Chapter 8 can be consulted. Table 11 presents an overview of the layout of Chapter 9. Lastly, Appendix E provides a complete overview of all simulation results, with the main aspects being presented in the following sections.

Table 11: Overview configurations for FDS simulations

Section	FDS model	Reference experiment (Olivier, 2019)
9.1	Simulation 1: left side wall exposed	Configuration 3
9.2	Simulation 2: both side walls exposed	Configuration 2
9.3	Simulation 3: ceiling exposed	Configuration 4

9.1 SIMULATION 1: LEFT SIDE WALL EXPOSED

This section presents simulation 1 which replicates the experimental setup of configuration 3 by Olivier (2019) with an exposed left sidewall (LSW). The importance of this simulation is found in assessing how the FDS model works in a compartment with one vertical combustible CLT surface. The observations during the simulation are presented with a focus on the HRR and gas temperature development within the compartment. The observed results are compared to the experimental results of configuration 3. A brief overview of simulation 1 is given in Table 12. A complete overview of all results is given in Appendix E.1.

Table 12: Overview simulation 1

Simulation 1	
Exposed CLT surface	Left side wall
Reference test setup	Configuration 3 (Olivier, 2019)
HRR burner	41 kW
Simulation length	4359 seconds
Time to turning burner off (heating phase)	1989 seconds
Simulation running time (with 20 meshes)	13 hours

9.1.1 Observations HRR

The simulated HRR development is given in Figure 35 in combination with the experimental result of configuration 3 by Olivier (2019). The output of the simulated gas burner is given to provide a clear visualisation of the contribution to the HRR of the burning CLT left side wall. The observations of the simulation are discussed stepwise in Table 13. Subsequently, the difference between the simulation and the reference experiment by Olivier (2019) is quantified.

Table 13: Observations HRR simulation 1

Step	Description simulation 1
1	At the start of the simulation the burner instantly reaches its full capacity at 41 kW.
2	After 60 seconds the first signs of ignition of the left side wall are observed. Ignition starts in the far lower corner from the compartment opening.
3	Gradual increase in HRR as more cells in the CLT surface reach the lower limit of the pyrolysis temperature range and start to release pyrolysis gases that combust in access of oxygen.
4	After 500 seconds the entire left side wall is in flaming combustion where the HRR levels out at 67 kW. This is based on assessing the burning rate of the wall, which is visualised after 500 seconds in Figure 34.
5	Subsequently, the HRR fluctuates around an average of 67 kW while reaching a peak of 71 kW after 800 seconds.
6	Followed by a period where the HRR decreases slightly due to less combustion occurring at the left side wall until the HRR reaches a lower limit of 63 kW after 1900 seconds.
7	Next, combustion increases again ultimately reaching a HRR of 67 kW after 1985 seconds.
8	The gas burner is turned off after 1989 seconds.
9	Once the burner is turned off, the HRR drops almost instantly to approximately 0 kW which indicates that the CLT wall is considered to be extinguished after 2000 seconds.

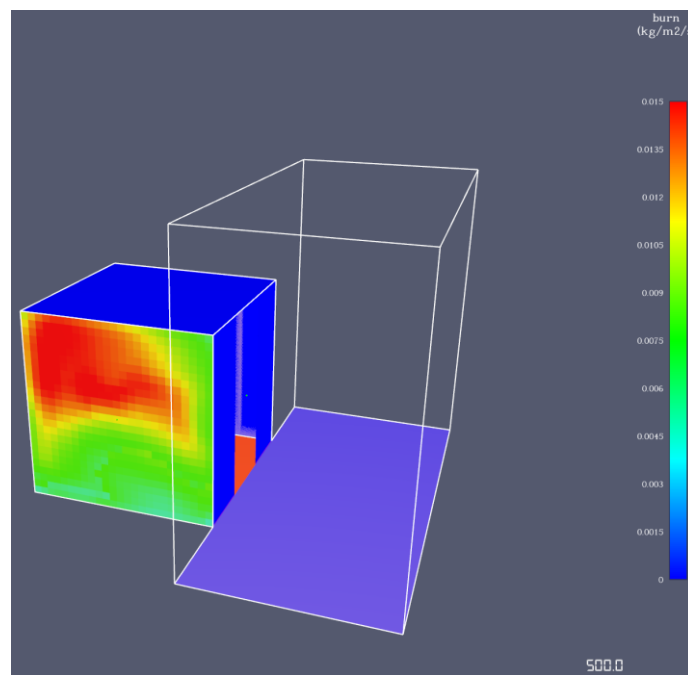


Figure 34: Simulation 1 visualisation burning rate after 500 seconds

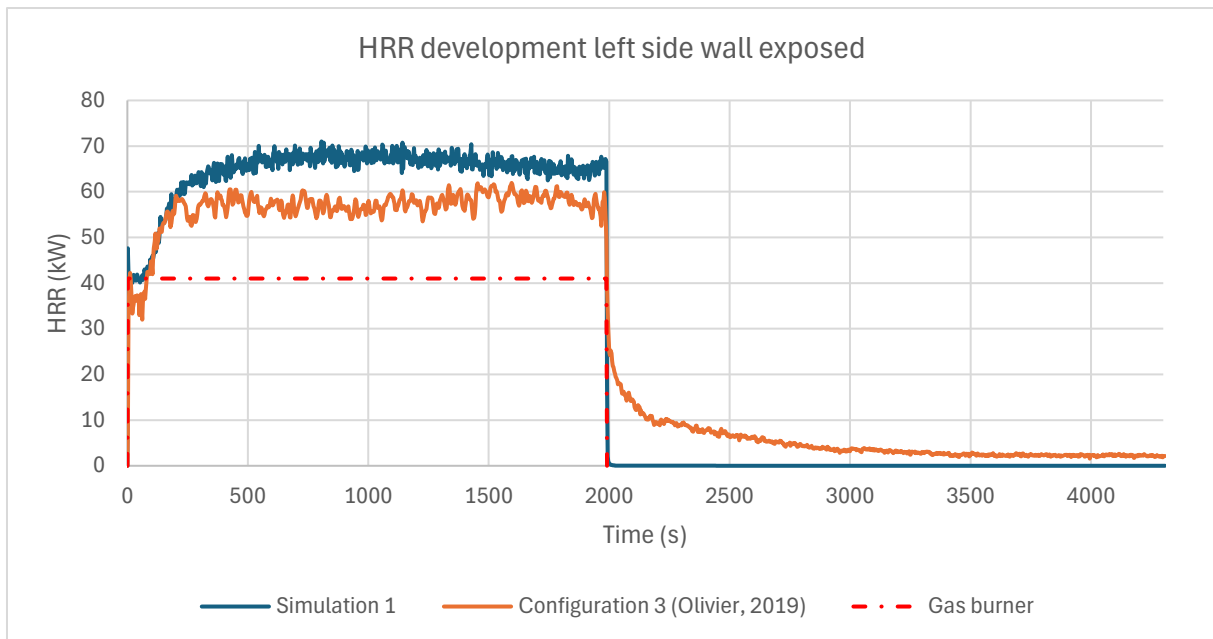


Figure 35: Simulation 1 HRR development

In Figure 35 it can be observed that for the first 240 seconds, the simulation approximates the experimental result adequately. Subsequently, the experimental HRR stagnates around 57 kW, while the simulated HRR increases further until it stagnates around 67 kW after 500 seconds.

Both graphs follow a similar trend during the heating phase, where the gas burner is turned on. Once the burner is turned off, the experimental HRR drops with 41 kW corresponding with the gas burner output and subsequently shows a gradual decay phase. However, the simulated HRR drops almost instantaneously towards 0 kW, thus not showing any decay phase. This is further discussed in Chapter 10.1.1.

For quantifying the percentual difference between the simulated and experimental HRR, only the heating phase is considered to allow for a reasonable comparison. Table 14 provides an overview of the HRR difference between the simulation and configuration 3 in the heating phase. It can thus be concluded that simulation 1 overestimates the HRR compared with configuration 3 by Olivier (2019).

Table 14: Quantification HRR simulation 1 vs configuration 3 in heating phase

	Simulation 1	Configuration 3 (Olivier, 2019)
Average HRR	64,3 kW	56,3 kW
Average HRR contribution of exposed CLT compared to the 41kW burner output	23,3 kW	15,3 kW
Average HRR increase compared to the 41kW burner output	57%	37%
Maximum HRR	71,0 kW	61,9 kW

9.1.2 Observations temperature

This section presents the simulated compartment temperatures, compared with the experimentally measured gas temperatures by Olivier (2019). For this the gas temperature is compared in the middle of the compartment at both 0,2 m and 0,4 m height. Figure 36 presents both the simulated as well as the experimental results. It can be observed that both at 0,2 m and 0,4 m height in the middle of the compartment the gas temperature is underestimated in the model. The trend of all graphs is

approximately similar during the heating phase. However, once the burner is turned off after 1989 seconds, the experiment shows a more gradual decrease in compartment temperatures compared to the simulated temperatures. This is further discussed in Chapter 10.1.2.

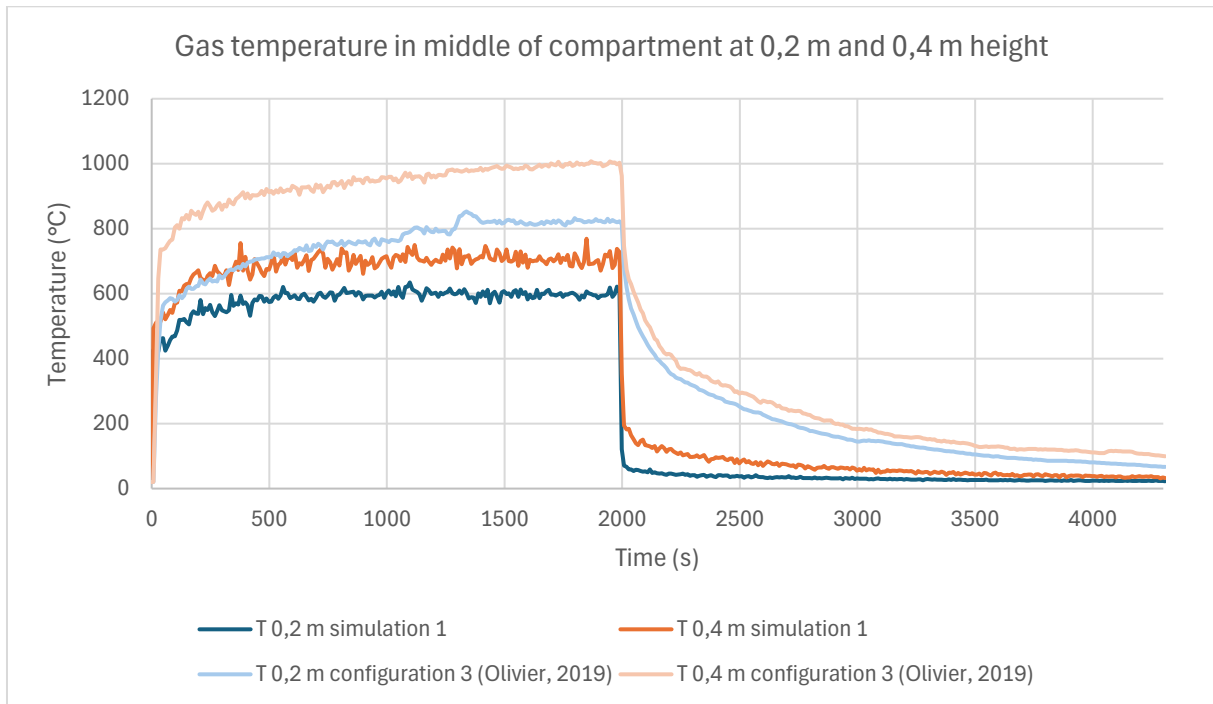


Figure 36: Simulation 1 gas temperature comparison

Table 15 provides an overview of the gas temperature differences in the middle of the compartment between simulation 1 and configuration 3 by Olivier (2019) in the heating phase. It can thus be concluded that simulation 1 underestimates the gas temperatures in the middle of the compartment.

Table 15: Quantification gas temperatures simulation 1 vs configuration 3 in heating phase

Temperature in the middle of the compartment	Simulation 1	Configuration 3 (Olivier, 2019)
Average temperature 0,2 m	581°C	747°C
Average temperature 0,4 m	688°C	931°C
Maximum temperature	769°C	1008°C
Average percentual difference simulation vs experiment at 0,2 m		-28%
Average percentual difference simulation vs experiment at 0,4 m		-35%

9.2 SIMULATION 2: 2 SIDE WALLS EXPOSED

This section presents simulation 2 which replicates the experimental setup of configuration 2 by Olivier (2019) with two exposed side walls (2SW). The importance of this simulation is found in assessing how the FDS model works with multiple combustible CLT surfaces to see if the burning behaviour is affected by each other. The observations during the simulation are presented with a focus on the HRR and gas temperature development within the compartment. The observed results are compared to the experimental results of configuration 2. A brief overview of simulation 2 is given in Table 16. A complete overview of the results is given in Appendix E.2.

Table 16: Overview simulation 2

Simulation 2	
Exposed CLT surface	Both side walls
Reference test setup	Configuration 2 (Olivier, 2019)
HRR burner	41 kW
Simulation length	17192 seconds
Time to turning burner off (heating phase)	1920 seconds
Simulation running time (with 20 meshes)	14 hours

9.2.1 Observations HRR

The simulated HRR development is given in Figure 37 in combination with the experimental result of configuration 2 by Olivier (2019). Due to the lack of decay phase in the simulation, Figure 38 shows a selected time frame at the start of the simulation to provide a better visualisation of the differences between simulated and experimental results. The output of the simulated gas burner is given to provide a clear visualisation of the contribution to the HRR of the burning CLT side walls. The observations of simulation 2 are discussed stepwise in Table 17. Subsequently, the difference between the simulation and the reference experiment by Olivier (2019) is quantified.

Table 17: Observations HRR simulation 2

Step	Description simulation
1	At the start of the simulation the burner instantly reaches its full capacity at 41 kW.
2	After 50 seconds the first signs of ignition of both side walls are observed simultaneously. Ignition starts in the far lower corner from the compartment opening for both side walls.
3	Gradual increase in HRR as more cells in both CLT side walls reach the lower limit of the pyrolysis temperature range and start to release pyrolysis gases that combust in access of oxygen.
4	After 300 seconds both side walls are in flaming combustion where the HRR levels out at 90 kW.
5	Subsequently, the HRR fluctuates around an average of 90 kW while reaching a peak of 96 kW after 560 seconds.
6	Followed by a period where the HRR decreases slightly due to less combustion occurring at both side walls until the HRR reaches a lower limit of 85 kW after 1750 seconds.
7	Next, combustion increases again ultimately reaching a HRR of 93 kW after 1900 seconds.
8	The gas burner is turned off after 1920 seconds.
9	Once the burner is turned off, the HRR drops almost instantly to approximately 0 kW which indicates that both CLT walls are considered to be extinguished after 1950 seconds.

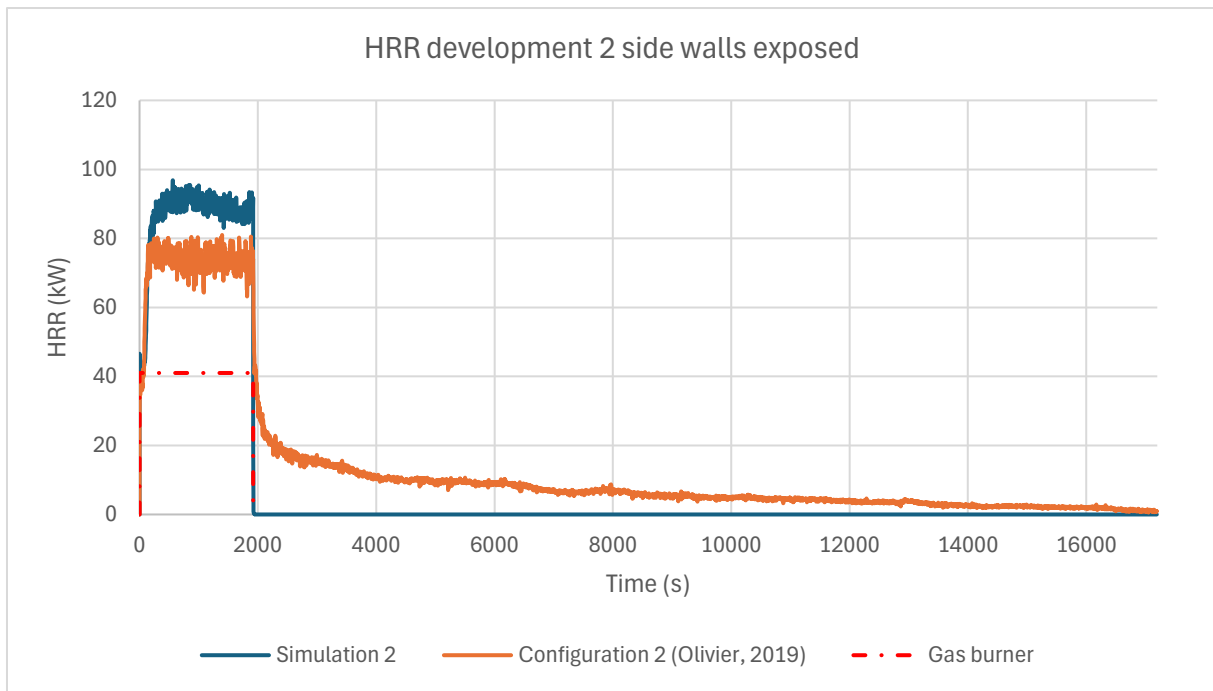


Figure 37: Simulation 2 full HRR development

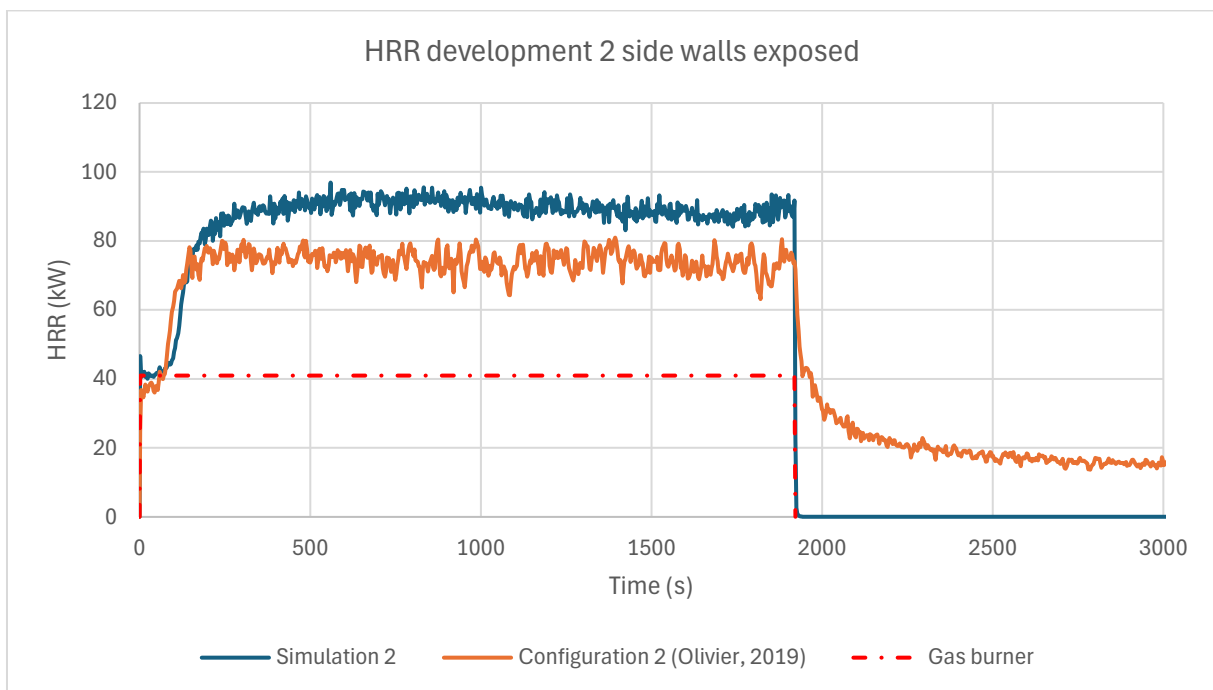


Figure 38: Simulation 2 HRR development first 3000 seconds

In Figure 38 it can be observed that for the first 160 seconds, the simulation approximates the experimental result adequately. Subsequently, the experimental HRR stagnates around 75 kW, while the simulated HRR increases further until it stagnates around 90 kW after 350 seconds.

Both graphs follow a similar trend during the heating phase, where the gas burner is turned on. Once the burner is turned off, the experimental HRR drops with 41 kW corresponding with the gas burner output and then shows a gradual decay phase. However, the simulated HRR drops almost

instantaneously towards 0 kW, thus not showing any decay phase. This is further discussed in Chapter 10.1.1.

For quantifying the percentual difference between the simulated and experimental HRR, only the heating phase is considered to allow for a reasonable comparison. Table 18 provides an overview of the HRR difference between the simulation and configuration 2. It can thus be concluded that simulation 2 overestimates the HRR compared with configuration 2 by Olivier (2019).

Table 18: Quantification HRR simulation 2 vs configuration 2 in heating phase

	Simulation 2	Configuration 2 (Olivier, 2019)
Average HRR	86,1 kW	72,5 kW
Average HRR contribution of exposed CLT compared to the 41kW burner output	45,1 kW	31,5 kW
Average HRR increase compared to the 41kW burner output	110%	77%
Maximum HRR	96,9 kW	81,0 kW

9.2.2 Observations temperature

This section presents the simulated compartment temperatures, compared with the experimentally measured gas temperatures by Olivier (2019). For this the gas temperature is compared in the middle of the compartment at both 0,2 m and 0,4 m height. Figure 39 and Figure 40 present the gas temperature comparison for the simulation vs the experimental results for the full simulation length and for a selected time frame, respectively. The selected time frame in Figure 40 provides a clearer visualisation of the temperature differences during the heating phase.

It can be observed that both at 0,2 m and 0,4 m height in the middle of the compartment the gas temperature is underestimated in the model. At the start of the simulation the gas temperatures follow a similar trend. However, after around 150 seconds, the simulated gas temperatures stagnate while the experimentally measured temperatures keep rising gradually until the gas burner is turned off. Once the burner is turned off after 1920 seconds, the experiment shows a significantly more gradual decrease in compartment temperatures compared to the simulated temperatures. This is further discussed in Chapter 10.1.2.

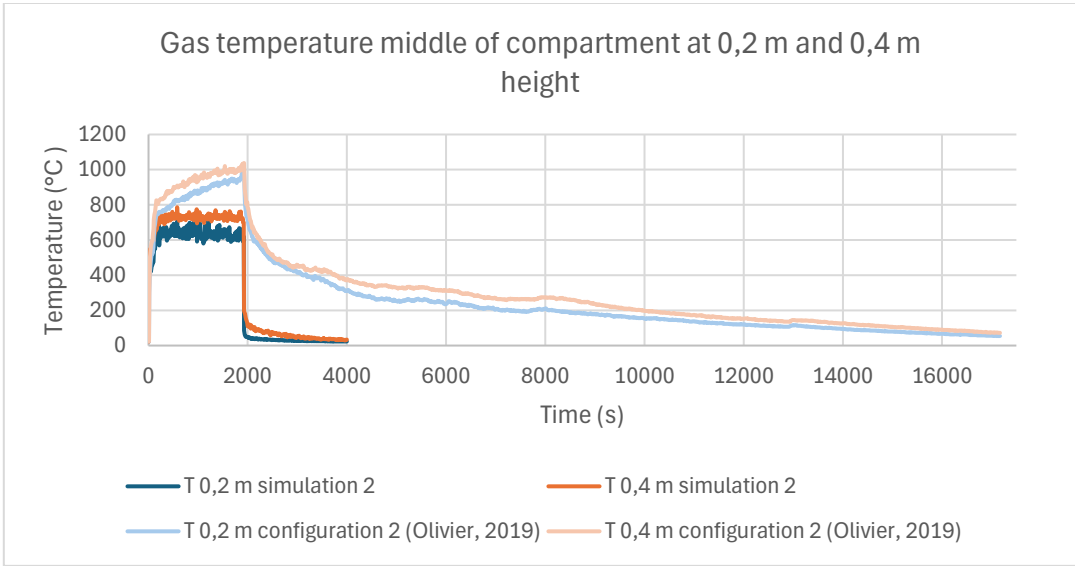


Figure 39: Simulation 2 gas temperature full comparison

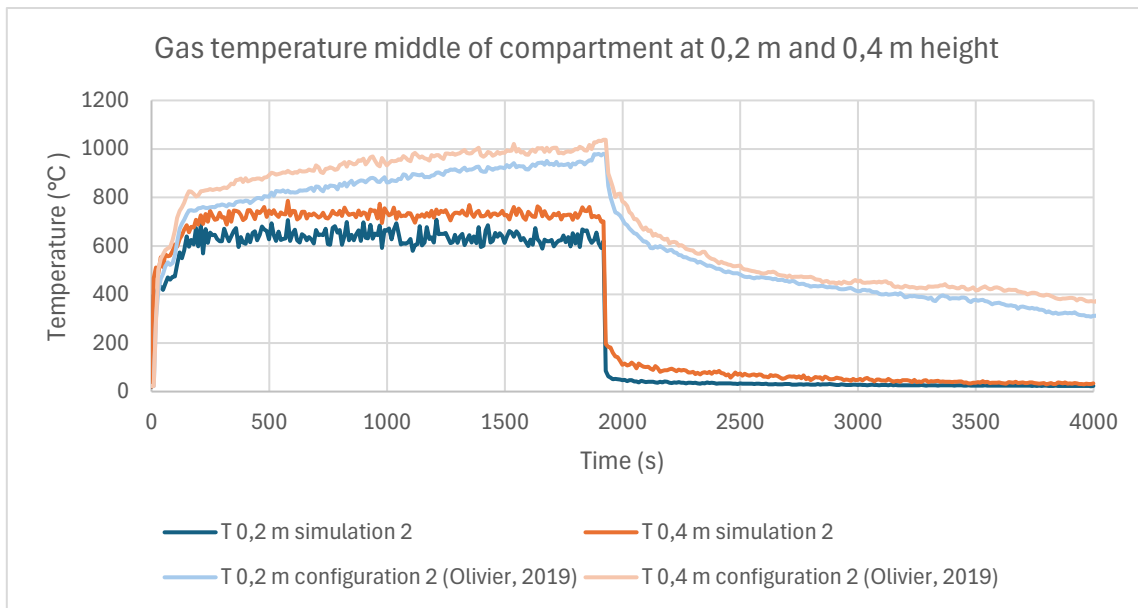


Figure 40: Simulation 2 gas temperature comparison first 4000 seconds

Table 19 provides an overview of the gas temperature differences in the middle of the compartment between simulation 2 and configuration 2 by Olivier (2019) in the heating phase. It can thus be concluded that simulation 2 underestimates the gas temperatures in the middle of the compartment.

Table 19: Quantification gas temperatures simulation 2 vs configuration 2 in heating phase

Temperature in the middle of the compartment	Simulation 2	Configuration 2 (Olivier, 2019)
Average temperature 0,2 m	625°C	842°C
Average temperature 0,4 m	717°C	914°C
Maximum temperature	787°C	1038°C
Average percentual difference simulation vs experiment at 0,2 m		-35%
Average percentual difference simulation vs experiment at 0,4 m		-27%

9.3 SIMULATION 3: CEILING EXPOSED

This section presents simulation 3 which replicates the experimental setup of configuration 4 by Olivier (2019) with an exposed ceiling (C). The importance of this simulation is found in assessing how the FDS works with a horizontally oriented combustible CLT surface. The observations during the simulation are presented with a focus on the HRR and gas temperature development within the compartment. The observed results are compared to the experimental results of configuration 4. A brief overview of simulation 3 is given in Table 20. A complete overview of the results is given in Appendix E.3.

Table 20: Overview simulation 3

Simulation 3	
Exposed CLT surface	Ceiling
Reference test setup	Configuration 4 (Olivier, 2019)
HRR burner	41 kW
Simulation length	4737 seconds
Time to turning burner off (heating phase)	1830 seconds
Simulation running time (with 20 meshes)	13 hours

9.3.1 Observations HRR

The simulated HRR development is given in Figure 41 in combination with the experimental result of configuration 4 by Olivier (2019). The output of the simulated gas burner is given to provide a clear visualisation of the contribution to the HRR of the burning CLT ceiling. The observations of the simulation are discussed stepwise in Table 21. Subsequently, the difference between the simulation and the reference experiment by Olivier (2019) is quantified.

Table 21: Observations HRR simulation 3

Step	Description simulation
1	At the start of the simulation the burner instantly reaches its full capacity at 41 kW.
2	After 100 seconds the first signs of ignition of the ceiling are observed. Ignition starts simultaneously in the far left and right corner from the compartment opening.
3	Gradual increase in HRR as more cells in the CLT ceiling reach the lower limit of the pyrolysis temperature range and start to release pyrolysis gases that combust in access of oxygen.
4	After 500 seconds the entire ceiling is in flaming combustion where the HRR levels out at 70 kW.
5	Subsequently, the HRR fluctuates around an average of 70 kW while reaching a peak of 73 kW after 700 seconds.
6	Followed by a period where the HRR decreases slightly due to less combustion occurring at the ceiling until the HRR reaches a lower limit of 66 kW after 1820 seconds.
7	The gas burner is turned off after 1830 seconds.
8	Once the burner is turned off, the HRR drops almost instantly to approximately 0 kW which indicates that the ceiling is considered to be extinguished after 1850 seconds.

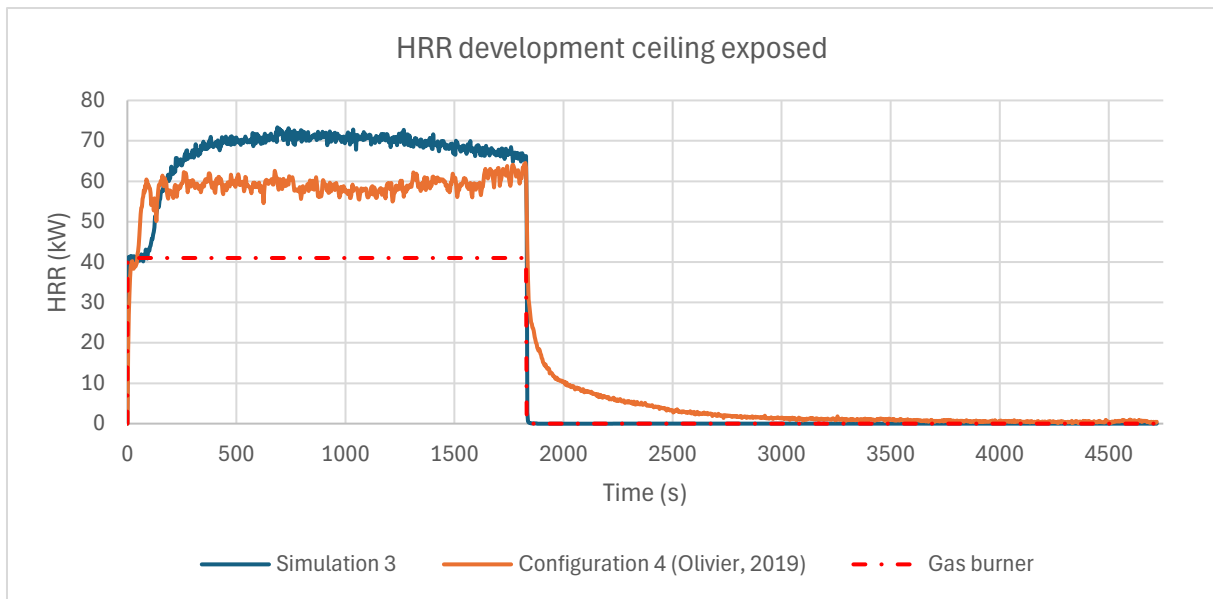


Figure 41: Simulation 3 HRR development

In Figure 41 it can be observed that for the first 160 seconds, the simulation approximates the experimental result adequately. Subsequently, the experimental HRR stagnates around 60 kW, while the simulated HRR increases further until it stagnates around 70 kW after 450 seconds.

Both graphs follow a similar trend during the heating phase, where the gas burner is turned on. Once the burner is turned off, the experimental HRR drops with 41 kW corresponding with the gas burner output and then shows a gradual decay phase. However, the simulated HRR drops instantaneously towards 0 kW, thus not showing a realistic gradual decay phase. This is further discussed in Chapter 10.1.1.

For quantifying the percentual difference between the simulated and experimental HRR, only the heating phase is considered to allow for a reasonable comparison. Table 22 provides an overview of the HRR difference between the simulation and configuration 4. It can thus be concluded that simulation 3 overestimates the HRR compared with configuration 4 by Olivier (2019).

Table 22: Quantification HRR simulation 3 vs experiment in heating phase

	Simulation 3	Configuration 4 (Olivier, 2019)
Average HRR in heating phase	67,0 kW	58,4 kW
Average HRR contribution of exposed CLT compared to the 41kW burner output	26 kW	17,4 kW
Average HRR increase compared to the 41kW burner output in heating phase	63%	42%
Maximum HRR	73,3 kW	64,5 kW

9.3.2 Observations temperature

This section presents the simulated compartment temperatures, compared with the experimentally measured gas temperatures by Olivier (2019). For this the gas temperature is compared in the middle of the compartment at both 0,2 m and 0,4 m height. Figure 42 present the gas temperature comparison for simulation 2 vs the experimental results for the full simulation length.

It can be observed that both at 0,2 m and 0,4 m height in the middle of the compartment the gas temperature is underestimated in the model. The initial temperature increase in the experiment is significantly underestimated in simulation 3. In general, during the heating phase the temperatures follow a similar trend in the simulation and the experiment. However, once the burner is turned off after 1830 seconds, the experiment shows a significantly more gradual decrease in compartment temperatures compared to the simulated temperatures. This is further discussed in Chapter 10.1.2.

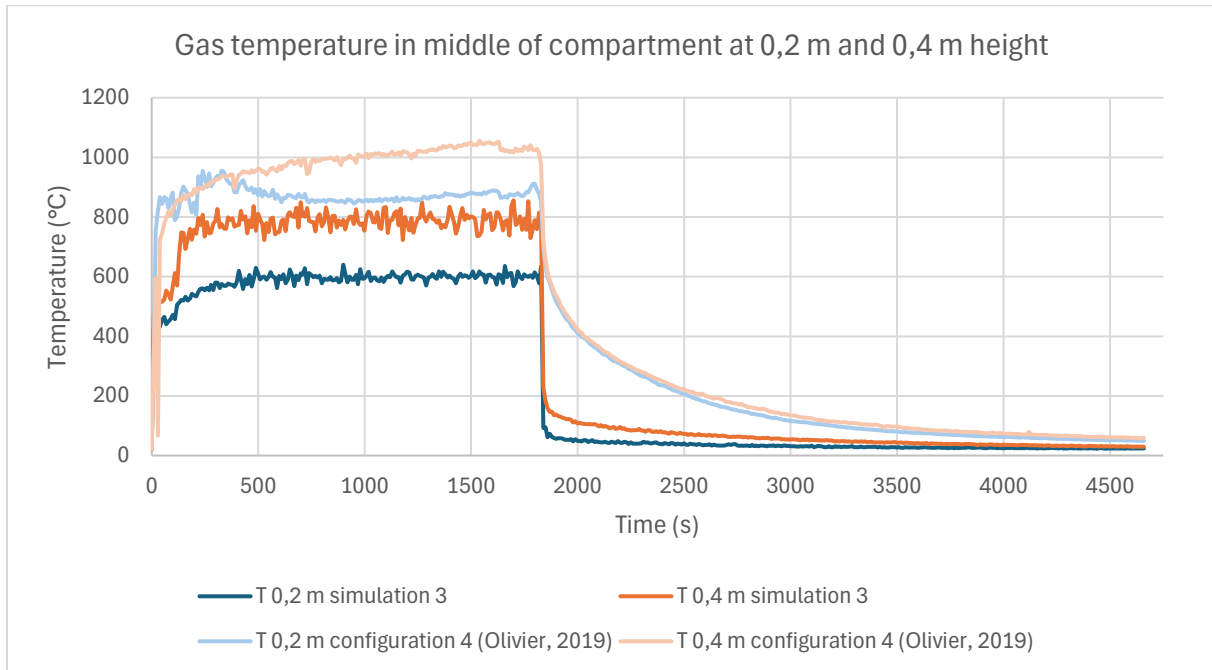


Figure 42: Simulation 3 gas temperature comparison

Table 23 provides an overview of the gas temperature differences in the middle of the compartment between simulation 3 and configuration 4 by Olivier (2019) in the heating phase. It can thus be concluded that simulation 3 underestimates the gas temperatures in the middle of the compartment.

Table 23: Quantification gas temperatures simulation 3 vs configuration 4 in heating phase

Temperature in the middle of the compartment	Simulation 3	Configuration 4 (Olivier, 2019)
Average temperature 0,2 m	582°C	869°C
Average temperature 0,4 m	767°C	969°C
Maximum temperature	856°C	1056°C
Average percentual difference simulation vs experiment at 0,2 m		-49%
Average percentual difference simulation vs experiment at 0,4 m		-26%

10 ANALYSIS

This chapter aims to combine the observations from the simulations presented in Chapter 9 to assess various important characteristics of the simulated compartment fire. Chapter 10.1 elaborates on the differences and similarities between the simulations and reference experiments regarding HRR and compartment temperatures.

Chapter 10.2 presents multiple sensitivity analyses to verify what input parameters highly affect the simulation results and to find the most fitting value for each parameter to match with the experimental result of configuration 3 by Olivier (2019).

10.1 COMPARISON SIMULATIONS AND EXPERIMENTS

10.1.1 HRR

This section combines the HRR observations from simulations 1, 2 and 3 as documented in Chapter 9. The goal of this section is to discuss the correspondence between the simulations and their reference experiments by Olivier (2019). Overarching trends, explaining similarities and differences, are analysed based on the simulated results to get a better understanding of the functionality of the FDS model for varying compartment configurations.

Table 24 provides a comprehensive overview of the burning behaviour of the exposed CLT for each simulation in the heating phase. To assess how well the FDS model approximates the burning behaviour, it is essential to only compare the additional HRR caused by the burning timber. In Table 24 it can be seen that the energy released by the exposed CLT is overestimated by approximately 50% for all simulations.

Subsequently, when comparing the burning rate between the simulations and the experiments, it can be noticed that the simulated burning rate is approximately a factor 2 higher. This burning rate is measured in the middle of the exposed surface, both in the simulation and the experiment. If the simulated burning rate would be uniform over the entire surface, it would mean that the HRR due to the burning wood should be overestimated with a factor 2 as well. However, as this is not the case, it means that in some parts of the exposed CLT surface the burning rate is significantly lower resulting from locally differing combustion conditions. Combustion conditions can differ based on gas temperature and oxygen concentration. For future research, it would be advisable to measure the burning rate at multiple locations in the exposed surface to get a better understanding of local differences.

By comparing simulation 1 and 2, it can be observed that doubling the area of exposed CLT results in doubling the energy released by the burning timber. This matches well with the experimentally obtained results. It was concluded by Olivier (2019) that the cross radiation between two opposing CLT panels results in a higher burning rate. In the simulations, the radiation between both exposed surfaces is thus considered adequately. Conclusively, based on the experimental results, extrapolating to a compartment with more exposed CLT can be done in the FDS model without resulting in significantly different fire dynamics within the compartment.

Table 24: HRR analysis simulation 1 – 3 in heating phase

	Simulation 1	Simulation 2	Simulation 3
Time to ignition	60 seconds	50 seconds	100 seconds
Average HRR simulation	64,3 kW	86,1 kW	67,0 kW
Average HRR reference experiment by Olivier (2019)	56,3 kW	72,5 kW	58,4 kW
Average simulated HRR contribution of exposed CLT compared to the 41kW burner output	23,3 kW	45,1 kW	26,0 kW
Average percentual difference of HRR contribution due to burning exposed CLT of simulation vs reference experiment by Olivier (2019)	+52%	+44%	+50%
Burning rate (middle of the exposed surface) simulation	1,15 mm/min	1,33 mm/min	1,32 mm/min
Burning rate reference experiment by Olivier (2019)	0,60 mm/min	0,63 mm/min	0,66 mm/min

Figure 43 visualises the HRR over time for all simulations and their reference experiment by Olivier (2019). The first thing to be noticed is the similarity between all simulations regarding the trend of the HRR development. Especially, when comparing simulation 1 and 3, there is little difference between a horizontally oriented surface (ceiling) and a vertically oriented surface (wall). The HRR is thus mostly influenced by the area of the exposed CLT.

In the initial growth phase of the fire, all simulations approximate the experimentally obtained burning behaviour well. Subsequently, in all simulations the HRR keeps rising for a longer time before stagnating at a relatively constant value. In the experiments a similar trend can be observed, although stagnating earlier at a lower HRR.

The decay phase is where all simulations show an identical fire behaviour, which is where the main problem of the FDS model occurs. As soon as the gas burner is turned off, the HRR drops almost instantly to 0 kW, while the experimental results show a gradual decrease in HRR eventually changing from flaming to smouldering combustion. The hypothesis for the immediate decrease in HRR is that the conditions for pyrolysis are no longer met once the energy supply from the gas burner stops. To check this hypothesis, the gas temperatures are analysed within the compartment which is presented in Chapter 10.1.2.

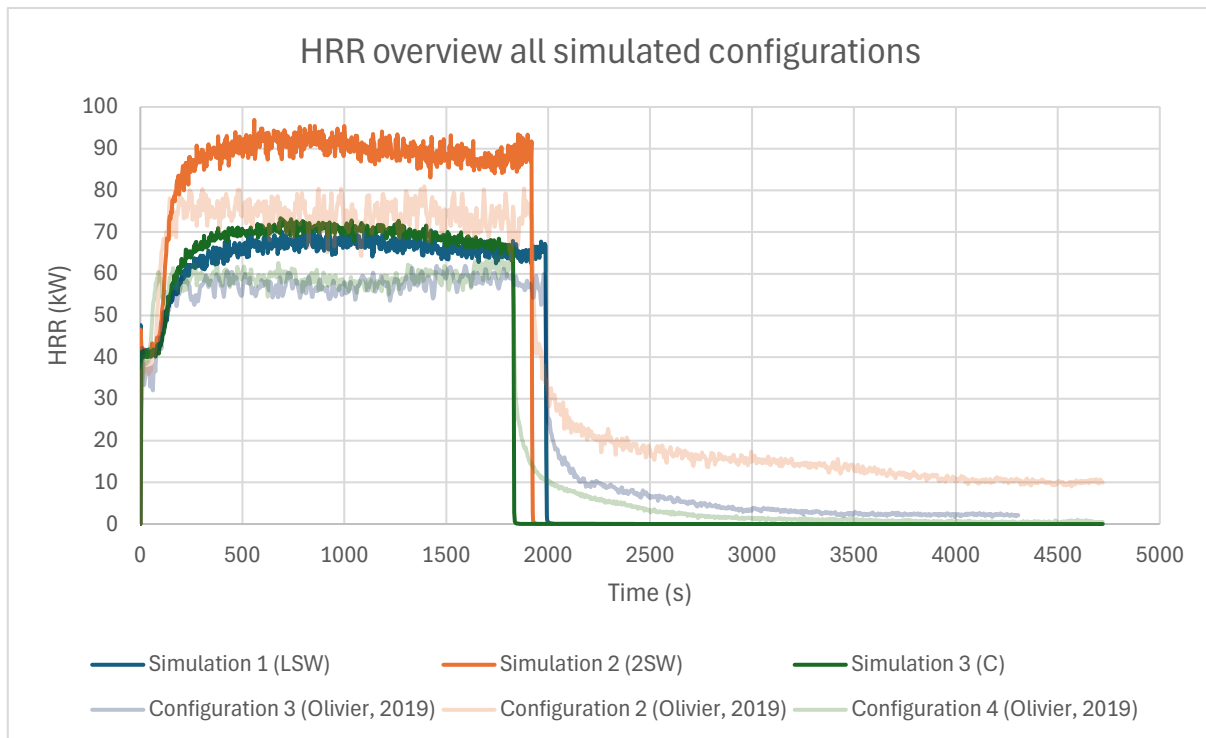


Figure 43: HRR overview simulations 1 – 3

In this section it was concluded that the additional HRR due to burning timber is overestimated by approximately 50% for all simulations. The overestimated energy release by the exposed CLT is directly linked to the heat of combustion that is assigned to wood in the FDS model. An effective heat of combustion of 10 MJ/kg is used as input, which is lower than the commonly assumed values between 16 – 20 MJ/kg. This is done to account for incomplete combustion that occurs in real-life experiments. For further elaboration on the modelling process of the heat of combustion, Chapter 10.2.2 can be consulted.

In the growth phase of the fire the model approximates the HRR well, which means that the initial heating of the exposed CLT is simulated adequately. However, at some point the FDS model starts to overestimate the pyrolysis reaction, which results in an overestimation of the HRR. A possible reason for this is that in experiments the char layer limits the pyrolysis speed at a certain point, which is not adequately imitated in the FDS model by replacing the char layer with an effective heat of combustion. The modelling process, resulting in the exclusion of the char layer, is documented extensively in Appendix G.

10.1.2 Compartment temperatures

This section combines the gas temperature observations from simulations 1, 2 and 3 as documented in Chapter 9. The goal of this section is to discuss the correspondence between the simulations and their reference experiments by Olivier (2019). Overarching trends, explaining similarities and differences, are analysed based on the simulated results to get a better understanding of the functionality of the FDS model for varying compartment configurations.

The simulated thermocouples, measuring the temperature within the CLT wall at various depths, are not discussed here. The reason for this is the poor simulated results which is caused by placing the thermocouples at a fixed distance from the fire-exposed side of the wall. Therefore, as the wall burns

away at a certain rate, the thermocouples move along at the same speed. This can be fixed by placing the thermocouples at a fixed distance from the back side of the wall. The simulated thermocouples can be found in Appendix E.

Table 25 presents an overview of the gas temperatures in the heating phase, measured in the middle of the compartment at 0,2 m and 0,4 m height. For each simulation, a comparison is given with the corresponding experiment by Olivier (2019). In all simulations the gas temperature is underestimated by approximately 30%. Only in simulation 3, with an exposed ceiling, the difference is 49% at 0,2 m height. The horizontal orientation could be a reason for a poorly approximated heat transfer from the burning ceiling to the compartment gas. The heat most likely remains near the ceiling in the simulation, which underestimates the heat flow at lower heights.

FDS calculates the gas temperature for each cell within the 3-dimensional mesh, which means that local differences can affect the mathematics resulting in the simulation results. Figure 44 shows a top view of simulation 1 halfway the simulation, presenting the gas temperature over a 2-dimensional field at 0,2 m height. It can be observed that the temperature distribution is far from uniform with higher temperatures near the left side wall and in the corners of the compartment. Nonetheless, the general trend is a significant underestimation of the temperature development due to the gas burner and the burning CLT.

Table 25: Gas temperature analysis simulation 1 - 3 in heating phase

	Simulation 1	Simulation 2	Simulation 3
Average simulated temperature at 0,2 m height	581°C	625°C	582°C
Average temperature at 0,2 m height reference experiment (Olivier, 2019)	747°C	842°C	869°C
Average simulated temperature at 0,4 m height	688°C	786°C	767°C
Average temperature at 0,4 m height reference experiment (Olivier, 2019)	930°C	914°C	969°C
Maximum temperature simulation	769°C	1056°C	856°C
Maximum temperature reference experiment (Olivier, 2019)	1008°C	1038°C	1056°C
Average percentual difference simulation vs reference experiment (Olivier, 2019) at 0,2 m	-29%	-35%	-49%
Average percentual difference simulation vs reference experiment (Olivier, 2019) at 0,4 m	-35%	-27%	-26%

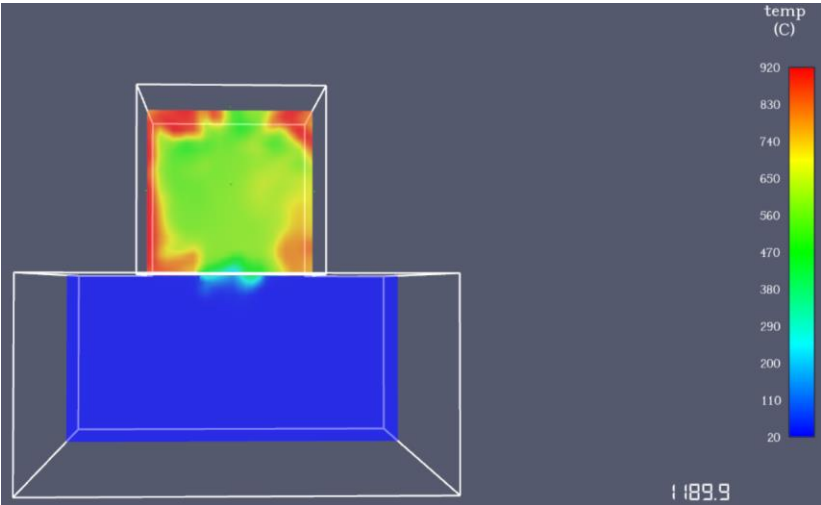


Figure 44: Top view compartment gas temperature slice at 0,2 m height simulation 1

As briefly discussed in Chapter 10.1.1, the decay phase of the fire remains a large point of attention in the FDS model. Figure 45 presents the gas temperature in the middle of the compartment at 0,4 m height for all simulations and their reference experiment. From this graph it can be concluded that the simulated gas temperature drops immediately to approximately 200°C, before gradually decreasing back to ambient conditions. This means that, as soon as the gas burner is turned off, the gas temperature drops below the pyrolysis range of 200 - 400°C. Once pyrolysis stops, the combustion of the pyrolysis gases also quickly stops. Therefore, the exposed CLT can be regarded as extinguished once the gas burner is turned off. In the experiments by Olivier (2019) a significantly more gradual decay phase can be observed, with temperatures remaining above 200°C for a long time.

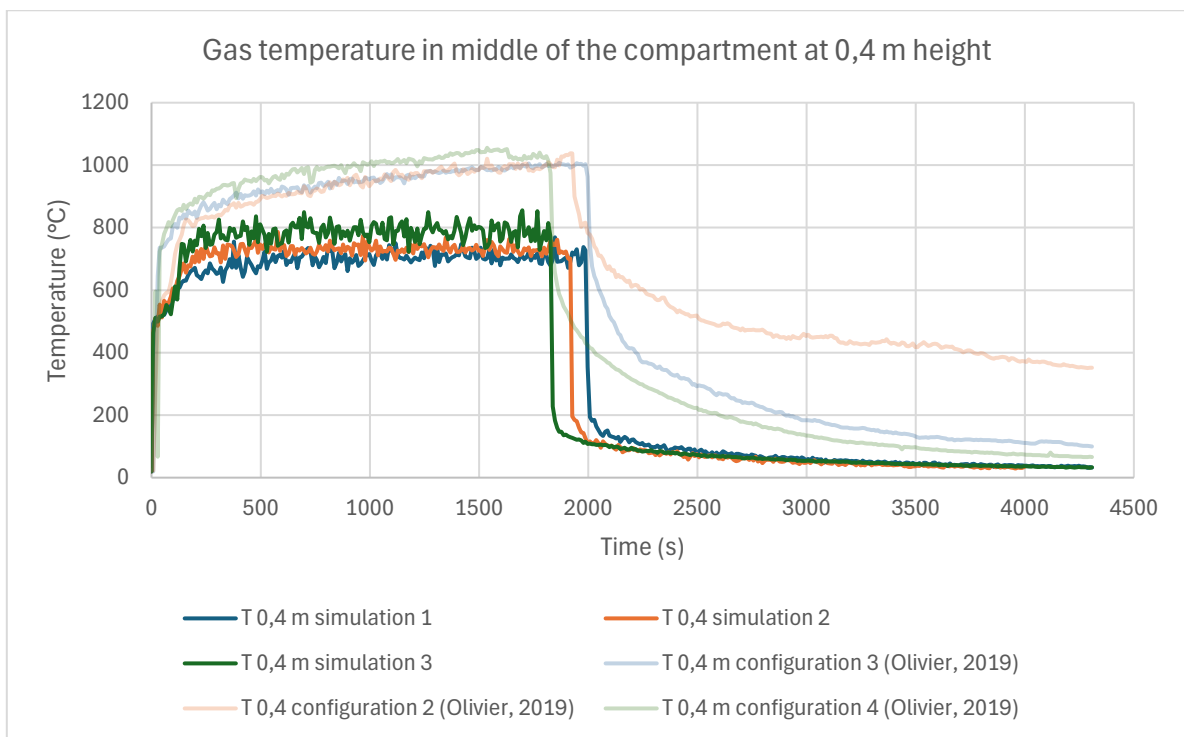


Figure 45: Analysis gas temperature simulation 1 - 3 at 0,4 m height

The next step is to find out why the gas temperature drops, causing the pyrolysis to stop. The availability of sufficient oxygen is required for sustaining the combustion process. It was decided to measure the oxygen concentration over a 2-dimensional plane. Figure 46 presents the oxygen concentration in simulation 1 with the time in the lower right corner, right before and after turning the gas burner off (at 1990 seconds). In the left image it can be seen that outside the compartment and near the compartment opening the oxygen concentration corresponds to ambient conditions of 20%, meaning an oxygen fraction of 0,2 in the air. Within the compartment the oxygen concentration is significantly lower, especially near the burning exposed left side wall.

The right image shows the oxygen concentration right after turning the burner off, which shows that the oxygen fraction goes back to ambient conditions within seconds. This corresponds with the HRR observation in Chapter 10.1.1 that combustion stops instantly once the energy supply of the gas burner stops. The fact that the oxygen concentration goes back to ambient conditions so quickly suggests a fast inflow of ambient air. This cold ambient air enters the compartment and then pushes the hot gases out of the compartment opening. This explains the steep decrease in gas temperatures.

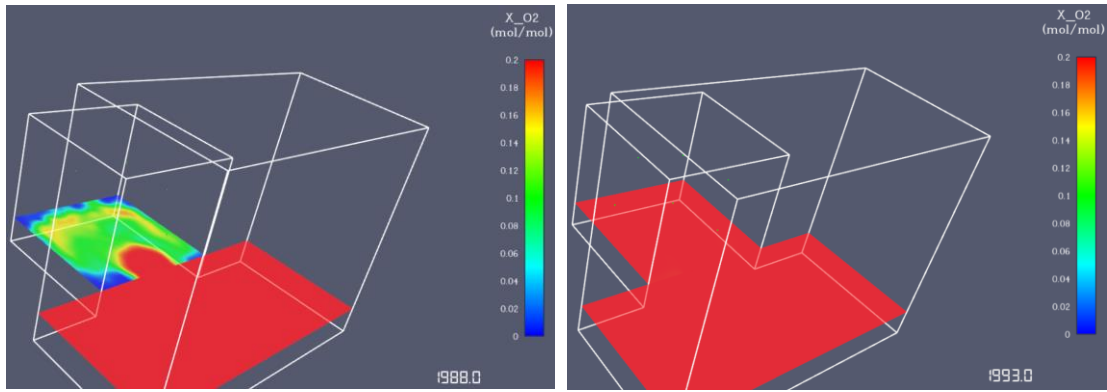


Figure 46: Compartment oxygen concentration right before and after turning the gas burner off

Conclusively, in the FDS model the burning of exposed CLT surfaces cannot be sustained without the presence of an external heat source. Additionally, the compartment temperatures are significantly underestimated while on the other hand the HRR is overestimated. Therefore, there is a trade-off between adequately validating the HRR or the gas temperature.

10.2 SENSITIVITY ANALYSIS

This section provides a sensitivity analysis for multiple input parameters in the FDS model. The goal of the sensitivity analyses is to assess which parameters significantly influence simulation results by comparing multiple values for each parameter. For the sensitivity analyses, the simulation results are compared with the experimental results by Olivier (2019) for a specific test configuration:

EXPERIMENTAL SETUP FOR SENSITIVITY ANALYSES: CONFIGURATION 3 = LEFT SIDE WALL EXPOSED

The HRR and gas temperatures are used as quantity for comparing various simulation setups. For the sensitivity analysis, only the heating phase is considered where the burner is turned on to clearly visualise the differences between parameter values. The percentual difference between the reference experiment and the simulations is used as a tool for quantifying the sensitivity of various input parameters on the simulation results.

Table 26 provides an overview of the assessed parameters and their default values. Each subsection discusses a varying parameter, while the other parameters are kept at their default values.

Table 26: Default values FDS model before sensitivity analysis

Section	Parameter	Default value
10.2.1	Mesh size	20 mm cubical cells
10.2.2	Heat of combustion	10 MJ/kg
10.2.3	Wood moisture content	12%
10.2.4	Ventilation factor	0,042 m ^{0,5}

10.2.1 Mesh size

The cell size within the 3-dimensional mesh is an important factor in FDS models according to the literature presented in Chapter 7.3. Within an FDS model, the goal is to reduce the cell size until simulation results no longer significantly vary. To achieve this, three cubical cell sizes are used of 20 mm, 10 mm and 5 mm. It is important to note that the simulation with 5 mm cubical cells only ran for 400 seconds. This is due to the fact that this simulation was already running over 50 hours at this point. For practical reasons it was decided to stop the simulation at this point and compare with the 10 mm and 20 mm simulations. The results of the three simulations in the heating phase compared with the experimental result are plotted in Figure 47.

It can be seen that all three simulations follow the same HRR and gas temperature trend. Table 27 presents an overview of the simulated results in the first 400 seconds to provide a clear comparison between the simulations with a varying mesh cell size. It can thus be concluded that the reduction in cell size does not result in further refinement of the simulated HRR and gas temperatures. Therefore, it is advised to continue with the 20 mm cell size to minimise the computing time of simulations.

Conclusively, 20 mm cubical cells provide adequate simulation results. Further refinement of the mesh does not notably influence simulation. The required simulation time is minimised to the best extent possible by choosing the largest adequate mesh cell size.

Table 27: Results mesh size sensitivity analysis first 400 seconds

	Simulation 5 mm mesh	Simulation 10 mm mesh	Simulation 20 mm mesh	Configuration 3 (Olivier, 2019)
Average HRR in heating phase	56,7 kW	56,2 kW	55,1 kW	50,7 kW
Average T at 0,2 m in middle of compartment	547	539	521	598
Average T at 0,4 m in middle of compartment	643	613	625	804

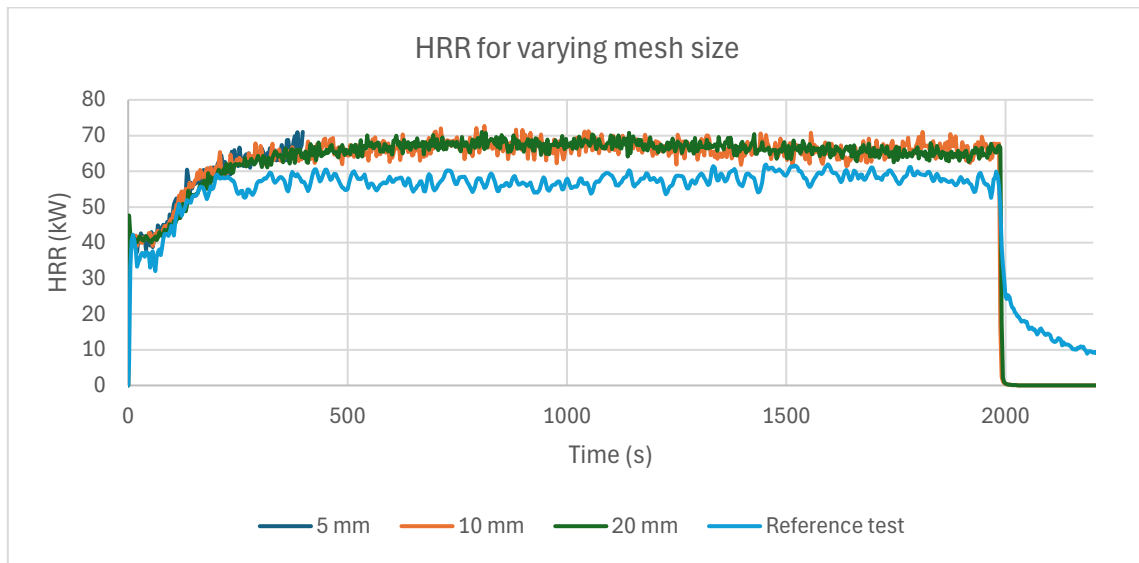


Figure 47: HRR for varying mesh cell size in heating phase

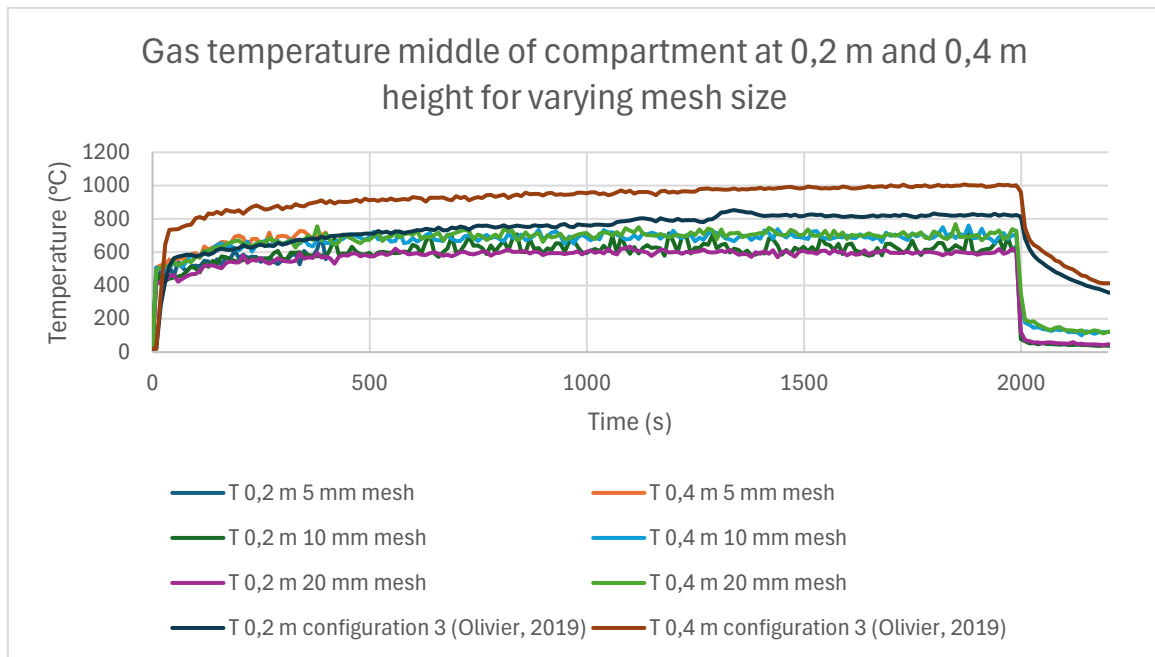


Figure 48: Gas temperatures for varying mesh cell size in heating phase

10.2.2 Heat of combustion

The heat of combustion of wood is a crucial input parameter in FDS for accurately assessing the additional heat release due to burning timber in a compartment fire. This subsection presents the simulation results for heat of combustion values varying between 7,5-20 MJ/kg. The goal of this sensitivity analysis is to determine the most fitting heat of combustion value which fits with the experimental results of configuration 3 by Olivier (2019) with an exposed left side wall.

Table 28 provides an overview of the simulated HRR and gas temperatures in the heating phase for the simulations with varying heat of combustion. In line with the expectations, a higher heat of combustion results in more energy being released in the compartment. Additionally, the percentual increase in HRR is given due to the burning timber. From this it can be concluded that in the 7,5 MJ/kg simulation the CLT wall ignites very slowly and limited as the HRR barely increases above the gas burner output of 41 kW. From the 10 MJ/kg simulation onwards, it can be noticed that the contribution of the burning CLT is significant.

Based on the average HRR, the simulation with a heat of combustion of 10 MJ/kg fits best with the experimental result of configuration 3 by Olivier (2019). However, the gas temperatures in the middle of the compartment are underestimated significantly.

Based on the average gas temperatures in the middle of the compartment, the simulation with a heat of combustion of 20 MJ/kg fits best with the experimental result of configuration 3 by Olivier (2019). However, the HRR is severely overestimated in this simulation. Therefore, a trade-off needs to be made between approximating the HRR or gas temperatures in an adequate manner. The HRR is chosen as main criterium because the gas temperatures are sensitive to local differences while the energy release is calculated for the entire compartment.

Table 28: Results heat of combustion sensitivity analysis heating phase

	7,5 MJ/kg	10 MJ/kg	12,5 MJ/kg	15 MJ/kg	17,5 MJ/kg	20 MJ/kg	Configuration 3 (Olivier, 2019)
Average HRR	42 kW	64 kW	80 kW	100 kW	121 kW	143 kW	56 kW
Average heating phase HRR increase compared to the 41kW burner output	2,9%	57%	94%	143%	195%	248%	37%
Average T at 0,2 m in middle of compartment	357°C	581°C	612°C	644°C	676°C	756°C	747°C
Average T at 0,4 m in middle of compartment	399°C	688°C	728°C	785°C	847°C	902°C	931°C

Figure 49 visualises the simulated HRR results. The experimental result of configuration 3 by Olivier (2019) is plotted and the burner output of 41 kW is visualised to clearly identify the contribution of the exposed CLT to the HRR. Except from the 7,5 MJ/kg simulation, all simulations follow a similar HRR trend during the largest part of the heating phase. Once the gas burner is turned off, the HRR of the simulations drops quickly to 0 kW except for the 17,5 MJ/kg simulation.

Initially, once the gas burner is turned off, the HRR drops to 0 kW for a short period of time in the 17,5 MJ/kg simulation before a steep increase reaching 80 kW. Subsequently, the HRR starts to decrease again until reaching 0 kW after 2200 seconds. A similar period of regrowth is not observed in any of the

other simulations which makes it difficult to explain the reasoning behind the simulated result. The observed HRR means that the burning of the CLT wall increases again once the burner is turned off. At the point of turning the burner off, the HRR is the highest for the 17,5 MJ/kg simulation. This could imply that the timber is burning at a sufficiently high rate such that the flaming can be sustained for a short period of time even without the energy emitted by the gas burner. Although, it would be more logical if the HRR would then gradually decrease instead of the regrowth phase that is now observed.

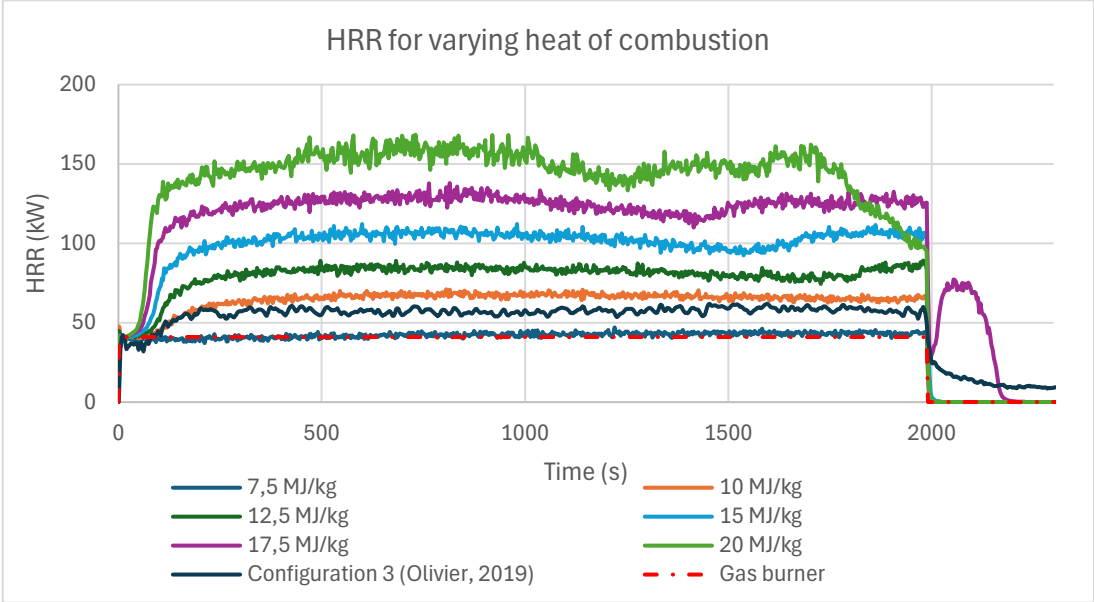


Figure 49: HRR for varying heat of combustion in heating phase

During the heating phase, it can be noticed that the HRR in the 20 MJ/kg simulation gradually decreases from 1700 seconds onwards before dropping to 0 kW once the gas burner is turned off. After an extensive analysis of the results for this simulation, it was concluded that this decrease in HRR is caused by the partly burn through of the exposed CLT wall. The burn rate of the wall is at a level that the timber burns away within the heating phase. Subsequently, it was decided to analyse the burning rate in the other simulations as well to check if the same problem occurs.

Figure 50 visualises the decrease in wall thickness over time, which is measured in the middle of the wall. It can be observed that the wall burns through in the middle of the wall in the 17,5 and 20 MJ/kg simulations. Table 29 provides an overview of the burning rate in the middle of the exposed left side wall with the time to burn through mentioned if relevant. The charring rate as measured in configuration 3 by Olivier (2019) is also given for reference. It can thus be concluded that the burning rate of the modelled timber is significantly overestimated compared to the experimentally measured charring rate. This goes hand in hand with the overestimation of the HRR, as this is approximately linearly related to the amount of timber that is combusting.

Table 29: Overview burning rate for varying heat of combustion in heating phase

	Burning rate	Time to burn through
Simulation 7,5 MJ/kg	0,15 mm/min	/
Simulation 10 MJ/kg	1,15 mm/min	/
Simulation 12,5 MJ/kg	1,69 mm/min	/
Simulation 15 MJ/kg	2,33 mm/min	/
Simulation 17,5 MJ/kg	2,87 mm/min	2088 seconds
Simulation 20 MJ/kg	3,54 mm/min	1696 seconds
Configuration 3 (Olivier, 2019)	0,61 mm/min	/

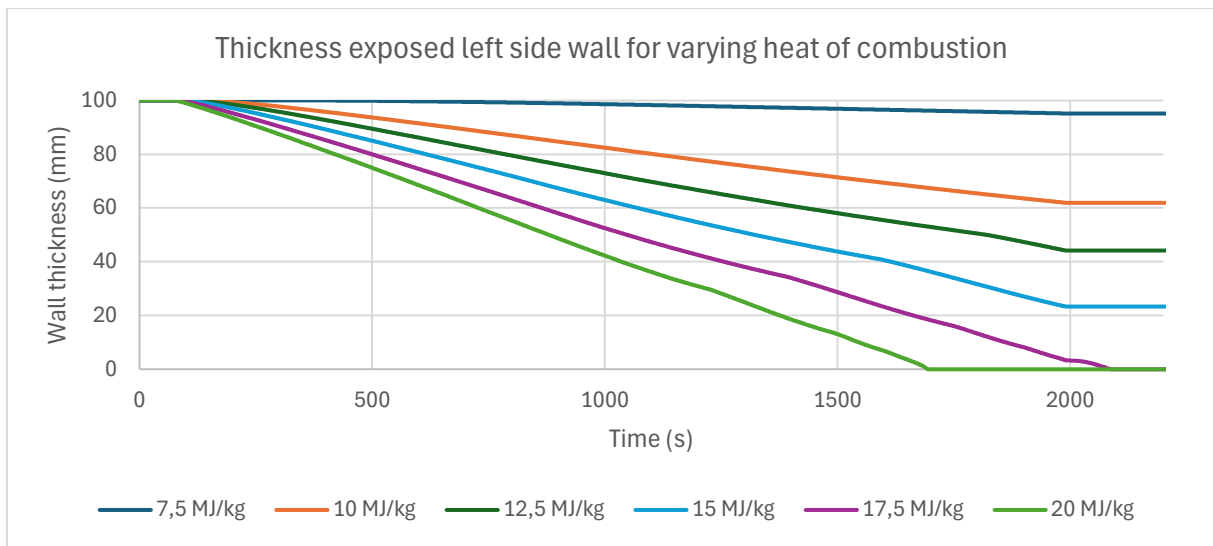


Figure 50: Thickness exposed CLT wall over time for varying heat of combustion

Conclusively, the heat of combustion value of 10 MJ/kg is chosen for the final FDS model as this approximates the energy release in the best manner, although still overestimating the burning rate of the exposed CLT. The underestimation of the gas temperature can be dealt with by using a heat of combustion value of 20 MJ/kg, but this comes with a significant overestimation of the burning behaviour of timber and thus a poorly matching HRR.

In the literature presented in Chapter 7.3, heat of combustion values between 10 – 15 MJ/kg are commonly used as input in FDS models. The chosen value of 10 MJ/kg is therefore in accordance with the limited available literature.

10.2.3 Wood moisture content

The moisture content (MC) of the CLT surfaces in the FDS model is fixed at 12%, in correspondence with the samples used by Olivier (2019) in the reference experiments. However, it is interesting to assess the influence of the moisture content on simulation results to investigate extrapolation possibilities of the FDS model to other test setups. The moisture content is difficult to control in practice and therefore a low sensitivity to the moisture content would be desirable. Therefore, three simulations are performed with varying moisture content (4%, 8% and 12%). The HRR results in the heating phase are plotted in Figure 51.

Based on the results shown in Table 30, Figure 51 and Figure 52, it can be concluded that the moisture content of the CLT surfaces has very limited influence on the simulation results. Slightly higher HRR values and similar gas temperatures are recorded with a lower moisture content but the shape of the HRR graphs remains the same. This is in accordance with the findings of Dai et al. (2022). The moisture is quickly evaporated in the model when reaching 100°C in the CLT wall. Therefore, small differences can potentially be observed in the temperature development through the cross section of the CLT wall at the start of the simulation as more energy is required to increase the temperature of surfaces with a higher moisture content.

Table 30: Results moisture content sensitivity analysis heating phase

	4% MC	8% MC	12% MC	Configuration 3 (Olivier, 2019)
Average HRR	66,8 kW	65,5 kW	64,3 kW	56,3 kW
Average T at 0,2 m in middle of compartment	582°C	579°C	581°C	747°C
Average T at 0,4 m in middle of compartment	687°C	686°C	688°C	931°C

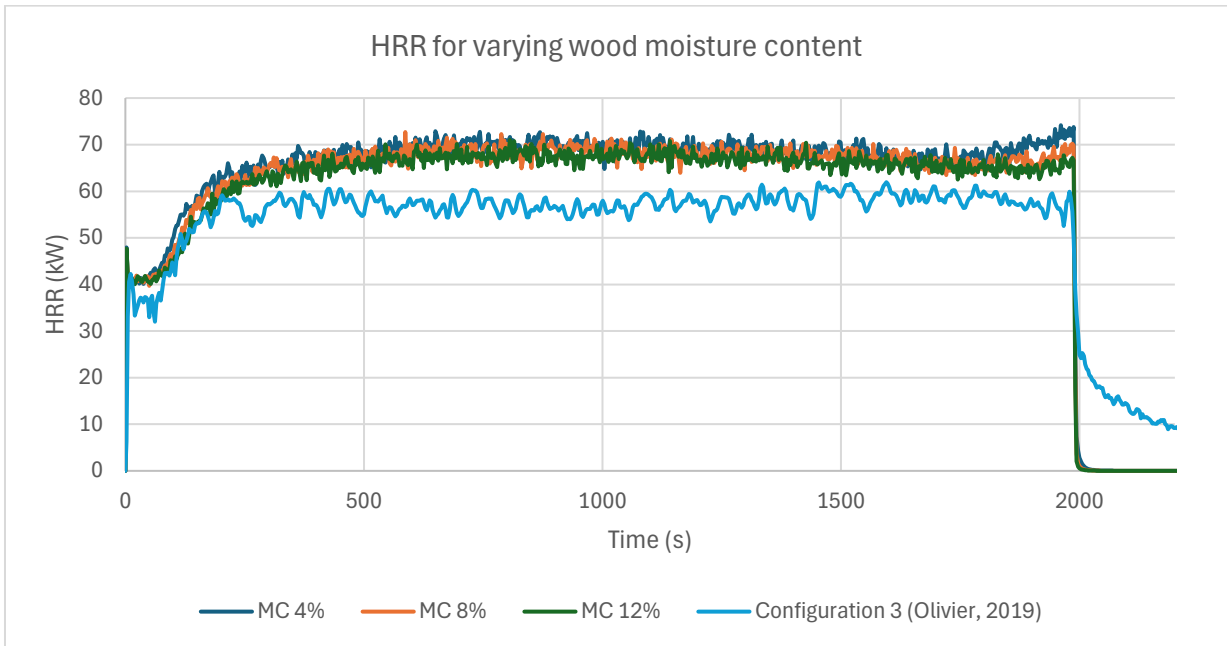


Figure 51: HRR for varying wood moisture content in heating phase

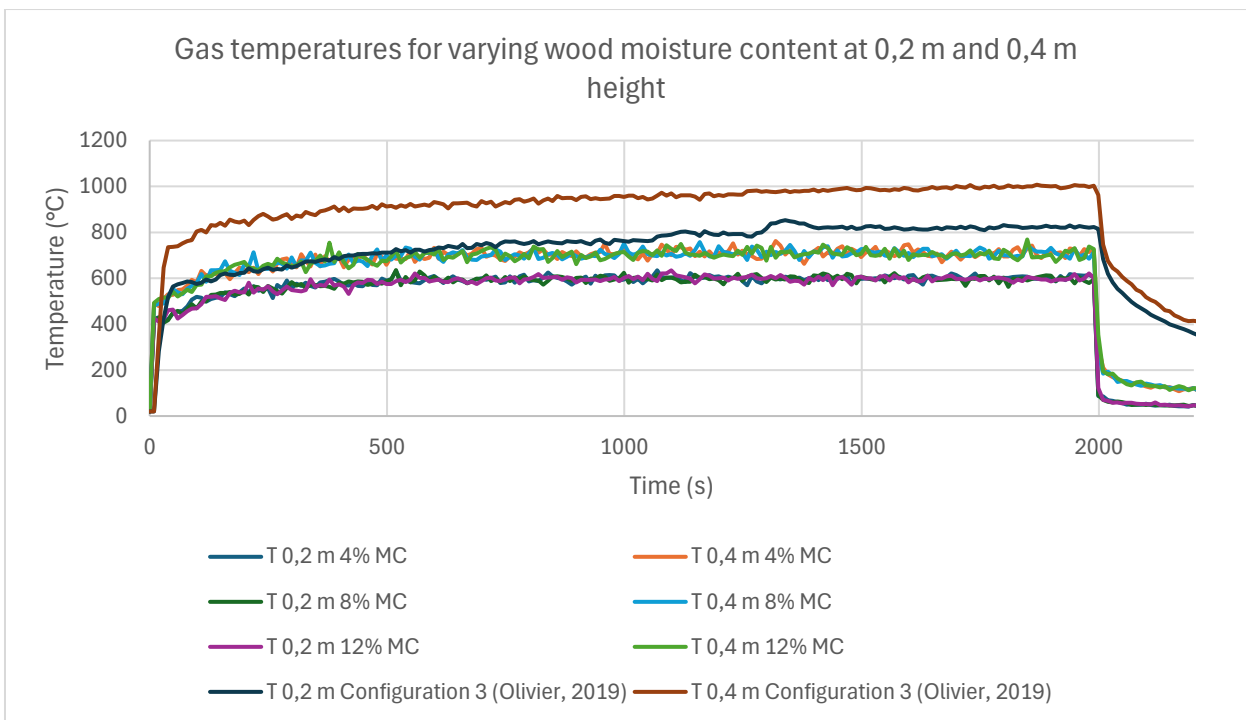


Figure 52: Gas temperatures for varying wood moisture content in heating phase

10.2.4 Ventilation factor

This section discusses the influence of the ventilation factor on the simulated compartment fire dynamics in FDS. Hereby, the extrapolation possibilities of the FDS model are investigated for compartments with different ventilation conditions. For this analysis, three varying ventilation factors are considered which are calculated based on Equation (3). The default opening, corresponding to the experimental setup by Olivier (2019), is 0,18 m x 0,50 m (WxH) which results in a ventilation factor of 0,042 m^{1/2}. Subsequently, a simulation is performed with an opening of 0,36 m x 0,50 m (WxH) which results in a ventilation factor of 0,085 m^{1/2}. The goal of this simulation is to allow for an abundant inflow of oxygen into the compartment to satisfy the required combustion conditions. Lastly, a simulation is performed with an opening of 0,18 m x 0,25 m (WxH) which results in a ventilation factor of 0,015 m^{1/2}. The goal of this simulation is to assess the influence of reduced oxygen inflow on the burning behaviour of exposed CLT. All three configurations are depicted in Figure 53 with an increasing ventilation factor from left to right.

$$\text{Ventilation factor} = \frac{A_0 \sqrt{H_0}}{A_l}$$

(3)

- A_0 = area of the opening [m²]
- H_0 = height of the opening [m]
- A_l = total internal compartment surface area [m²]

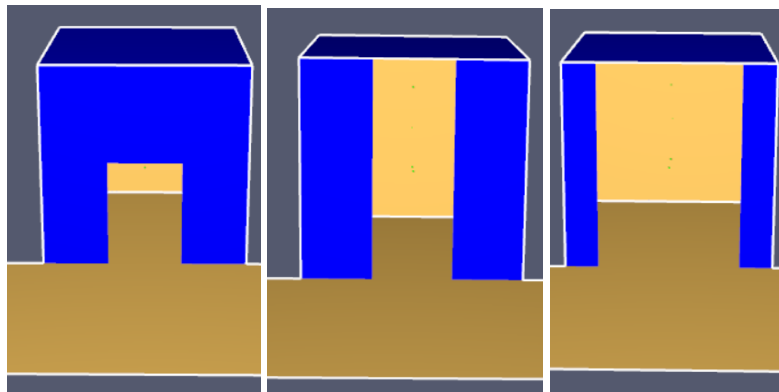


Figure 53: Compartment configurations with varying ventilation factor

Table 31 summarises the results of all three above-mentioned simulations. In Figure 54 it can be observed that a larger ventilation opening results in a slower growth phase of the fire. This can be attributed to the increased inflow of cold ambient air. Eventually, this simulation reaches a similar HRR as the default simulation but requiring a longer time for the exposed left side wall to fully ignite.

The simulation with a smaller ventilation factor depicts a heavily fluctuating HRR. On average, the HRR equals to the gas burner output. It is remarkable that lower HRR values than the burner output of 41 kW are simulated. This means that the gas burner is restrained by the availability of oxygen in the compartment. The fluctuating HRR can be attributed to the combustion conditions within the compartment. When analysing Figure 55, it is noticed that it takes a considerable amount of time for gas temperatures to increase in this simulation. This means that pyrolysis is going slower compared to the other two simulations. Subsequently, the dependency on oxygen concentration within the compartment results in an inconsistent burning behaviour of the exposed CLT. In some locations there is sufficient oxygen available for the combustion reaction to persist, while other locations may not reach

the required combustion conditions. This means that pyrolysis gases are released without combusting which can lead to dangerous phenomena in real-life.

The gas temperatures in Figure 55 show that a larger ventilation factor results in lower temperatures which is in line with expectations due to the inflow of cold ambient air. Compared with the other simulations, the smaller ventilation factor results in a significantly more gradual temperature decay at 0,4 m height. This can be explained by the fact that in this particular simulation the opening is only 0,25 m in height, meaning that hot air is trapped above the opening. At 0,2 m height the temperature decay is similar for all simulations, which thus supports the conclusion that the height of the opening is an important factor for the decay phase.

Table 31: Results ventilation factor sensitivity analysis heating phase

	2x smaller	Default	2x bigger	Configuration 3 (Olivier, 2019)
Ventilation factor	0,015 m ^{1/2}	0,042 m ^{1/2}	0,085 m ^{1/2}	0,042 m ^{1/2}
Average HRR	40,0 kW	64,3 kW	60,9 kW	56,3 kW
Average T at 0,2 m in middle of compartment	402°C	581°C	315°C	747°C
Average T at 0,4 m in middle of compartment	398°C	688°C	471°C	931°C

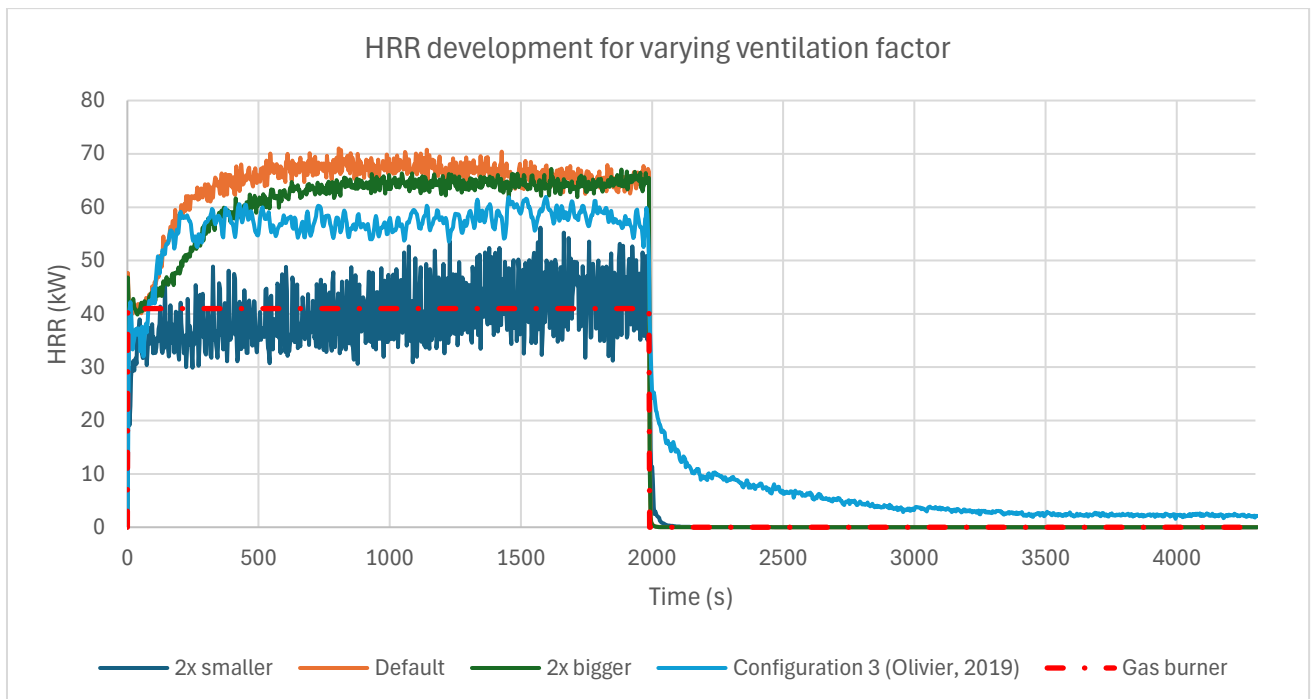


Figure 54: HRR development for varying ventilation factor

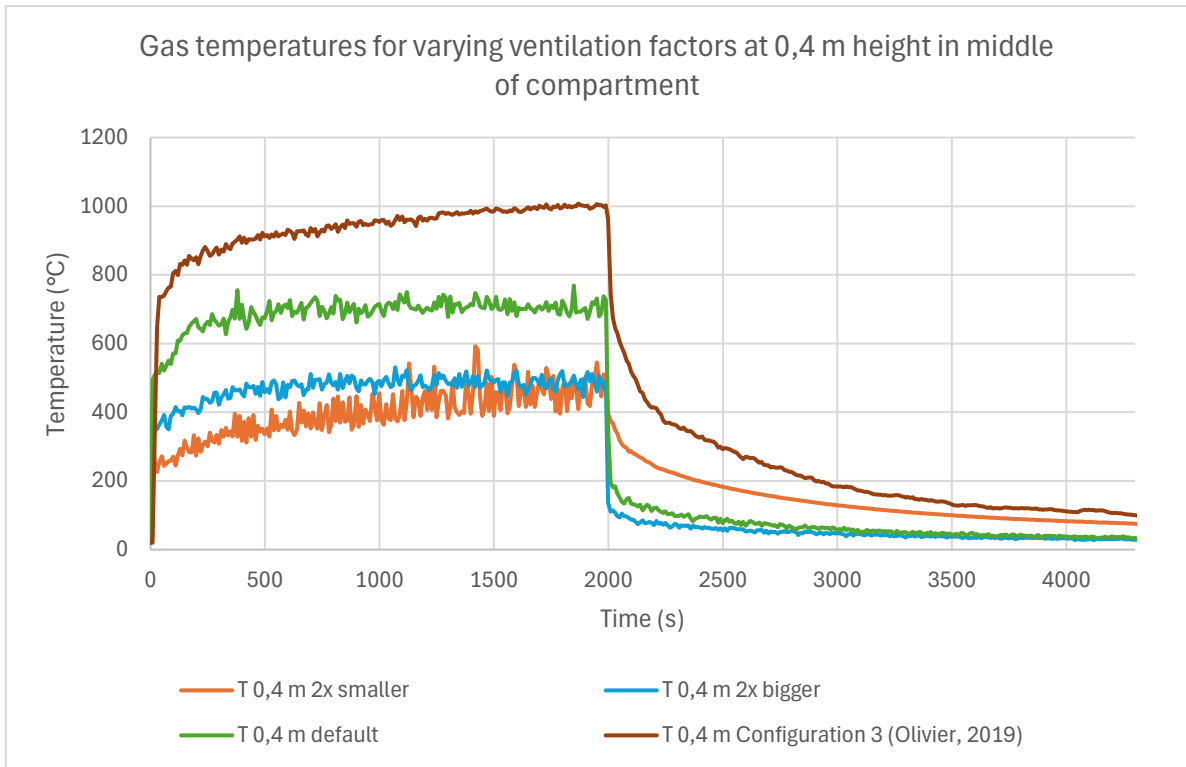


Figure 55: Gas temperatures for varying ventilation factor

Conclusively, the ventilation factor significantly influences the simulated HRR and gas temperatures in the FDS model. Small ventilation factors result in a high dependency of the available oxygen, resulting in a heavily fluctuating HRR. Large ventilation factors result in a slower growth phase but eventually reaching full ignition of the exposed CLT. Therefore, the interaction between the interior compartment and the ambient surrounding air is crucial for reaching the right pyrolysis and combustion conditions for the exposed CLT. This highlights the importance of modelling an exterior volume outside the compartment to simulate realistic gas flows.

PART 4: PRACTICAL APPLICATION

After extensively analysing the presented FDS model in previous chapters, the practical applications for engineers are explored. The ultimate goal is to be able to use the FDS model to obtain quick insights into the fire dynamics within a CLT compartment without having the need for large-scale experiments.

- CHAPTER 11: MODELLING IMPLEMENTATION IN PRACTICE
 - Chapter 11.1: Charring rate from model to practice
 - Chapter 11.2: Extrapolation model to larger compartment
 - Chapter 11.3: Conclusion

11 MODELLING IMPLEMENTATION IN PRACTICE

This chapter aims to explore the practical applications of the FDS model which is extensively discussed in previous chapters. The following analyses assess to what extent FDS can be a useful tool for engineers to use in practice for predicting the fire dynamics within a CLT compartment. Chapter 11.1 determines the charring depth based on the simulated temperature development in FDS. Chapter 11.2 discusses the extrapolation possibility of the FDS model to larger compartment geometries.

11.1 CHARRING RATE FROM MODEL TO PRACTICE

This section assesses the charring development over time based on the simulated gas temperatures in the FDS model. To achieve this, a newly proposed formula from prEN 1995-1-2 (EC5) is used as discussed in Chapter 4.1.3.3 and presented in Equation (2). This formula allows for estimating the charring depth based on the locally measured gas temperatures in the FDS model. This way the FDS model can be a useful tool for structural engineers and fire safety specialists to gain quick insights into the charring behaviour for varying fire scenarios. As of now there is little knowledge of the additional fire load due to exposed CLT surfaces. The impact of the additional fire load should be considered when estimating a representative charring rate for structural calculations. Henceforth, it is important to assess to what extent the presented FDS model can contribute to bridging this knowledge gap.

This section emphasises the advantage of CFD software like FDS due to its ability to calculate local temperatures, while other software such as two-zone models only allow for average compartment temperatures. Equation (2) calculates the charring depth based on the gas temperature right above the surface of the burning timber. This formula follows from the research by Werther (2015) who recommended to apply the formula in cases where wood is only exposed to a fire from one side. Additionally, the charring depth should be calculated over the entire burning phase of wood, thus including the growth and decay phase.

$$d_{char} = \left(\frac{\int_0^t T^2 dt}{1,35 * 10^5} \right)^{\frac{1}{1,6}} \quad (2)$$

- d_{char} = charring depth [mm]
- T = gas temperature right above the exposed surface [Kelvin]
- t = time [minutes]

First of all, it is important to analyse the development of the required simulated gas temperature. For this analysis, simulation 1 and 2 are compared, each focusing on the gas temperature development above the middle of the exposed left side wall. In Figure 56, it can be observed that there is very little difference between simulation 1 and 2. This means that in the FDS model the gas temperature near the flaming left side wall is barely influenced by the addition of an exposed right side wall. This suggests that similar charring rates can be expected in both simulations. When looking at the temperature development in the corresponding experiments by Olivier (2019), it can be noted that simulation 1 overestimates the temperature in the heating phase, while simulation 2 underestimates the temperature. Therefore, in the experiments, the addition of an exposed right-side wall does affect the temperature development near the left side wall.

It is remarkable that the gas temperature near the left side wall is overestimated in simulation 1, while underestimating the temperature in the middle of the compartment by 30% as discussed in

Chapter 10.1.2. Therefore, it can be concluded that local temperature differences are more significant in the FDS model compared to the real-life experiments by Olivier (2019).

Lastly, the decay period is assessed. As soon as the gas burner is turned off, a steep decrease in the simulated gas temperature can be observed which corresponds with the previously discussed observations that the flaming stops almost instantly. Therefore, very little charring is expected after this point. A notable observation is that the simulated gas temperature in the middle of the compartment, as presented in Chapter 10.1.2, shows a significantly more gradual decay phase than the gas temperature near the wall in Figure 56. In the experiments a more gradual temperature decay is observed near the exposed left side wall.

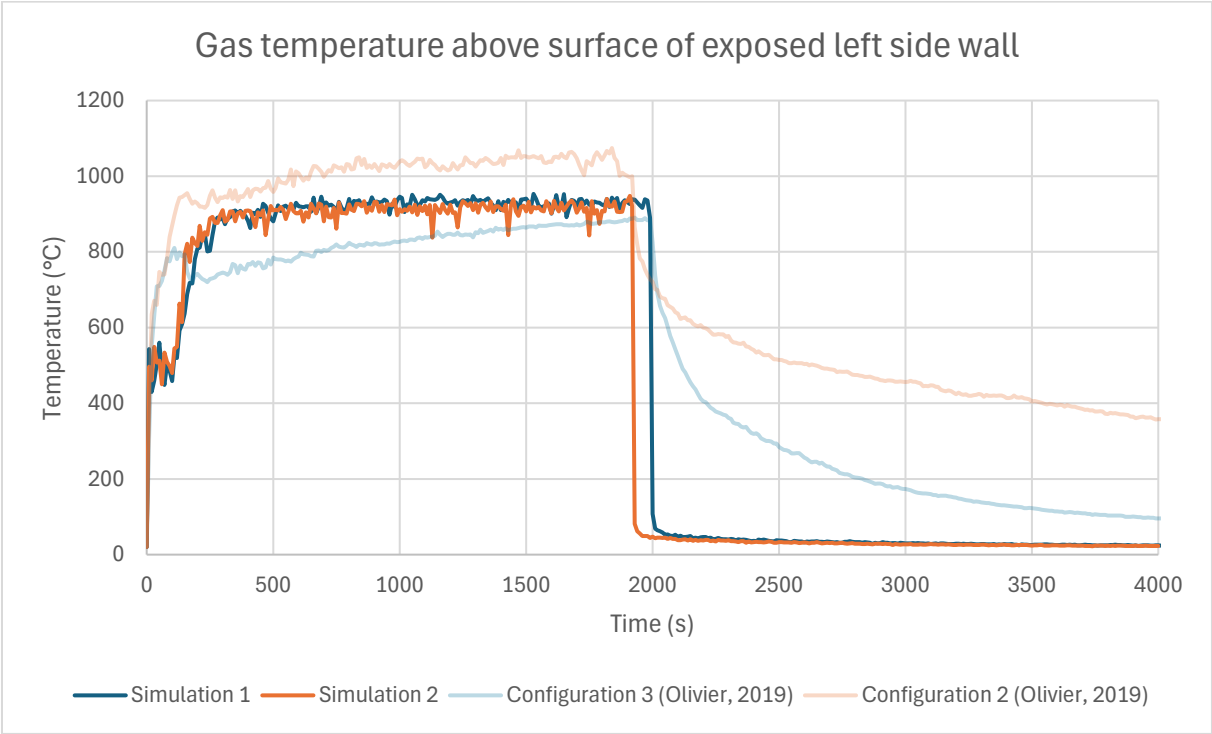


Figure 56: Gas temperature above the surface of exposed left side wall

For determining the charring rate, only the heating phase is considered to get an accurate estimation of the functionality of the FDS model because the simulated gas temperatures are not representative after turning the gas burner off. However, it is important to note that the intended use of Equation (2) also includes the decay phase of the fire.

Figure 57 and Figure 58 show the calculated charring development in the middle of the exposed left side wall for both simulation 1+2 and their corresponding reference experiments by Olivier (2019). It can be seen that by using Equation (2), simulation 1 and configuration 3 show a well matching development of the charring depth. This can be attributed to the good correspondence in average gas temperature near the CLT surface. On the other hand, simulation 2 slightly underestimates the charring depth during the heating phase and consequently in the decay phase the experimental data of configuration 2 shows a longer propagation of charring. The moment at which the gas burner is turned off corresponds to the point where the experimentally measured charring depth has reached 20 mm in the middle of the fire exposed CLT surface.

From Table 32 it can be concluded that the calculated charring rate is not influenced by the amount of exposed CLT within the simulated compartment. A charring rate of 1,14 mm/min is calculated for both simulation 1 and 2 during the heating phase based on Equation (2). This corresponds well with the

simulated burning rate of 1,15 mm/min for simulation 1 as discussed in Chapter 10.1.1. For simulation 2 a slightly higher burning rate of 1,33 mm/min is simulated. This can be linked to the higher gas temperatures on average in simulation 2 compared to simulation 1. Important to note is that the temperature used for calculating the charring development is taken at one specific point which is therefore sensitive to local differences. Extrapolating the calculated charring rate to the entire exposed wall should be done with caution.

The correspondence between the simulated burning rate and calculated charring rate suggests that the modelling of the pyrolysis and combustion process is in line with the temperatures that are generated due to the released energy of the combusting wood. However, the calculated charring rate is significantly higher than the charring rate of 0,60 mm/min which is measured in the reference experiments by Olivier (2019).

The charring development is also calculated with Equation (2) for both configuration 2 and 3, to compare with the measured charring rate by utilizing the 300°C isotherm in the experiments. Based on Table 32, Figure 57 and Figure 58 it can be concluded that the charring rate is significantly overestimated with Equation (2) compared to the experimentally measured charring rate. This is in line with the expectations because the average gas temperatures of the simulations are similar to those measured in the experiments. When applying Equation (2) to the total duration of the experiments, charring rates of 0,76 and 0,59 mm/min are calculated for configuration 2 and 3, respectively. This brings the charring rate significantly closer to the experimentally measured charring rate, while still overestimating the speed at which the char layer propagates through the cross section of the wall. In general, this supports the recommendation by Werther (2015) to apply the formula to the total burning phase, hereby including the decay phase. It is therefore recommended to only use the final calculated charring depth and not use Equation (2) for estimating the charring depth at intermediate points during the burning phase of a CLT element. In practice, this means that for CLT panels this formula cannot be used to determine the moment at which the glue layer between two CLT lamellae is reached. Due to this reason, delamination is not considered in the development of this formula, thus applying it for CLT compartment fires is only recommended when using non-delaminating CLT.

Table 32: Overview EC5 charring left side wall

	Simulation 1	Configuration 3 (Olivier, 2019)	Simulation 2	Configuration 2 (Olivier, 2019)
Exposed CLT surface	Left side wall	Left side wall	Both side walls	Both side walls
Length heating phase	33 minutes	33 minutes	32 minutes	32 minutes
Charring depth heating phase	37,5 mm	20 mm	36,6 mm	20 mm
Charring rate heating phase	1,14 mm/min (EC5 formula)	1,05 mm/min (EC5 formula) (measured = 0,60 mm/min)	1,14 mm/min (EC5 formula)	1,29 mm/min (EC5 formula) (measured = 0,63 mm/min)
Average gas temperature near left side wall	885°C	817°C	878°C	996°C

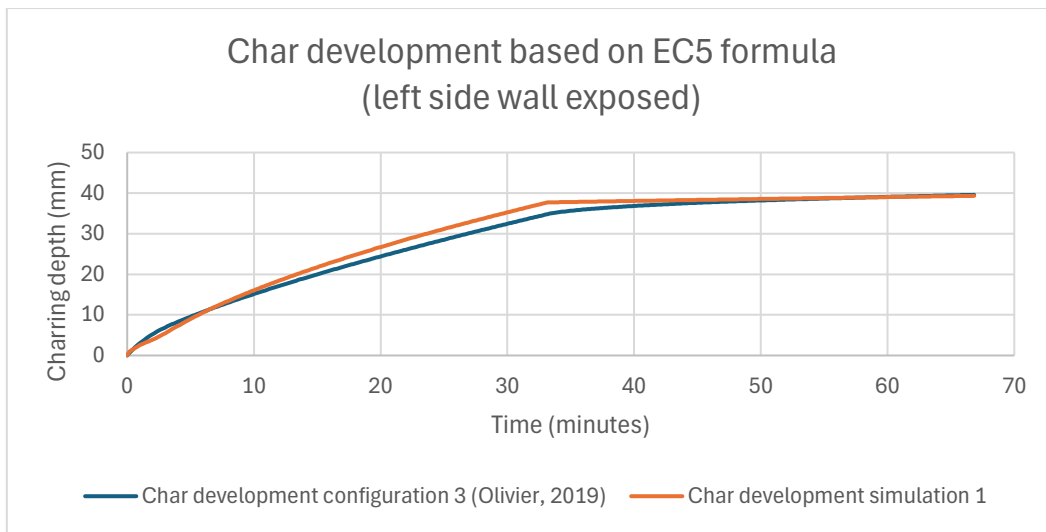


Figure 57: Charring depth simulation 1 vs configuration 3 according to EC5 formula

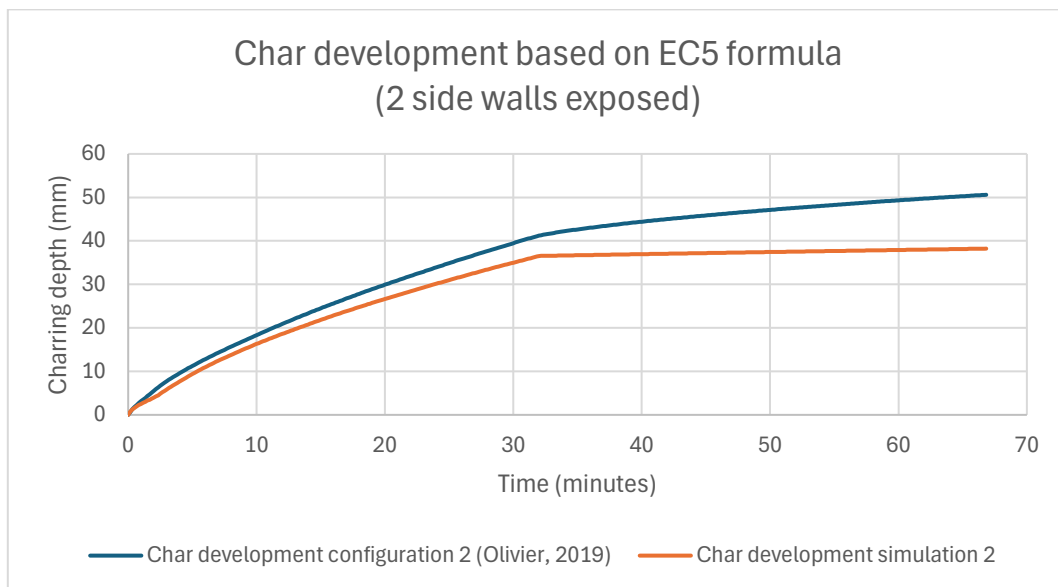


Figure 58: Charring depth simulation 2 vs configuration 2 according to EC5 formula

Conclusively, using the simulated gas temperatures, Equation (2) presented in prEN 1995-1-2 calculates a charring depth which is in line with the simulated burning rate in the FDS model. However, extrapolation to different compartment configurations should be done with care because the simulated gas temperature near one exposed wall is barely influenced by the addition of a second exposed wall. Additionally, the overall applicability of Equation (2) should be treated carefully. It is recommended to only use this equation to calculate the final charring depth that can be expected after the decay phase of a burning timber element. Using this equation for determining intermediate charring depths results in a significant overestimation of the charring depth. The use of this equation is therefore not recommended for CLT panels that are sensitive to delamination.

It is advisable to include the above-mentioned additional sidenotes in prEN 1995-1-2 about the usability of Equation (2) to prevent wrongful applications.

11.2 EXTRAPOLATION MODEL TO LARGER COMPARTMENT

This section explores the extrapolation possibilities of the presented FDS model to larger compartment geometries. Up to this point, a small-scale cubical compartment with 0,5 m sides is used to assess the functionality of the FDS model. However, the model can only be useful for engineers if the model works in an adequate manner for real-scale compartments. The simulations of the small-scale compartment have shown that the FDS model functions reasonably for obtaining a rough estimate of the fire dynamics within a CLT compartment. Therefore, it is important to investigate if the size of the simulated geometry has significant influence on the burning behaviour of wood and the deviations regarding HRR.

For extrapolating the model to a full-scale compartment, a reference experiment is used as performed by McGregor (2013) which is presented in Chapter 6.1.1. The goal of the experimental series by McGregor (2013) was to compare the fire dynamics within a fully protected CLT compartment versus a fully exposed CLT compartment. This experimental series is used because full-scale experiments have been conducted with a propane burner. This burner is easy to model in FDS, while other large-scale experiments mostly use furniture or wood cribs as fuel load.

The reference compartment has the following dimensions: 3,5 m x 4,5 m x 2,5 m (x, y, z). Additionally, a door opening is added of 1,1 m x 2,0 m (x, z) which corresponds to a ventilation factor of $0,042 \text{ m}^{1/2}$. The ventilation conditions are therefore identical to the small-scale experiment by Olivier (2019). For this analysis, a fully exposed CLT compartment is simulated with only the floor being non-combustible. The propane burner outputs 3 MW, with a growth and decay phase, and is placed as given in the floor plan in Figure 59.

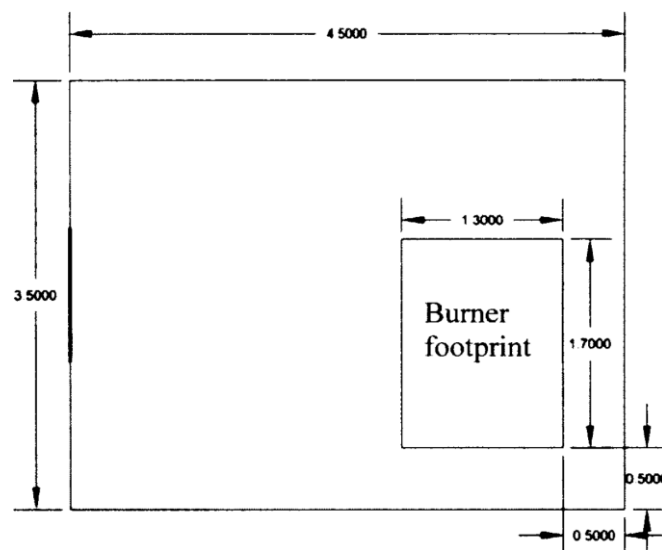


Figure 59: Floor plan full-scale compartment (McGregor, 2013)

In Chapter 10.2.1 it was concluded that a mesh consisting of 20 mm cubical cells is appropriate for running the FDS model. However, it is noted that running a full-scale compartment with 20 mm cells is extremely time consuming regarding required computing power. Therefore, alternatives are investigated to enhance the computational efficiency of the process. These alternative solutions for the mesh division are first applied to the small-scale compartment by Olivier (2019).

- Alternative 1: use 100 mm cubical cells for the entire computational domain.

- Alternative 2: use 20 mm cubical cells near the exposed CLT surfaces to obtain a more accurate gas flow near the burning surfaces. This is done for all cells within 0,2 m of the exposed CLT surfaces. The remainder of the computational domain is constructed of 100 mm cubical cells.

Figure 60 compares the above-mentioned alternatives to the simulation with a uniform mesh consisting of 20 mm cubical cells. It can be concluded that 100 mm cubical cells do not result in adequate results, depicting a too low and highly fluctuating HRR. On the other hand, alternative 2 approaches the 20 mm simulation very well. It is interesting to notice that a finer mesh can efficiently be combined with a coarser mesh, without decreasing the accuracy of the simulated results. Based on these observations, it is decided to continue with alternative 2 for running the full-scale simulation.

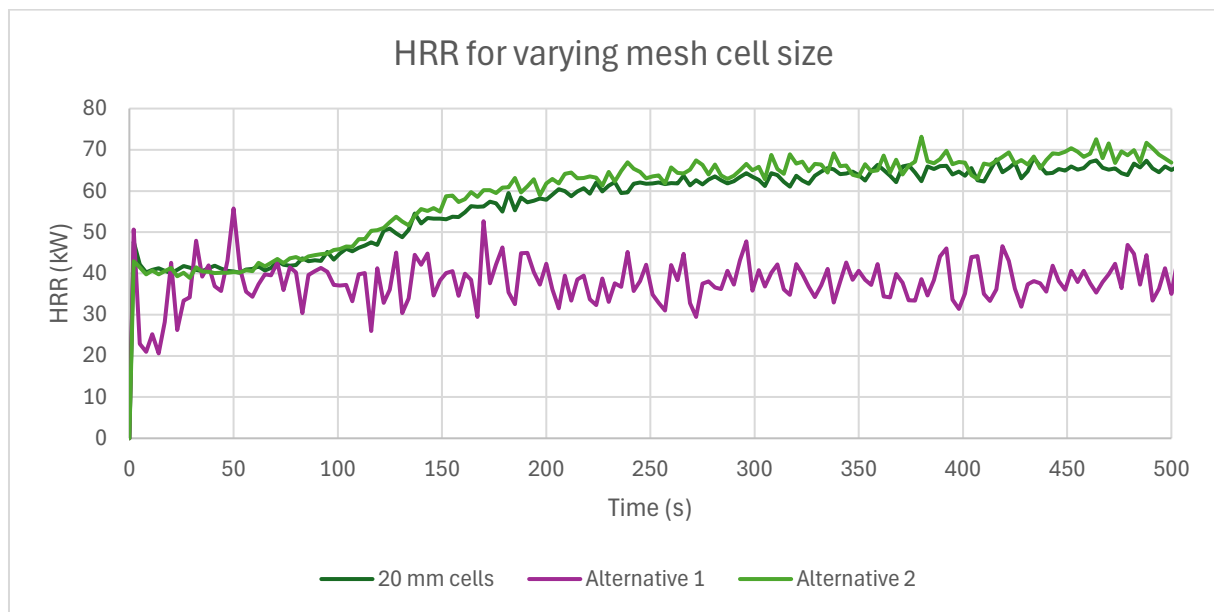


Figure 60: Mesh size comparison for using in full-scale compartment

The full-scale simulation is compared with the fully exposed compartment by McGregor (2013) regarding the HRR, with a special focus on the contribution of the burning CLT to the energy release within the compartment. Figure 61 and Figure 62 show the HRR of the experiment and the simulation, respectively. The propane burner is simulated adequately. However, the simulated contribution of the burning CLT to the HRR is largely underestimated. In the heating phase, where the propane burner is active, the total HRR is on average 8 MW in the experiment while the simulation levels out around 4 MW. This contradicts the observations of the small-scale simulations in Chapter 9 where the HRR due to the burning CLT is overestimated by approximately 50%.

Once the propane burner is turned off, the experiment shows a period of sustained burning of the CLT with subsequently a gradual decay phase. Eventually, at the end of the experiment only smouldering combustion was observed in the CLT panels. The simulated HRR does not show any decay phase with the total HRR remaining around 4 MW. In the simulation results, it is observed that the CLT surfaces are burning more heavily once the propane burner is turned off. This is not in line with the expectations based on the previously discussed simulations in Chapter 9. Up to this point, all presented simulations resulted in immediate extinguishment once the gas burner was removed.

From an FDS modelling perspective, it is good to observe that the modelled CLT panels can sustain flaming combustion without the need for a gas burner fuelling the fire. Most likely, the simulation

results in sustained flaming due to the fully exposed CLT compartment where all surfaces are burning and radiating heat towards each other. It is therefore recommended to investigate the functionality of the FDS model in similar sized compartments with less exposed CLT surfaces. Potentially, a gradual HRR decay can be simulated in full-scale compartments.

Based on the results of the discussed full-scale compartment simulation, it is concluded that the size of the simulated geometry significantly influences the correspondence between experimental and simulated results. Especially the decay phase is a notable point of attention, which depicts sustained burning in the full-scale simulation while resulting in immediate extinguishment in the small-scale simulations. Additionally, the underestimation of the HRR in the full-scale simulation versus the overestimation in the small-scale simulations is a point of attention that needs to be further investigated. Potentially, a larger heat of combustion needs to be assigned to wood in the full-scale compartments, compared to small-scale test setups. In general, due to the high complexity of fire dynamics, scaling the compartment size does not result in realistic energy scaling.

However, it is important to note that the conclusions in this section are based on simulating one specific test configuration. It is recommended to simulate more full-size compartments to analyse if similar trends are observed.

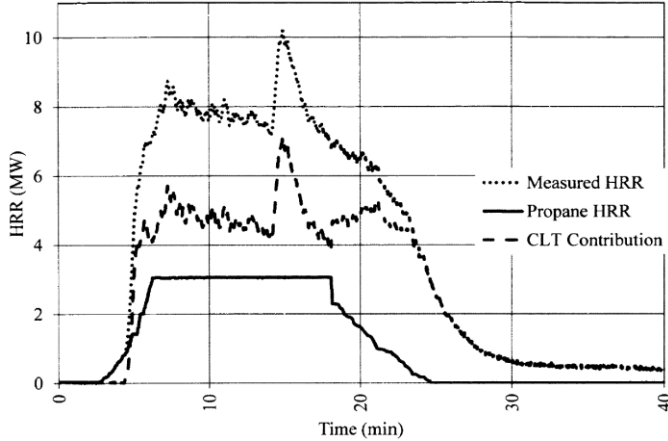


Figure 61: HRR fully exposed CLT compartment with propane burner (McGregor, 2013)

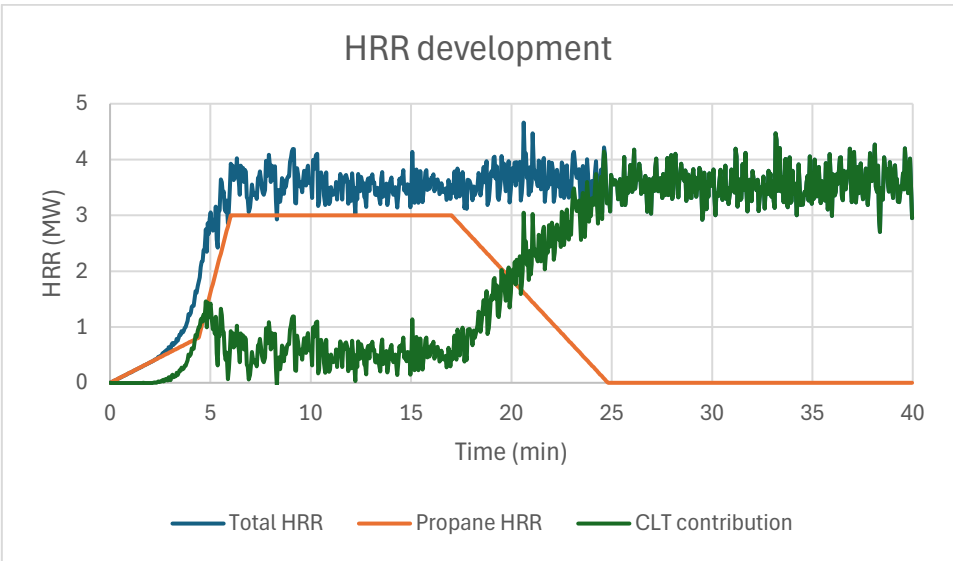


Figure 62: HRR simulation full-scale compartment

11.3 CONCLUSION

In this chapter the possibilities have been explored for implementing the presented FDS model in real-life engineering practices. In Chapter 11.1 the applicability of Equation (2) for compartment fires is assessed with gas temperature input from the FDS model. Hereby, it is concluded that Equation (2) should solely be used for determining the final charring depth after the full burning phase, including the decay phase. Using the formula to calculate intermediate points during the burning phase results in a significant overestimation of the charring depth. The small-scale FDS model, based on the experiments by Olivier (2019), should not be used to predict the charring behaviour due to the lack of a realistic decay phase in the simulations. Henceforth, it is not recommended to use Equation (2) for predicting the charring depth in compartments with delamination sensitive CLT.

Chapter 11.2 analysed the impact of the size of the simulated geometry on the accuracy of the FDS model. Hereby, it is concluded that applying the FDS model to a full-scale compartment results in some notable differences compared to simulating small-scale compartments. In the full-scale simulation the HRR is underestimated and sustained burning is observed, showing no decay phase. On the other hand, the small-scale simulation overestimates the HRR and results in immediate extinguishment of the burning CLT once the gas burner is removed. It is recommended to simulate a larger variety of full-scale CLT compartments to get a better understanding of the functionality of the FDS model for larger geometries.

Answer subquestion 5:

Based on the literature presented in previous chapters, subquestion 5 can be answered to the best extent.

SUBQUESTION 5: "IN WHAT WAY CAN CFD SOFTWARE PROVIDE A SOLUTION IN PRACTICAL ENGINEERING SITUATIONS?"

CFD software, specifically FDS, allows for a large range of insightful analyses for predicting the fire dynamics within a structure. The following conclusion is solely based on the presented simulations in this thesis, while a larger field of applications might be possible in multistorey buildings (e.g. assessing smoke development and evacuation strategies).

The presented FDS model shows significant differences in HRR contribution due to the exposed CLT and the decay phase for the small-scale versus large-scale simulations. Validation of the small-scale compartment showed more potential for predicting the fire growth and serving as a conservative tool for estimating the HRR. Unfortunately, the simulated full-scale compartment does not show the same potential based on the specific test configuration that is used for validation.

Further optimisation of the FDS model is therefore required for being useful for engineers to predict the severity of a CLT compartment fire. If the decay phase can be modelled in a more gradual manner, Equation (2) can be a fast and easy to use tool for predicting the final charring depth of timber elements based on the simulated gas temperatures in the FDS model. However, the applicability to CLT panels can be questioned due to the inability of Equation (2) to consider delamination by calculating intermediate charring depths during the burning phase.

Conclusively, it should be noted that setting up a CFD model requires significant in-depth knowledge and the computing times for simulating the fire dynamics in larger geometries can be very large, resulting in rather costly operations.

PART 5: FINAL REMARKS

This part of the master thesis aims to answer the main research question and the adherent subquestions to the best extent possible. The results are comprehensively discussed and recommendations for applications in practice and future research are given.

- CHAPTER 12: CONCLUSIONS

- CHAPTER 13: Recommendations and future research
 - Chapter 13.1: Recommendations
 - Chapter 13.2: Future research

12 CONCLUSIONS

This thesis explores the possibilities for utilising CFD software, specifically FDS, to assess the fire dynamics within a CLT compartment. A well validated FDS model can replace the need for large-scale experiments which are costly and time-consuming to setup. By using adequate FDS models engineers can explore the effects of different fuel loads, compartment geometries, ventilation conditions, and fire suppression strategies in a fast way by varying the input parameters of the model.

Existing research on CFD modelling of the burning behaviour of wood is limited. Most of the available research utilises the ignition temperature method to simplify the burning behaviour. Hereby, an ignition temperature is specified and subsequently a predefined burning rate is imposed. The applicability of this approach can be questioned due to the complexity of the real burning behaviour of wood. This thesis therefore researches the possibility of modelling the burning behaviour of wood in FDS by utilising chemical reactions for the pyrolysis and combustion process.

Concluding this thesis, the main research question can be answered based on the presented existing theoretical framework and the newly gained insights from the performed simulations. By doing so, this thesis contributes significantly to the research field of CFD modelling within FSE.

MAIN RESEARCH QUESTION:

“Under what conditions can a computational model be developed which accurately assesses the influence of exposed CLT surfaces on compartment fire dynamics using chemical reactions?”

Based on the presented validation study of the FDS model corresponding to the experiments by Olivier (2019), the following conclusions are drawn for accurately modelling the fire dynamics within a small-scale CLT compartment. This serves as a comprehensive answer to the main research question:

- The three-dimensional mesh should consist of 20 mm cubical cells positioned within a proximity of 10 – 20 cm from the CLT surfaces. Larger cell sizes result in a poor approximation of the fire dynamics, while smaller cells do not notably refine the simulated results but do require significantly longer computing time. In the remainder of the computational domain 100 mm cubical cells should be used to minimise the number of cells in the simulation while maintaining simulation accuracy.
- An effective heat of combustion of 10 MJ/kg should be considered for wood to account for incomplete combustion in real-life fire scenarios. Hereby, an overestimating of the burning behaviour of the fire exposed CLT surfaces is avoided to the best extent possible.
- The pyrolysis process of wood should be modelled between a range of 200 – 400°C with a reaction peak at 300°C to accurately simulate the ignition of fire-exposed CLT surfaces. This pyrolysis reaction should assume a fully efficient combustion process, thus resulting solely in pyrolysis gases and not include a char layer.

The above listed conclusions should be considered when setting up a model in FDS that aims to simulate the fire dynamics within a CLT compartment. Additionally, the following aspects are important to consider regarding the model development:

- The utilisation of predefined surface properties in FDS, such as INERT and ADIABATIC, for modelling non-combustible surfaces in a compartment results in a poor approximation of the burning behaviour of timber surfaces. INERT surfaces result in a significant underestimation of the gas temperatures and HRR due to its constant surface temperature of 20°C, while ADIABATIC surfaces overestimate the growth phase of burning timber due to the absence of heat dissipation through the surface.

- Including the formation of a physical char layer, as a consequence of the pyrolysis reaction in the FDS model, results in a heavily fluctuating HRR without adequate explanation for this phenomenon based on the input given in the FDS model.
- The impact of the wood moisture content is neglectable in the FDS model.
- The ventilation factor significantly influences the FDS model due to the ability of ambient air to flow in and out of the compartment. Large openings result in a slow fire growth while a small opening results in a more fluctuating HRR due to the limited oxygen availability within the compartment.

The conclusions in this thesis are largely based on the FDS simulations that aims to replicate the small-scale CLT compartment experiments by Olivier (2019). This validation of the FDS model, including relevant deviations in results, has led to the following conclusions:

- Extrapolation of the FDS model to similar sized compartments with varying configurations regarding exposed CLT is possible, resulting in approximately the same percentual deviation for each simulation compared to its reference experimental setup.
- The presented FDS model overestimates the energy that is released by the burning of exposed CLT by approximately 50% compared to the experimental results by Olivier (2019). Therefore, the FDS model is a conservative tool for predicting the fire dynamics in a small-scale CLT compartment.
- The simulated gas temperatures differ significantly locally, hereby underestimating the experimentally obtained gas temperatures by approximately 30% compared to the real-life measurements in the middle of the compartment by Olivier (2019). While on the other hand the gas temperatures near the exposed CLT wall are approximated reasonably or even overestimated. Consequently, it is hypothesised that the radiation generated from the burning CLT surfaces is underestimated in the simulations as compared to the experiments, where radiating CLT surfaces elevate gas temperatures more significantly in the middle of the compartment.
- The simulated burning rate in the middle of the fire-exposed CLT surface ranges between 1,15 – 1,33 mm/min in the small-scale simulations. However, these findings are sensitive to local differences, hence extrapolating this burning rate to the entire surface is not recommended.
- The ignition point and growth phase of the fire exposed CLT surface are approximated adequately which can be concluded based on the HRR development of the small-scale simulations and experiments. Subsequently, the fully developed fire shows a relatively constant HRR and gas temperature. Once the external heat source is removed in the small-scale simulations, the rapid inflow of cold ambient air results in the immediate extinguishment of the burning CLT therefore not showing a gradual decay phase which is notably present in the experiments by Olivier (2019).

After validating the FDS model for small-scale CLT compartments, the practical applications of the FDS model are explored for engineers to use in daily practice. This part of the master thesis has led to the following conclusions:

- Utilising Equation (2), as presented in prEN 1995-1-2, to calculate the charring depth based on the compartment gas temperature results in a charring rate similar to the simulated burning rate during the heating phase in the FDS model. Therefore, with the presence of an external heat source, the modelling of the pyrolysis and combustion process is in line with the gas temperatures that are generated due to the released energy of the combusting wood.

- Equation (2) should solely be used to calculate the charring depth over the entire burning phase of a timber element. Therefore, the simulated gas temperatures from the FDS model are not suitable for implementing in this equation due to the lack of a gradual decay phase in the small-scale simulations. Using Equation (2) to calculate intermediate charring depths during the burning phase of timber results in a significant overestimation of the charring rate. Subsequently, it is not recommended to apply this formula to delamination sensitive CLT due to its inability to predict the moment when the char layer reaches the glue layer bonding two CLT lamellae.
- Based on the results of the full-scale compartment simulation, corresponding to the fully exposed experiment by McGregor (2013), it is concluded that the size of the simulated geometry significantly influences the correspondence between experimental and simulated results. Especially the decay phase is a notable point of attention, which depicts sustained burning in the fully exposed large simulation while resulting in immediate extinguishment in the small-scale simulations. The FDS model needs to be applied to a larger variety of full-scale CLT compartments and optimised based on the overarching outcomes before application by engineers is reasonable.

13 RECOMMENDATIONS AND FUTURE RESEARCH

Based on the presented conclusions in Chapter 12, recommendations can be given for an advisable modelling approach in FDS for simulating the fire dynamics within a CLT compartment. Subsequently, recommendations for future research are given, emphasising the current unknowns and limitations of the presented FDS model.

13.1 RECOMMENDATIONS

- It is recommended for small-scale CLT compartments to utilise the presented FDS model for predicting the growth phase of the fire development. Additionally, in the fully developed fire phase, the simulated HRR in the FDS model can be used as a conservative tool for predicting the additional energy release due to burning CLT surfaces. This provides quick insights into the severity of the fire dynamics.
- It is recommended for large-scale CLT compartments to further optimise the energy release due to burning CLT before utilising the FDS model to predict the fire dynamics within full-scale CLT compartments.
- When modelling the burning behaviour of CLT through chemical reactions, it is recommended to assume a fully efficient combustion process, without the formation of a char layer. Alternatively, the more realistic incomplete combustion is taken into account by specifying an effective heat of combustion of 10 MJ/kg for wood. This value is notably lower than commonly assumed values for the heat of combustion, ranging from 16 – 20 MJ/kg for a fully efficient combustion process.
- It is recommended in FDS to self-specify a material with the relevant thermal properties for assigning to non-combustible surfaces in a CLT compartment to simulate the HRR and gas temperature more accurately. Using predefined settings in FDS such as INERT and ADIABATIC is not recommended due to the inaccurate representation of thermal properties.
- It is recommended to solely use Equation (2) for determining the final charring depth of a timber element. Using this equation at intermediate points during the burning phase results in an overestimation of the charring depth at the assessed moment. Subsequently, applying this equation to CLT sensitive to delamination is not recommended. Due to the lack of a realistic decay phase in the presented FDS model the application of Equation (2) is not yet advisable.
- It is recommended to specify thermocouples in the FDS model at a fixed distance from the back side of the burning CLT wall. Specifying a fixed distance from the fire-exposed side results in the thermocouples moving along with the burn rate of the wall therefore not showing a representable temperature development through the cross section.
- It is recommended to utilise external servers for running the FDS simulations to significantly enhance the computational efficiency of the research process. The largest benefit is the ability to split the FDS model in a significant larger amount of meshes compared to the technical limitations of a normal laptop. Subsequently, the simulation can be performed by means of MPI processing to minimise the simulation time.

13.2 FUTURE RESEARCH

- It is advisable to run the FDS model for a different set of large-scale experiments to assess if the simulated results show similar trends compared with the observations presented in this master thesis. This would provide important insights into the general applicability of the FDS model to full-scale CLT compartment fires. Based on the gained insights, further optimisation of the FDS model can be required.
- Further research is especially crucial for improving the input criteria for modelling the char layer in FDS. The attempted approach presented in this thesis needs to be altered to obtain a more realistic impact of the char layer on the burning behaviour of timber. In the current approach a continuous increase in char layer thickness is assumed, while it would be better to model fall-off criteria for the char layer to simulate a more realistic behaviour of the char layer. In general, there is little knowledge available for modelling a char layer in FDS. Contributing to bridging this knowledge gap provides significant added value for being able to approximate the burning behaviour of wood to the best extent possible.
- For the presented FDS model it would be highly beneficial to find improved input conditions for the FDS model to more adequately simulate the decay phase of burning timber. In the small-scale simulations special attention should be given to the fast inflow of cold ambient air in the decay phase which results in a rapid decrease in gas temperatures and the immediate extinguishment of the burning timber. On the other hand, in the full-scale simulations attention should be given to varying amounts of exposed CLT and its impact on the decay phase because a fully exposed compartment results in sustained burning. For example, a larger external volume can be modelled around the compartment to assess if this results in a more gradual flow of hot and cold gases in and out of the compartment. Another interesting topic is to model smouldering combustion of wood to bridge the gap between flaming combustion and extinguishment.
- The presented FDS model overestimates the energy released by the burning of exposed timber in the small-scale simulations, while underestimating the HRR in the large-scale simulations. Therefore, further research is required for bringing the simulated burning behaviour closer to the real-life behaviour. Improving the fire spread over the exposed timber surface can be an adequate starting point for minimising the deviations in HRR. It is advisable to deal with this problem by analysing the overall setup of the model to assess which input parameters impact the burning behaviour of the CLT surfaces.
- It is worthwhile to investigate the optimisation of the mesh division in the presented FDS model even further. Reducing the number of cells in the simulated compartment without affecting the accuracy of the simulated fire dynamics significantly increases the application possibilities of the FDS model for engineers due to the minimised required computing time. Further research is thus required for utilising larger cubical cell sizes near the CLT surfaces and/or in the remainder of the computational domain.
- It would be interesting to apply the developed FDS model to a larger structure, consisting of multiple compartments. Further research can be conducted into modelling a fire in a multi-storey CLT structure and then analysing the fire spread within the structure. Subsequently, the ability of one compartment to limit the fire expansion for the required fire resistance time can be assessed in a fast and relatively low-cost manner.
- Further research is required for assessing the accuracy of the smoke development in the FDS model due to the burning CLT surfaces. Especially, for multi-storey CLT buildings it is relevant to be able to predict the smoke spread through the building for evacuation strategies.

REFERENCES

- Bahrani, B. (2015). Effects of weathering on performance of intumescent coatings for structure fire protection in the wildland-urban interface. *PhDT*.
<https://ui.adsabs.harvard.edu/abs/2015PhDT.....278B/abstract>
- Bartlett, A. I., Hadden, R. M., & Bisby, L. (2018). A review of factors affecting the burning behaviour of wood for application to tall timber construction. *Fire Technology*, 55(1), 1–49. <https://doi.org/10.1007/s10694-018-0787-y>
- Brandner, R., Flatscher, G., Ringhofer, A., Schickhofer, G., & Thiel, A. (2016). Cross laminated timber (CLT): overview and development. *European Journal of Wood and Wood Products*, 74(3), 331–351. <https://doi.org/10.1007/s00107-015-0999-5>
- Brandon, D., Qvist, S., Van Straalen, I., Watez, Y., & Steenbakkens, P. (2022). *Literatuurstudie - Brandveiligheid en Bouwen met Hout*. RISE Safety and Transport.
- Browne, F. L. (1958). Theories of the combustion of wood and its control. In *Madison, Wis. : U.S. Dept. of Agriculture, Forest Service, Forest Products Laboratory eBooks*.
<https://ir.library.oregonstate.edu/downloads/3r074z89g>
- Brunkhorst, S., & Zehfuß, J. (2020). Experimental and Numerical Analysis of Fire Development in Compartment Fires with Immobile Fire Load. In *Springer eBooks* (pp. 185–190). https://doi.org/10.1007/978-3-030-41235-7_28
- Carley, K. (2017). *Validating Computational Models*. Carnegie Mellon University.
<http://www.casos.cs.cmu.edu/publications/papers/CMU-ISR-17-105.pdf>
- Crielaard, R. (2015). *Self-extinguishment of cross-Laminated timber*. TU Delft Repositories.
<http://resolver.tudelft.nl/uuid:c7e7ade5-3c04-4268-b370-8e2c33e3e0ee>
- Dai, X., Gamba, A., Liu, C., Anderson, J., Charlier, M., Rush, D., & Welch, S. (2022). An engineering CFD model for fire spread on wood cribs for travelling fires. *Advances in Engineering Software*, 173, 103213. <https://doi.org/10.1016/j.advengsoft.2022.103213>
- Drysdale, D. (2011). *An introduction to fire dynamics*. John Wiley & Sons.

- Emberley, R., Putynska, C. G., Bolanos, A., Lucherini, A., Solarte, A., Soriguer, D., González, M. G., Humphreys, K. L., Hidalgo, J. P., Maluk, C., Law, A., & Torero, J. L. (2017). Description of small and large-scale cross laminated timber fire tests. *Fire Safety Journal*, *91*, 327–335. <https://doi.org/10.1016/j.firesaf.2017.03.024>
- Falk, A., Dietsch, P., & Schmid, J. (2016). Proceedings of the Joint Conference of COST Actions FP1402 a FP1404 Cross Laminated Timber : A competitive wood product for visionary and fire safe buildings. *COST*. <http://www.diva-portal.org/smash/record.jsf?pid=diva2:951846>
- FDS. (2022, March 30). *Your first FDS simulation*. FDS tutorial. <https://fdstutorial.com/your-first-fds-simulation/#cap3>
- Frangi, A., Fontana, M., Hugi, E., & Jübstl, R. (2009). Experimental analysis of cross-laminated timber panels in fire. *Fire Safety Journal*, *44*(8), 1078–1087. <https://doi.org/10.1016/j.firesaf.2009.07.007>
- Friquin, K. L. (2010). Material properties and external factors influencing the charring rate of solid wood and glue-laminated timber. *Fire and Materials*, *35*(5), 303–327. <https://doi.org/10.1002/fam.1055>
- Hadden, R. M., Bartlett, A. I., Hidalgo, J. P., Santamaria, S., Wiesner, F., Bisby, L., Deeny, S., & Lane, B. (2017). Effects of exposed cross laminated timber on compartment fire dynamics. *Fire Safety Journal*, *91*, 480–489. <https://doi.org/10.1016/j.firesaf.2017.03.074>
- Hakkarainen, T. (2002). Post-Flashover fires in light and heavy timber construction compartments. *Journal of Fire Sciences*, *20*(2), 133–175. <https://doi.org/10.1177/0734904102020002074>
- Hayajneh, S. M., & Naser, J. (2023). Fire spread in Multi-Storey timber building, a CFD study. *Fluids*, *8*(5), 140. <https://doi.org/10.3390/fluids8050140>

- Hejtmánek, P., Ševčík, L., & Cábová, K. (2017). INPUT DATA OF BURNING WOOD FOR CFD MODELLING USING SMALL-SCALE EXPERIMENTS. *Stavební Obzor*, 26(4). <https://doi.org/10.14311/cej.2017.04.0038>
- Hevia, M., & Ramón, A. (2018). *Fire resistance of partially protected Cross-Laminated timber rooms*. <https://doi.org/10.22215/etd/2015-10728>
- International Organisation for Standardization. (2014). *ISO 834 Fire Curve*. ISO 834 Fire Resistance Tests. <https://www.iso.org/standard/57577.html>
- Janardhan, R. K., & Hostikka, S. (2019). Predictive computational fluid dynamics simulation of fire spread on wood cribs. *Fire Technology*, 55(6), 2245–2268. <https://doi.org/10.1007/s10694-019-00855-3>
- Johansson, N. (2020). *MULTI-ZONE MODELS – BRIDGING THE GAP BETWEEN TWO-ZONE MODELS AND CFD MODELS*. Lund University Sweden. <https://www.sfpe.org/publications/periodicals/sfpeeuropedigital/sfpeurope19/europeissue19feature6>
- Just, A., Brandon, D., Mager, K. N., Lange, D., & Pukk, R. (2018). *CLT compartment fire* [World Conference on Timber Engineering].
- Karlsson, B., & Quintiere, J. G. (1999). Enclosure fire dynamics. In *CRC Press eBooks*. <https://doi.org/10.1201/9781420050219>
- MacLeod, C., Law, A., & Hadden, R. M. (2023). Quantifying the heat release from char oxidation in timber. *Fire Safety Journal*, 138, 103793. <https://doi.org/10.1016/j.firesaf.2023.103793>
- McGrattan, K., Hostikka, S., Floyd, J., McDermott, R., Vanella, M., & Mueller, E. (2023). *Fire Dynamics Simulator User's Guide*. National Institute of Standards and Technology. https://github.com/firemodels/fds/releases/download/FDS-6.8.0/FDS_User_Guide.pdf

- McGregor, C. (2013). *Contribution of cross laminated timber panels to room fires*.
<https://www.semanticscholar.org/paper/Contribution-of-cross-laminated-timber-panels-to-McGregor/9a8a165f18a9c5094fccbd49c4604fd338e64e32#citing-papers>
- Mindeguia, J., Mohaine, S., Bisby, L., Robert, F., McNamee, R., & Bartlett, A. I. (2020). Thermo-mechanical behaviour of cross-laminated timber slabs under standard and natural fires. *Fire and Materials*, 45(7), 866–884. <https://doi.org/10.1002/fam.2938>
- Nakrani, D., Tiwari, M. K., Wani, T., & Srivastava, G. (2023). Characterization of combustion of hardwood and softwood through experimental and computer simulations. *Journal of Thermal Analysis and Calorimetry*, 148(15), 7727–7745. <https://doi.org/10.1007/s10973-023-12261-7>
- NEN. (2011). *NEN-EN 1995-1-2+C2: Eurocode 5: Design of timber structures - Part 1-2: General - Structural fire design*.
- NEN. (2023). *prEN 1995-1-2: Eurocode 5 - Design of timber structures - Part 1-2: Structural fire design*.
- Olivier, G. (2019). *Fire performance of cross- laminated timber: investigating adhesives, compartment configuration and design guidelines*.
<http://resolver.tudelft.nl/uuid:aef55a03-9216-48b8-ae9a-d1a2b3eee60e>
- Östman, B. (1985). Wood tensile strength at temperatures and moisture contents simulating fire conditions. *Wood Science and Technology*, 19(2), 103–116. <https://doi.org/10.1007/bf00353071>
- Östman, B. (2021). National fire regulations for the use of wood in buildings – worldwide review 2020. *Wood Material Science and Engineering*, 17(1), 2–5. <https://doi.org/10.1080/17480272.2021.1936630>
- Rego, F. C., Morgan, P., Fernandes, P., & Hoffman, C. (2021). *Fire science: From Chemistry to Landscape Management*. Springer Nature.

- Robbins, A. P., & Wade, C. A. (2007). Soot Yield Values for Modelling Purposes – Residential Occupancies: BRANZ Study Report 185. In *BRANZ Ltd.*
https://d39d3mj7qio96p.cloudfront.net/media/documents/SR185_Soot_yield_values_for_modelling_purposes_-_residential_occupancies.pdf
- Smith, S. G. L., & Brebbia, C. A. (1977). Improved stability techniques for the solution of Navier-Stokes equations. *Applied Mathematical Modelling*, 1(5), 226–234.
[https://doi.org/10.1016/0307-904x\(77\)90013-0](https://doi.org/10.1016/0307-904x(77)90013-0)
- Su, J. Z., Lafrance, P., Hoehler, M. S., & Bundy, M. F. (2018). Fire Safety Challenges of Tall Wood Buildings Phase 2: Task 3 - Cross Laminated Timber Compartment Fire Tests | NIST. *NRC CNRC*. <https://www.nist.gov/publications/fire-safety-challenges-tall-wood-buildings-150-phase-2-task-3-cross-laminated-timber>
- Sun, Q., Türkan, Y., & Fischer, E. C. (2022). A building information modeling-fire dynamics simulation integrated framework for the simulation of passive fire protection in a mid-scale cross-laminated timber compartment: Numerical implementation and benchmarking. *Fire and Materials*, 47(4), 525–541. <https://doi.org/10.1002/fam.3070>
- SWEDISH WOOD. (2019). *The CLT Handbook* [PDF].
<https://www.swedishwood.com/siteassets/5-publikationer/pdf/CLT-Handbook-2019-eng-m-svensk-standard-2019-2022.pdf>
- The Great Fire of London in 1666 - Museum of Fine Arts, Budapest*. (n.d.). Museum of Fine Arts, Budapest. <https://www.mfab.hu/artworks/the-great-fire-of-london-in-1666/>
- TU München. (2023). *Temperaturprofil in Holzkohle und Holz*.
- Wade, C. A. (2019). *A theoretical model of fully developed fire in mass timber enclosures* [Master thesis]. University of Canterbury.

Werther, N. (2015). *Factors influencing the charring rate of timber elements and their consideration within empirical and numerical assessment methods* [PhD dissertation].

Technische Universität Munchen.

Zelinka, S. L., Hasburgh, L. E., Bourne, K. J., Tucholski, D. R., & Ouellette, J. P. (2018).

Compartment fire testing of a two-story mass timber building.

<https://doi.org/10.2737/fpl-gtr-247>

APPENDIX

A INPUT DATA FDS MODEL SIMULATION 1

&HEAD CHID='Configuration3_LSW', TITLE='Configuration3_LSW'/

&TIME T_END=4311/

&DUMP NFRAMES=4311/

!MESH DEFINITION

&MESH ID='mesh1-01', IJK=10,25,13, XB=-0.24,-0.04,-0.3,0.2,0.0,0.26, MPI_PROCESS=0/

&MESH ID='mesh1-02', IJK=10,25,14, XB=-0.24,-0.04,-0.3,0.2,0.26,0.54, MPI_PROCESS=0/

&MESH ID='mesh1-03', IJK=10,25,13, XB=-0.24,-0.04,-0.3,0.2,0.54,0.8, MPI_PROCESS=1/

&MESH ID='mesh1-04', IJK=10,25,13, XB=-0.04,0.16,-0.3,0.2,0.0,0.26, MPI_PROCESS=1/

&MESH ID='mesh1-05', IJK=10,25,14, XB=-0.04,0.16,-0.3,0.2,0.26,0.54, MPI_PROCESS=2/

&MESH ID='mesh1-06', IJK=10,25,13, XB=-0.04,0.16,-0.3,0.2,0.54,0.8, MPI_PROCESS=2/

&MESH ID='mesh1-07', IJK=10,25,13, XB=0.16,0.36,-0.3,0.2,0.0,0.26, MPI_PROCESS=3/

&MESH ID='mesh1-08', IJK=10,25,14, XB=0.16,0.36,-0.3,0.2,0.26,0.54, MPI_PROCESS=3/

&MESH ID='mesh1-09', IJK=10,25,13, XB=0.16,0.36,-0.3,0.2,0.54,0.8, MPI_PROCESS=4/

&MESH ID='mesh1-10', IJK=10,25,13, XB=0.36,0.56,-0.3,0.2,0.0,0.26, MPI_PROCESS=4/

&MESH ID='mesh1-11', IJK=10,25,14, XB=0.36,0.56,-0.3,0.2,0.26,0.54, MPI_PROCESS=5/

&MESH ID='mesh1-12', IJK=10,25,13, XB=0.36,0.56,-0.3,0.2,0.54,0.8, MPI_PROCESS=5/

&MESH ID='mesh1-13', IJK=10,25,13, XB=0.56,0.76,-0.3,0.2,0.0,0.26, MPI_PROCESS=6/

&MESH ID='mesh1-14', IJK=10,25,14, XB=0.56,0.76,-0.3,0.2,0.26,0.54, MPI_PROCESS=6/

&MESH ID='mesh1-15', IJK=10,25,13, XB=0.56,0.76,-0.3,0.2,0.54,0.8, MPI_PROCESS=7/

&MESH ID='mesh2', IJK=25,5,25, XB=0.0,0.5,0.2,0.3,0.0,0.5, MPI_PROCESS=7/

&MESH ID='mesh3', IJK=25,5,25, XB=0.0,0.5,0.3,0.4,0.0,0.5, MPI_PROCESS=8/

&MESH ID='mesh4', IJK=25,5,25, XB=0.0,0.5,0.4,0.5,0.0,0.5, MPI_PROCESS=8/

&MESH ID='mesh5', IJK=25,5,25, XB=0.0,0.5,0.5,0.6,0.0,0.5, MPI_PROCESS=9/

&MESH ID='mesh6', IJK=25,5,25, XB=0.0,0.5,0.6,0.7,0.0,0.5, MPI_PROCESS=9/

!DEFINITION SPECIES AND MATERIALS

&SPEC ID = 'PYROLYZATE', FORMULA = 'CH1.7O0.83' /

&SPEC ID = 'OXYGEN', LUMPED_COMPONENT_ONLY=.TRUE./

```

&SPEC ID ='NITROGEN', LUMPED_COMPONENT_ONLY=.TRUE./
&SPEC ID ='WATER VAPOR', LUMPED_COMPONENT_ONLY=.FALSE./
&SPEC ID ='CARBON DIOXIDE', LUMPED_COMPONENT_ONLY=.TRUE./
&SPEC ID ='CARBON MONOXIDE', LUMPED_COMPONENT_ONLY=.TRUE./
&SPEC ID ='SOOT'/
&SPEC ID='PRODUCTS',
    SPEC_ID(1)='CARBON DIOXIDE', VOLUME_FRACTION(1)=0.89,
    SPEC_ID(2)='CARBON MONOXIDE', VOLUME_FRACTION(2)=0.01,
    SPEC_ID(3)='WATER VAPOR', VOLUME_FRACTION(3)=0.85,
    SPEC_ID(4)='NITROGEN', VOLUME_FRACTION(4)=3.4148019,
    SPEC_ID(5)='SOOT', VOLUME_FRACTION(5)=0.1, /
&SPEC ID = 'AIR', BACKGROUND=.TRUE.,
    SPEC_ID(1)='OXYGEN', VOLUME_FRACTION(1)=0.2095,
    SPEC_ID(2)='NITROGEN', VOLUME_FRACTION(2)=0.7905,/
&REAC ID = 'PYROLYZATE',
    FUEL = 'PYROLYZATE',
    IDEAL=.TRUE.
    SPEC_ID_NU = 'PYROLYZATE','AIR','PRODUCTS'
    NU=-1,-4.3198,1
    SOOT_YIELD=0.02
    HEAT_OF_COMBUSTION = 10000./
&MATL ID = 'WATER'
    DENSITY = 1000.
    CONDUCTIVITY = 0.20
    SPECIFIC_HEAT = 4.186
    REFERENCE_TEMPERATURE = 100.
    PYROLYSIS_RANGE = 10.
    HEATING_RATE = 5.
    NU_SPEC = 1.
    SPEC_ID = 'WATER VAPOR'
    HEAT_OF_REACTION = 2500. /

```

&MATL ID = 'PROMATECT'

CONDUCTIVITY = 0.18

SPECIFIC_HEAT = 0.92

DENSITY = 870. /

&MATL ID = 'CHAR'

DENSITY = 100.

CONDUCTIVITY = 1.0

SPECIFIC_HEAT = 1.6 /

&MATL ID='PINE'

SPECIFIC_HEAT_RAMP = 'c_pine'

CONDUCTIVITY_RAMP = 'k_pine'

DENSITY = 520.

N_REACTIONS = 1

MATL_ID (1,1) = 'CHAR'

NU_MATL(1,1) = 0

SPEC_ID(1,1) = 'PYROLYZATE'

NU_SPEC(1,1) = 1

REFERENCE_TEMPERATURE(1) = 300.

PYROLYSIS_RANGE = 100

HEATING_RATE(1) = 5.

HEAT_OF_REACTION = 1047/

&RAMP ID='k_pine', T= 20., F=0.12 /

&RAMP ID='k_pine', T=200., F=0.15 /

&RAMP ID='k_pine', T=350., F=0.07 /

&RAMP ID='k_pine', T=500., F=0.09 /

&RAMP ID='k_pine', T=800., F=0.35 /

&RAMP ID='k_pine', T=1200., F=1.5 /

&RAMP ID='c_pine', T=20., F=1.5 /

&RAMP ID='c_pine', T=99., F=1.77 /

&RAMP ID='c_pine', T=100., F=13.6 /
&RAMP ID='c_pine', T=120., F=13.5 /
&RAMP ID='c_pine', T=121., F=2.12 /
&RAMP ID='c_pine', T=200., F=2.0 /
&RAMP ID='c_pine', T=300., F=0.71 /
&RAMP ID='c_pine', T=400., F=1.0 /
&RAMP ID='c_pine', T=800., F=1.65 /

&SURF ID ='PINE'

COLOR ='BROWN'
THICKNESS = 0.100
BURN_AWAY =.TRUE.
BACKING ='EXPOSED'
HEAT_TRANSFER_COEFFICIENT = 0.13
MATL_ID = 'PINE'
MOISTURE_FRACTION = 0.12 /

&SURF ID ='PROMATECT'

COLOR ='BLUE'
THICKNESS = 0.020
BURN_AWAY =.FALSE.
BACKING ='EXPOSED'
MATL_ID = 'PROMATECT' /

!DEFINITION BOUNDARIES

&OBST ID='Obstruction #1.1', XB=0.0,0.16,0.20,0.20,0.0,0.5, SURF_ID='PROMATECT'/
&OBST ID='Obstruction #1.2', XB=0.34,0.5,0.20,0.20,0.0,0.5, SURF_ID='PROMATECT'/
&OBST ID='Obstruction #2', XB=0.0,0.0,0.2,0.7,0.0,0.5, SURF_ID='PINE'/
&OBST ID='Obstruction #3', XB=0.5,0.5,0.2,0.7,0.0,0.5, SURF_ID='PROMATECT'/
&OBST ID='Obstruction #4', XB=0.0,0.5,0.7,0.7,0.0,0.5, SURF_ID='PROMATECT'/
&OBST ID='Obstruction #5', XB=0.0,0.5,0.2,0.7,0.5,0.5, SURF_ID='PROMATECT'/

&VENT ID='outside #1', SURF_ID='OPEN', XB=-0.24,0.76,-0.3,-0.3,0.0,0.8/
&VENT ID='outside #2', SURF_ID='OPEN', XB=-0.24,-0.24,-0.3,0.2,0.0,0.8/
&VENT ID='outside #3', SURF_ID='OPEN', XB=0.76,0.76,-0.3,0.2,0.0,0.8/
&VENT ID='outside #4', SURF_ID='OPEN', XB=-0.24,0.76,-0.3,0.2,0.8,0.8/
&VENT ID='outside #5', SURF_ID='OPEN', XB=-0.24,0.0,0.2,0.2,0.0,0.8/
&VENT ID='outside #6', SURF_ID='OPEN', XB=0.5,0.76,0.2,0.2,0.0,0.8/
&VENT ID='outside #7', SURF_ID='OPEN', XB=0.0,0.5,0.2,0.2,0.5,0.8/

!DEFINTION FIRE

&VENT ID='burner', XB= 0.0, 0.5, 0.2, 0.7, 0, 0.0, SURF_ID='fire'/
&SURF ID='fire', HRRPUA=164, RAMP_Q='fireramp' /
&RAMP ID='fireramp', T= 0, F=0 /
&RAMP ID='fireramp', T= 1, F=1 /
&RAMP ID='fireramp', T= 1989, F=1 /
&RAMP ID='fireramp', T=1990, F=0 /

!DEFINITION OUTPUT

&BNDF QUANTITY='BURNING RATE'/

&DEVC ID='MLR left wall', QUANTITY='BURNING RATE', XYZ=0.0,0.45,0.25, IOR=1/
&DEVC ID='Left wall thickness', QUANTITY='WALL THICKNESS', XYZ=0.0,0.45,0.25, IOR=1/
&DEVC ID='Back wall temp', QUANTITY='WALL TEMPERATURE', XYZ=0.25,0.7,0.25, IOR=-2/
&DEVC ID='L side wall temp', QUANTITY='WALL TEMPERATURE', XYZ=0.0,0.45,0.25, IOR=1/
&DEVC ID='R side wall temp', QUANTITY='WALL TEMPERATURE', XYZ=0.5,0.45,0.25, IOR=-1/

&DEVC ID='TC LSW 5mm', DEPTH=0.005, QUANTITY='INSIDE WALL TEMPERATURE',
XYZ=0.0,0.45,0.25, IOR=1/

&DEVC ID='TC LSW 10mm', DEPTH=0.010, QUANTITY='INSIDE WALL TEMPERATURE',
XYZ=0.0,0.45,0.25, IOR=1/

&DEVC ID='TC LSW 20mm', DEPTH=0.020, QUANTITY='INSIDE WALL TEMPERATURE',
XYZ=0.0,0.45,0.25, IOR=1/

&DEVC ID='TC LSW 30mm', DEPTH=0.030, QUANTITY='INSIDE WALL TEMPERATURE',
XYZ=0.0,0.45,0.25, IOR=1/

&DEVC ID='TC LSW 40mm', DEPTH=0.040, QUANTITY='INSIDE WALL TEMPERATURE',
XYZ=0.0,0.45,0.25, IOR=1/

&DEVC ID='TC LSW 50mm', DEPTH=0.050, QUANTITY='INSIDE WALL TEMPERATURE',
XYZ=0.0,0.45,0.25, IOR=1/

&DEVC ID='TC LSW 60mm', DEPTH=0.060, QUANTITY='INSIDE WALL TEMPERATURE',
XYZ=0.0,0.45,0.25, IOR=1/

&DEVC ID='T near back wall', QUANTITY='TEMPERATURE', XYZ=0.25,0.7,0.25/

&DEVC ID='T near L side wall', QUANTITY='TEMPERATURE', XYZ=0.0,0.45,0.25/

&DEVC ID='T near R side wall', QUANTITY='TEMPERATURE', XYZ=0.5,0.45,0.25/

&DEVC ID='T middle 0.2m', QUANTITY='TEMPERATURE', XYZ=0.25,0.45,0.2/

&DEVC ID='T middle 0.4m', QUANTITY='TEMPERATURE', XYZ=0.25,0.45,0.4/

&SLCF QUANTITY='TEMPERATURE', ID='Slice01', PBX=0.1/

&SLCF QUANTITY='TEMPERATURE', ID='Slice02', PBY=0.65/

&SLCF QUANTITY='TEMPERATURE', ID='Slice03', PBY=0.15/

&SLCF QUANTITY='TEMPERATURE', ID='Slice04', PBZ=0.2/

&SLCF QUANTITY='TEMPERATURE', ID='Slice05', PBZ=0.4/

&SLCF PBY=0.21, QUANTITY='VOLUME FRACTION', SPEC_ID='OXYGEN' /

&SLCF PBY=0.45, QUANTITY='VOLUME FRACTION', SPEC_ID='OXYGEN' /

&SLCF PBY=0.65, QUANTITY='VOLUME FRACTION', SPEC_ID='OXYGEN' /

&SLCF PBX=0.1, QUANTITY='VOLUME FRACTION', SPEC_ID='OXYGEN' /

&SLCF PBX=0.45, QUANTITY='VOLUME FRACTION', SPEC_ID='OXYGEN' /

&SLCF PBZ=0.10, QUANTITY='VOLUME FRACTION', SPEC_ID='OXYGEN' /

&SLCF PBZ=0.40, QUANTITY='VOLUME FRACTION', SPEC_ID='OXYGEN' /

&SLCF QUANTITY='TEMPERATURE', VECTOR=.TRUE., ID='3D Slice', XB=-0.24,0.76,-0.3,0.7,0.0,0.8/

&SLCF QUANTITY='VELOCITY', VECTOR=.TRUE., ID='3D Slice01', XB=-0.24,0.76,-0.3,0.7,0.0,0.8/

&DEVC ID='opening heat flux', QUANTITY='RADIATIVE HEAT FLUX', XYZ=0.25,0.20,0.25, IOR=-2/

&TAIL /

B OVERVIEW FDS NAMELIST RECORDS

Appendix B gives an overview of the used namelist records within the FDS model as presented in Appendix A. For each namelist record the input parameters are listed with a brief description. The namelist records are given in the same order as in the FDS model in Appendix A. '*variable*' suggests that there are many options for this parameter where the FDS user guide should be consulted.

Table 33: Description namelist records FDS

Namelist record	Parameter	Unit	Description
&HEAD	CHID	{name}	Tag for output files
	TITLE	{name}	Description of the simulation
&TIME	T_END	Seconds	End time of the simulation
&DUMP	N_FRAMES	Number of frames	Defines at how many moments during the simulation output is written to output files
&MESH	IJK	Number of cells	The number of cells in x, y and z direction per mesh
	XB	Coordinates	The boundaries per mesh in x, y and z direction
&SPEC	FORMULA	Chemical formula	The chemical formula for a gas species
	LUMPED COMPONENT ONLY	TRUE / FALSE	Determines if the gas species is tracked over time
	VOLUME FRACTION	Mole/mole	The ratio in which species are present in an assembled species
	BACKGROUND	TRUE / FALSE	Defines if a species is present in ambient conditions (air is default)
&MATL	DENSITY	kg/m ³	Density of a material
	CONDUCTIVITY	W/(m*K)	Thermal conductivity of a material
	SPECIFIC HEAT	kJ/(kg*K)	Specific heat capacity of a material
	REFERENCE TEMPERATURE	°C	Temperature at which the reaction rate peaks
	PYROLYSIS RANGE	°C	Temperature range below and above reference temperature at which the reaction is ongoing
	HEATING RATE	K/min	Rate at which the temperature of the test apparatus is increased
	NU_SPEC	Fraction	Fraction of the material mass that is transformed into gas species
	SPEC_ID	Gas species	Defines the gas species that is formed out of the reacting material
	MATL_SPEC	Fraction	Fraction of the material mass that is transformed into a new material
MATL_ID	Solid material	Defines the solid material that is formed out of the reacting material	
	HEAT OF REACTION	kJ/kg	The amount of energy consumed per unit mass of reactant that is converted into reaction products
&SURF	THICKNESS	m	Thickness of a surface

	BURN_AWAY	TRUE / FALSE	Defines if the thickness of the surface should reduce due to burning
	COLOR	Colour	Specifies the surface colour
	BACKING	{variable}	Defines the thermal boundary conditions for the non-fire exposed side of the surface
	HEAT TRANSFER COEFFICIENT	W/(m ² *K)	Defines the heat transmittance of the surface
	MOISTURE FRACTION	Fraction	Specifies the moisture percentage in the surface
	HRRPUA	kW/m ²	HRR output for a burner
&REAC	FUEL	Species	Defines the fuel species for the fire
	IDEAL	TRUE / FALSE	Defines if the heat of combustion should be reduced based on the soot yield
	SPEC_ID_NU	Species	Defines the species that are formed upon fuel consumption
	NU	Ratio	Defines the ratio in which species are formed upon fuel consumption
	SOOT YIELD	Fraction	The fraction of fuel mass that is converted into smoke particles
	HEAT OF COMBUSTION	kJ/kg	Energy released upon fuel consumption
&RAMP	T	Seconds	Defines a time moment in a ramped function
	F	{variable}	Specifies the value for a parameter at the time moment as specified by T in the same line (for burner it specifies a fraction of the maximum burner output)
&OBST	XB	Coordinates	Specifies the x, y and z coordinates of an obstacle in the computational domain
	SURF_ID	{variable}	Specifies which surface properties are assigned to the obstacle
&VENT	XB	Coordinates	Specifies the x, y and z coordinates of a vent
	SURF_ID	{variable}	Specifies the vent properties (OPEN is often used to allow for oxygen inflow)
&BNDF	QUANTITY	{variable}	Measures a boundary quantity for all surfaces
&DEVC	QUANTITY	{variable}	Device that measures a specified output quantity
	XYZ	Coordinates	Specifies the location for the device
	IOR	1/2/3/-1/-2/-3	Specifies the orientation in which measurements should be taken (can be positive / negative x, y or z direction)

	DEPTH	m	Depth at which measurements are taken within an obstacle
&SLCF	QUANTITY	<i>{variable}</i>	Outputs a 2D slice for various output quantities like temperature and oxygen concentration
	PBX / PBY / PBZ	m	Location and direction of the 2D slice

C THERMAL PROPERTIES OF WOOD

Appendix C provides an overview of the temperature-dependent thermal properties of wood. These properties are used as input values for simulating the burning behaviour of the CLT panels in the FDS model. The values and graphs are retrieved from the prEN 1995-1-2.

Table 34: Thermal properties for CLT panels

T [°C]	λ [W/(m*K)]	c [kJ/(kg*K)]
20	0,12	1,53
99	a*	1,77
100	a*	13,60
120	a*	13,50
121	a*	2,12
200	0,15	2,00
250	a*	1,62
300	a*	0,71
350	0,07	0,85
400	a*	1,00
500	0,09	a*
600	a*	1,4
800	0,35	1,65
1200	1,5	1,65

T: temperature
 λ : thermal conductivity
c: specific heat capacity
a*: linear interpolation may apply

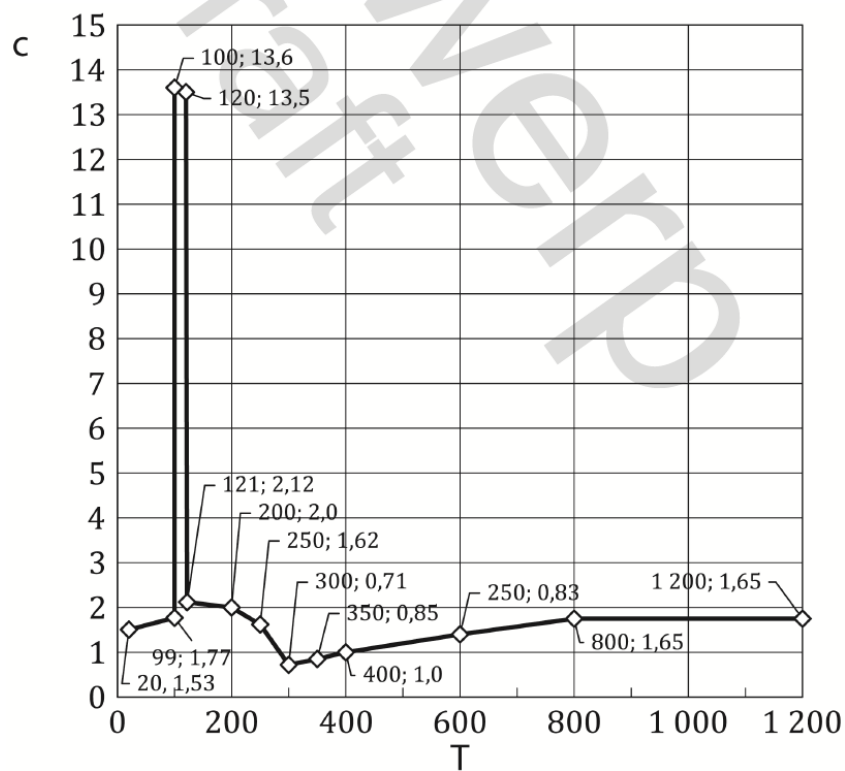


Figure 63: Specific heat capacity as function of temperature for CLT panels

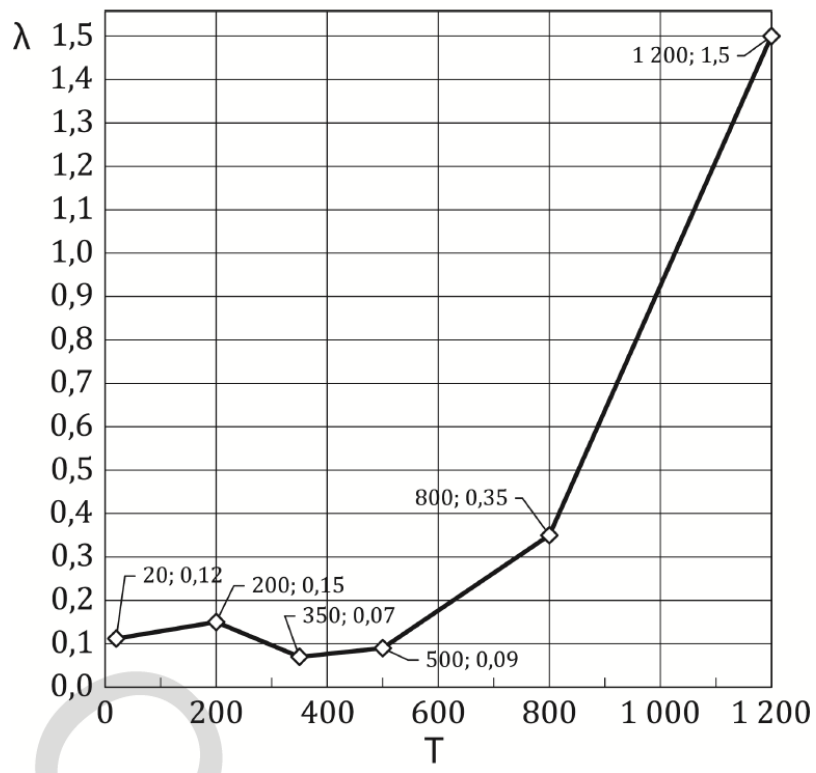


Figure 64: Thermal conductivity as function of temperature for CLT panels

D OVERVIEW EXISTING CLT FIRE EXPERIMENTS

Appendix D presents a comprehensive overview of the conclusions of each research as presented in Chapter 6.1. Table 35 provides a quick insight into the main problems arising in CLT constructions exposed to a fire.

Table 35: Overview existing CLT fire experiments

Research	Conclusions
McGregor (2013)	<ul style="list-style-type: none"> • Gypsum board prevents involvement of CLT exposed to a fire. • Furniture fuel gives more realistic results (compared to propane burner). • HRR doubled in a fully exposed CLT compartment. • Average charring rate of 0,85 mm/min in the fully exposed compartment.
Hevia and Ramón (2018)	<ul style="list-style-type: none"> • 2 opposing walls result in a higher HRR than 2 adjacent walls. • Compartment with 1 exposed wall had a similar HRR to a fully protected compartment. • Exposed CLT does not significantly influence temperatures in the early stages of the fire. • HRR is linked to the amount of exposed CLT. • Slightly higher charring rates than 0,65 mm/min were observed. • Compartments with 2 exposed walls showed no sign of self-extinguishment. • Gypsum board adequately protects underlying CLT.
Crielaard (2015)	<ul style="list-style-type: none"> • Delamination is too unpredictable to rely on self-extinguishment. • Average charring rate of 0,76 mm/min observed. • Delamination can occur safely at temperatures below 250 and heat flux below 4kW/m². • Delamination can be prevented by increasing the thickness of the outer lamella.
Emberley et al. (2017)	<ul style="list-style-type: none"> • Self-extinguishment started at the base of the exposed surface and progressed to the ceiling (ceiling and wall extinguished at about the same time). • No delamination was observed due to short fire duration.
Hadden et al. (2017)	<ul style="list-style-type: none"> • Exposed CLT ceiling results in faster combustion of interior fuel load, compared to exposed CLT wall (due to improved radiative view factors). • Lower charring depth observed at the ceiling. • Sustained burning observed after fuel is consumed due to radiation between CLT surfaces. • Exposed CLT did not significantly influence peak compartment temperatures. • Self-extinguishment in compartments with 2 exposed CLT surfaces is possible if delamination is prevented.
Su et al. (2018)	<ul style="list-style-type: none"> • Smaller opening factor results in longer fire duration due to increased involvement of CLT. • A larger opening factor results in a higher HRR, but for a shorter duration. • Peak compartment temperatures were similar to the fully protected compartment. • Delamination led to a second flashover or continuation of sustained burning. • Gypsum board is an effective way to delay/prevent ignition and involvement of CLT.
Just et al. (2018)	<ul style="list-style-type: none"> • Failed to demonstrate self-extinguishment due to second flashover. • Delamination occurred both above and below the critical charring temperature of 300°C. • Charring rates of approximately 0,50 mm/min. • Gypsum board adequately protects CLT as minimal charring was observed under the gypsum layer.

Olivier (2019)	<ul style="list-style-type: none"> • MUF bonded panels show greater resistance against delamination than polyurethane. • Charring rates around 0,65 mm/min were observed. • 2 adjacent walls self-extinguished about 3 times faster than 2 opposing walls. • An exposed ceiling gave the best results, potentially due to lower oxygen concentration limiting the pyrolysis process.
Mindeguia et al. (2020)	<ul style="list-style-type: none"> • A larger opening factor results in more rapid-fire progression and earlier decay. • Decreasing the opening factor results in a less severe fire, but longer fire duration. • Charring rates ranged between 0,80 and 1,43 mm/min depending on the opening factor. • A larger opening factor results in a smaller charring depth and is thus beneficial for preserving most of the load-bearing structure.

E SIMULATION RESULTS

Appendix E provides a complete overview of all simulation results which are discussed in Chapter 9 corresponding to the experiments by Olivier (2019). The presented graphs can be consulted to increase the understanding of the simulation results and the way the FDS model works. The following results are presented for simulations 1 – 3:

1. Heat release rate (HRR)
2. Mass loss rate (MLR) of the burning exposed CLT surface
3. Decreasing thickness of the exposed CLT surface
4. Gas temperature in the middle of the compartment at 0,2 m and 0,4 m height.
5. Gas temperatures near the middle of the exposed CLT surface (not for simulation 3)
6. Surface temperature in the middle of the exposed CLT surface
7. Thermocouple data at various depths in the middle of the exposed CLT surface

E.1 Overview results simulation 1

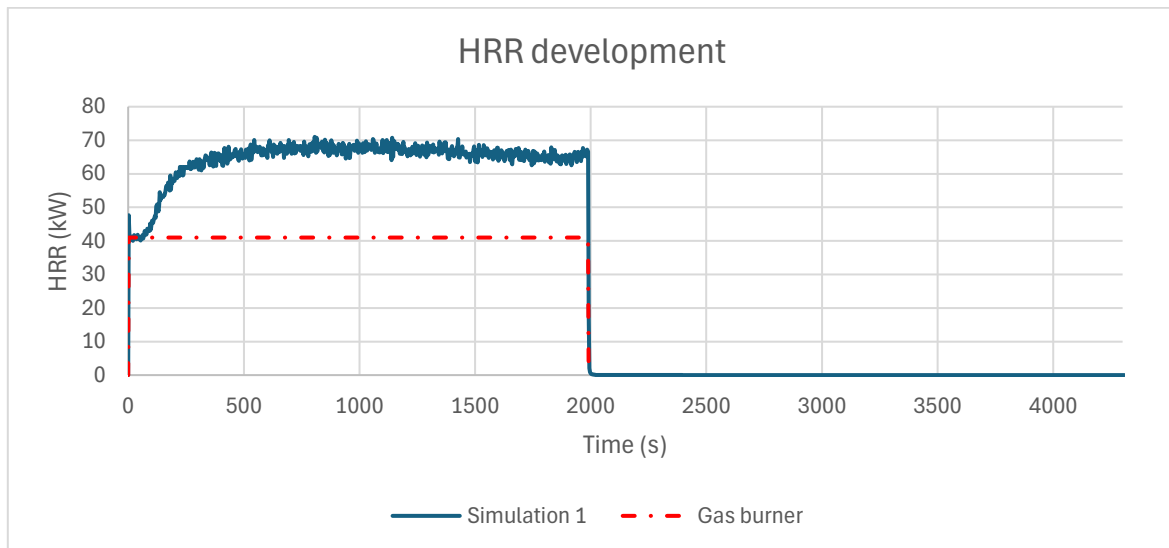


Figure 65: Simulation 1 HRR

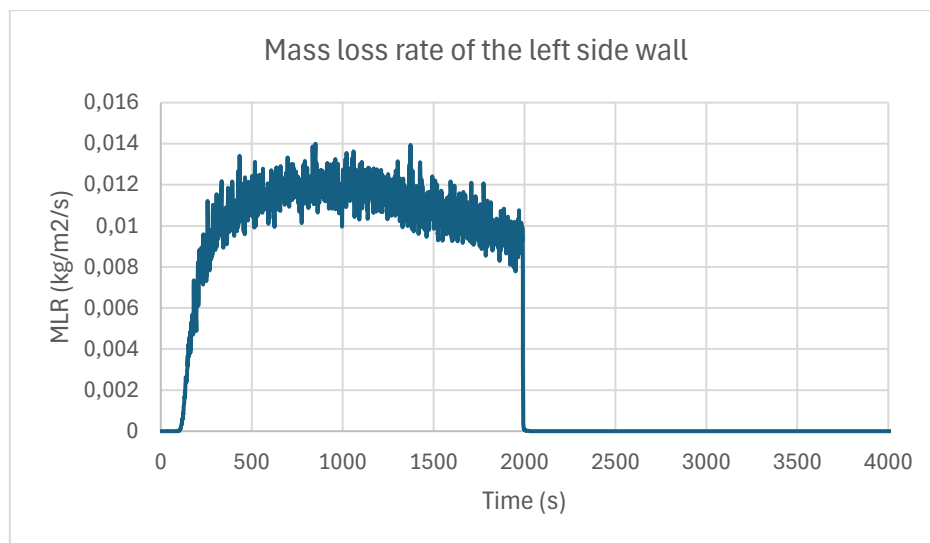


Figure 66: Simulation 1 mass loss rate

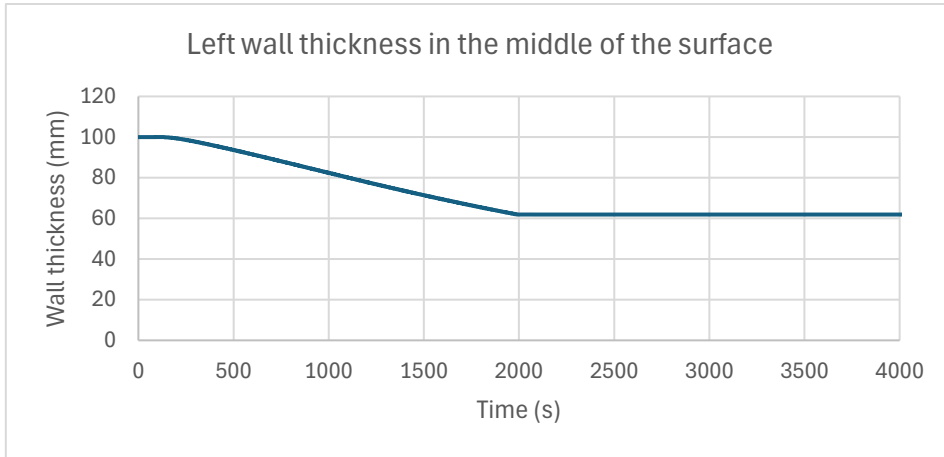


Figure 67: Simulation 1 decreasing wall thickness

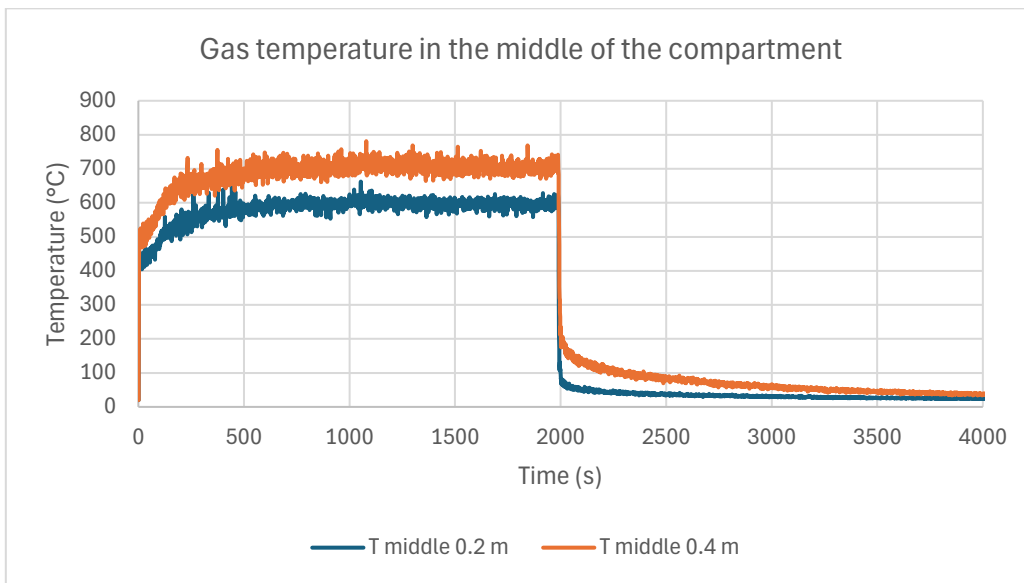


Figure 68: Simulation 1 gas temperatures in middle of compartment

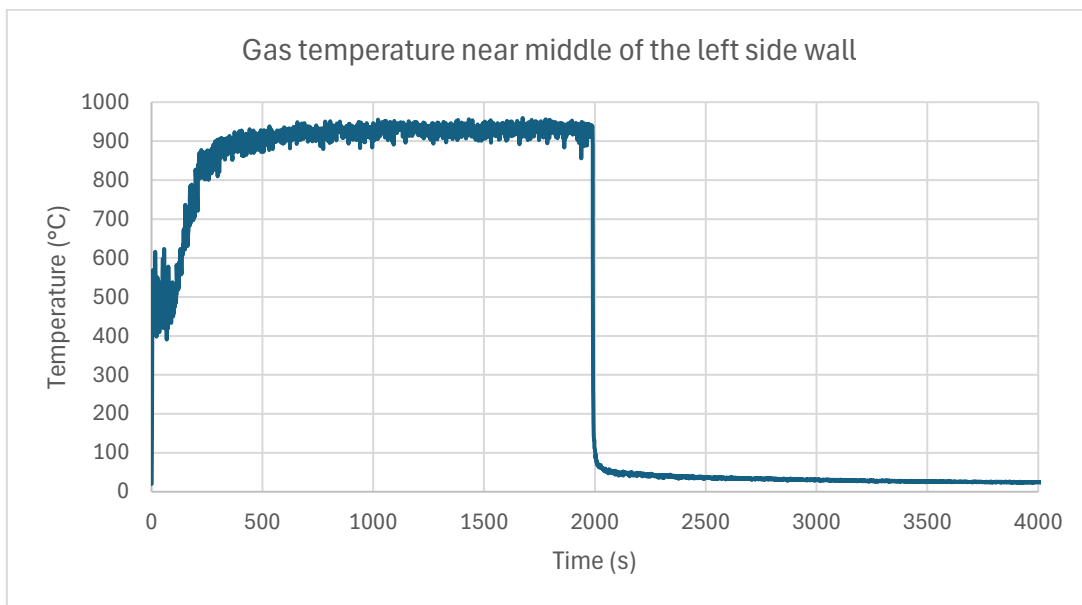


Figure 69: Simulation 1 gas temperature near CLT surface

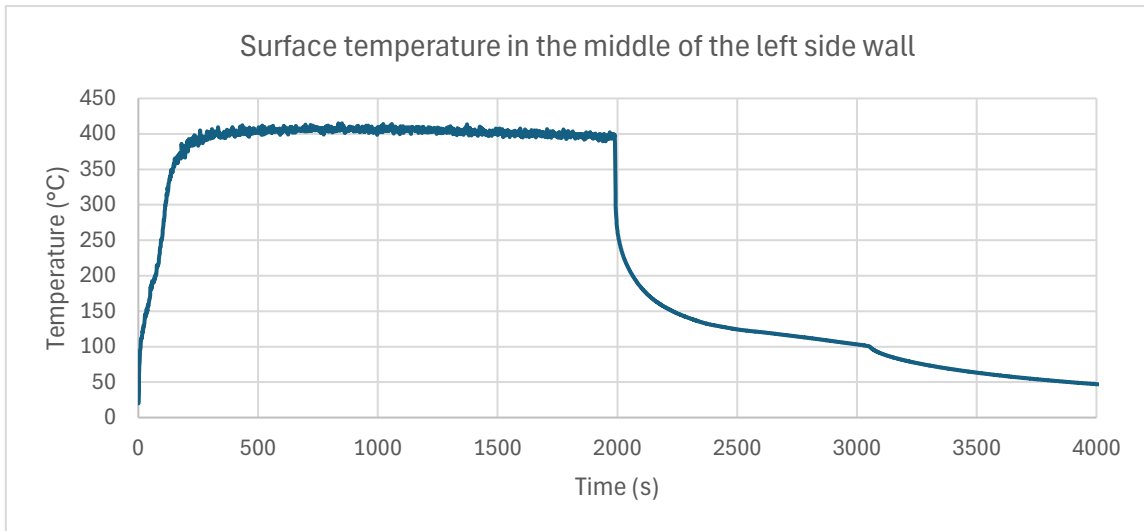


Figure 70: Simulation 1 CLT surface temperature

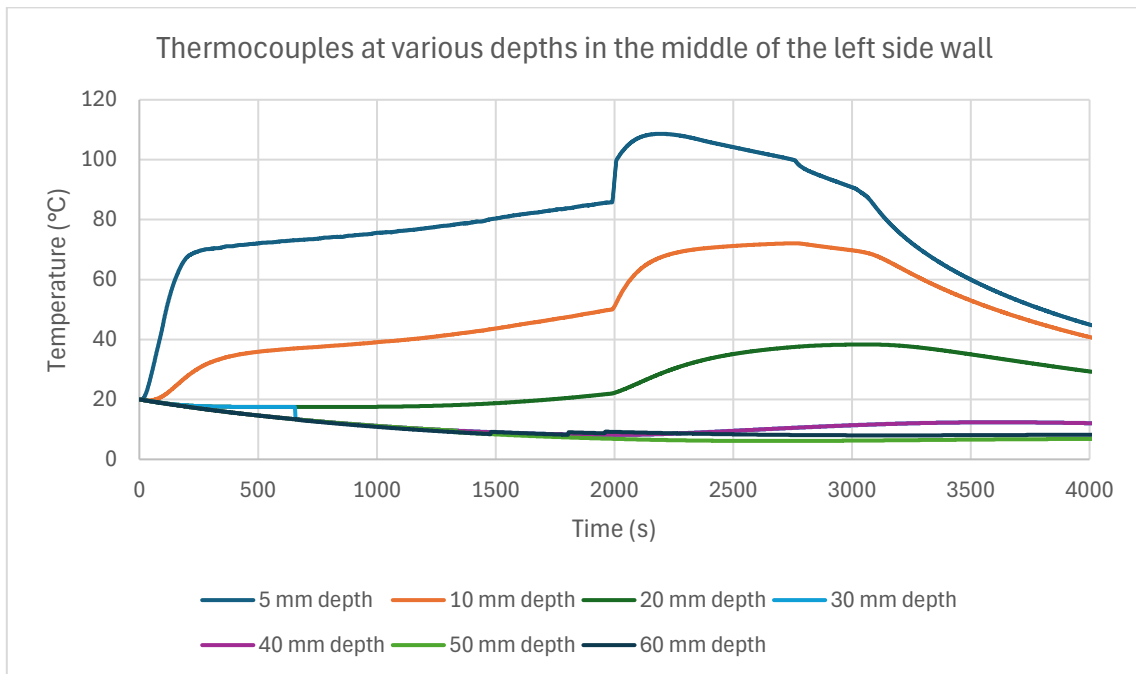


Figure 71: Simulation 1 thermocouples

E.2 Overview results simulation 2

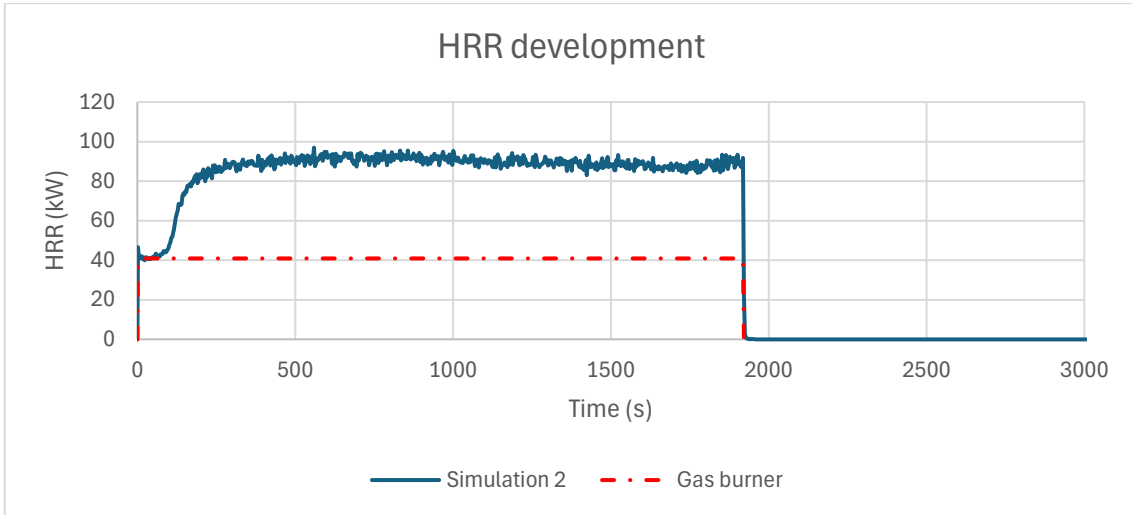


Figure 72: Simulation 2 HRR

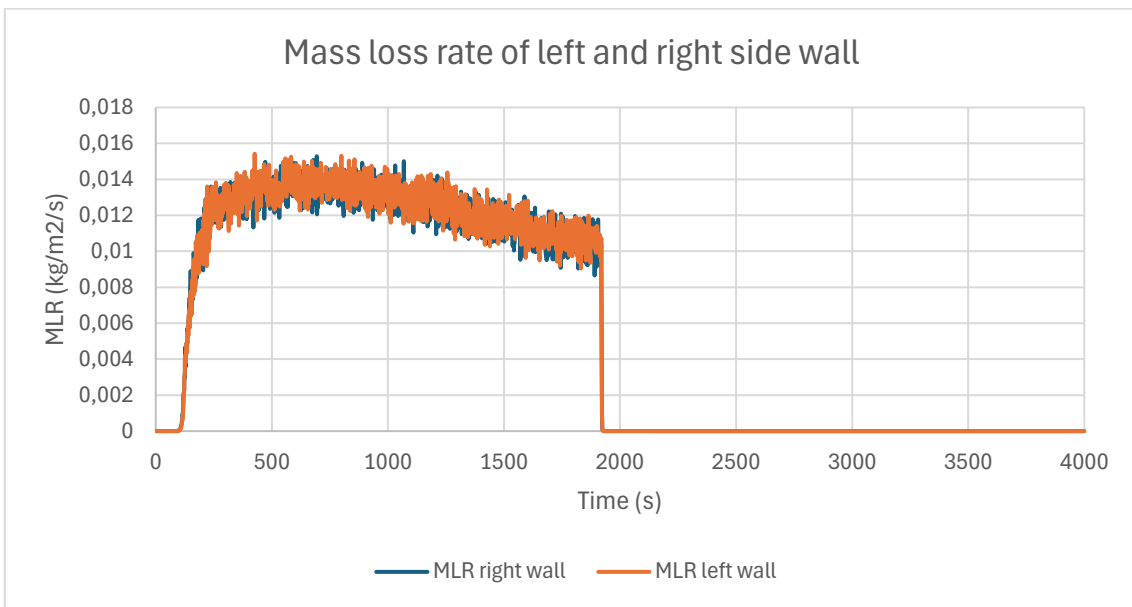


Figure 73: Simulation 2 mass loss rate

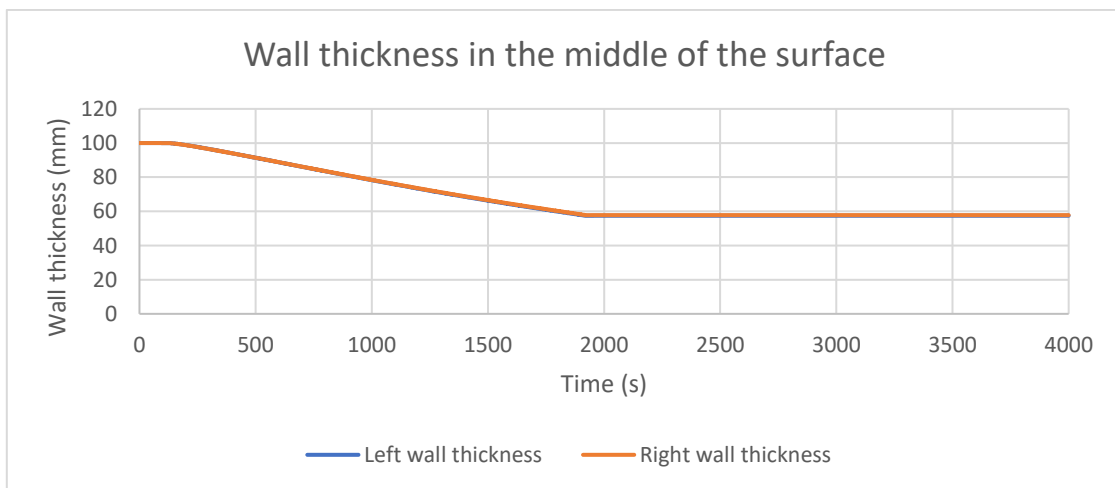


Figure 74: Simulation 2 decreasing wall thickness

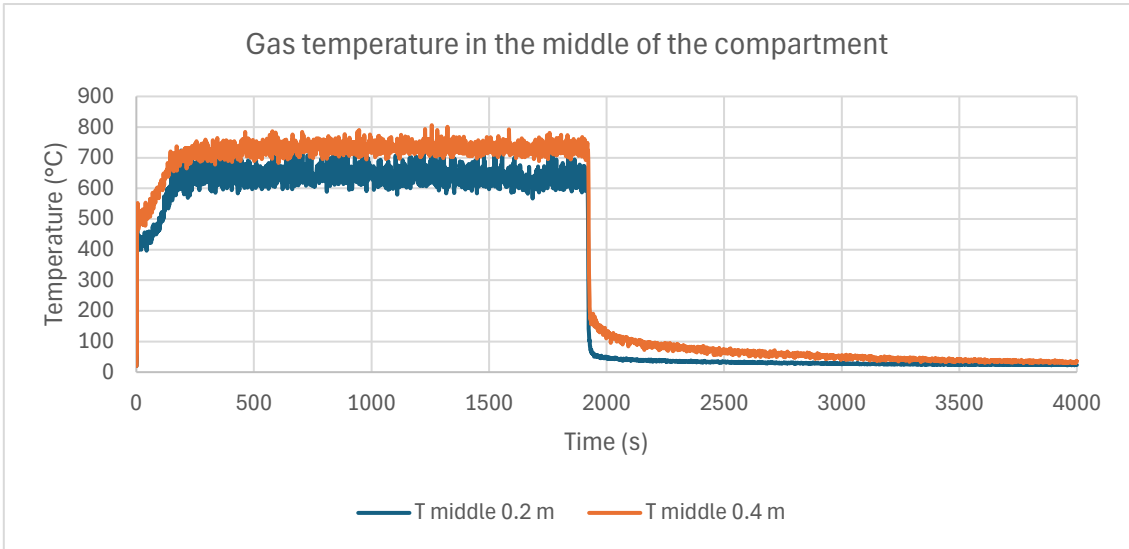


Figure 75: Simulation 2 gas temperatures in middle of compartment

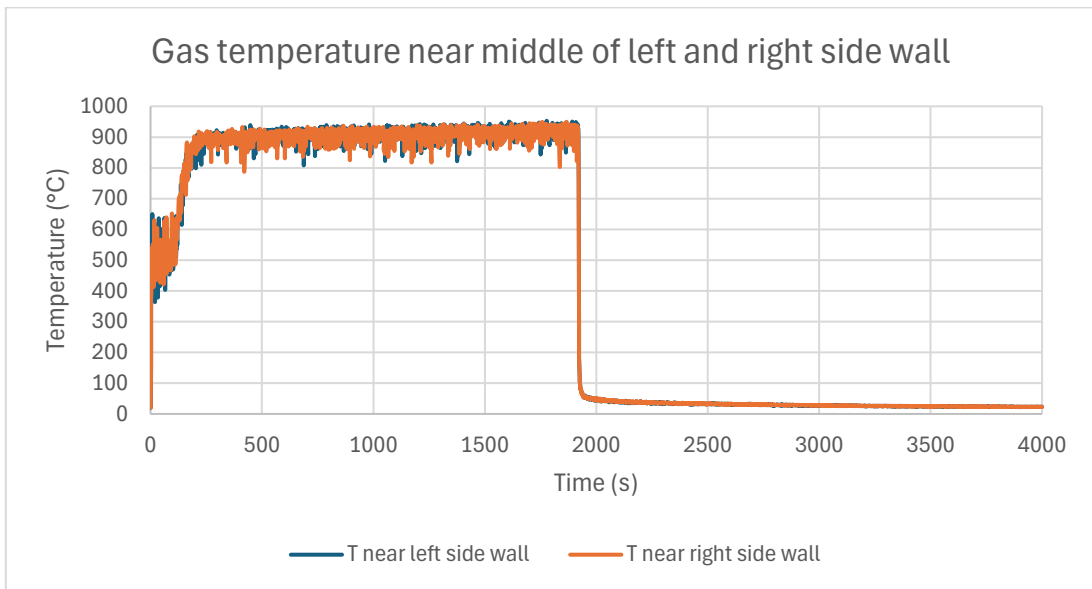


Figure 76: Simulation 2 gas temperature near CLT surface

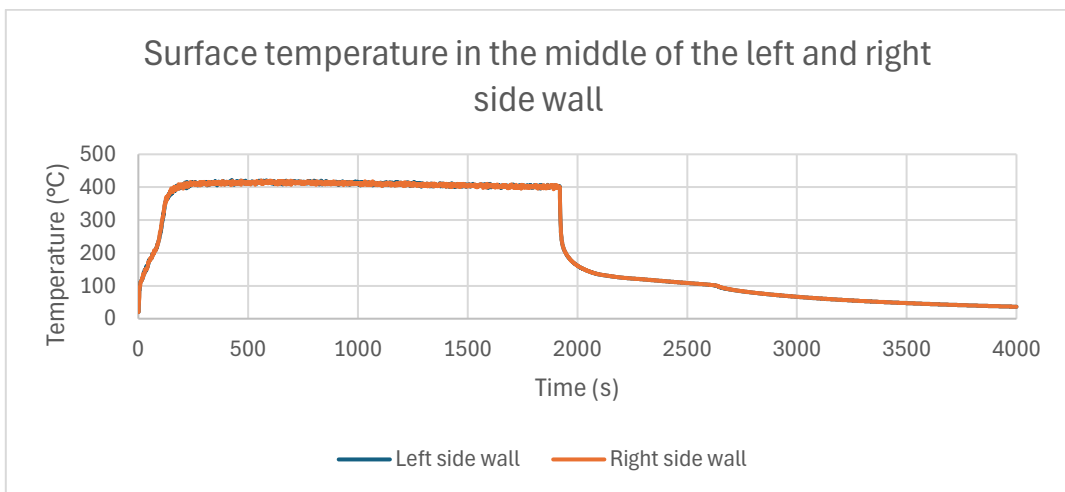


Figure 77: Simulation 2 CLT surface temperatures

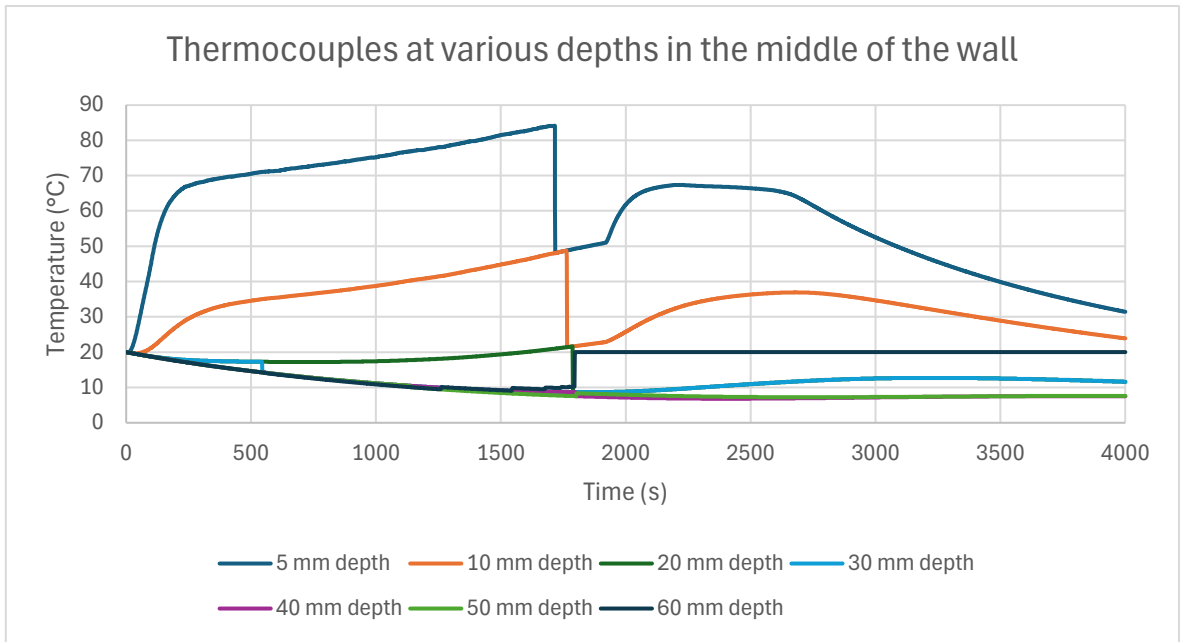


Figure 78: Simulation 2 thermocouples

E.3 Overview results simulation 3

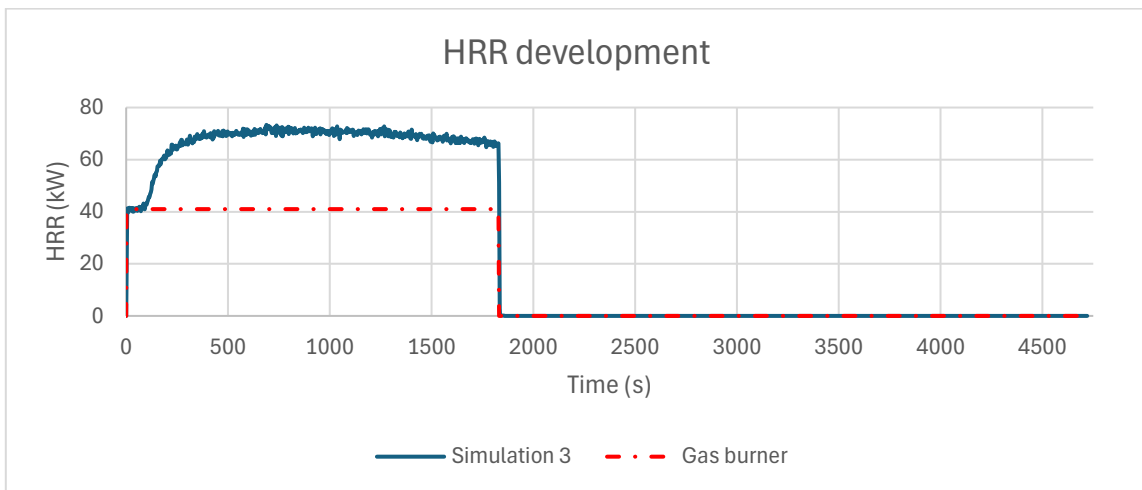


Figure 79: Simulation 3 HRR

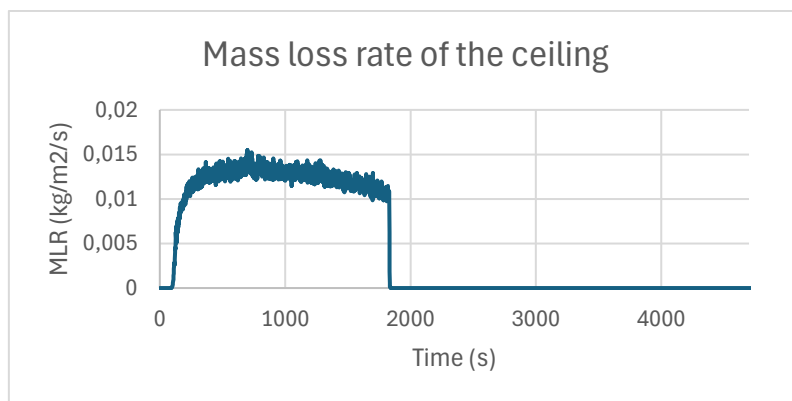


Figure 80: Simulation 3 mass loss rate

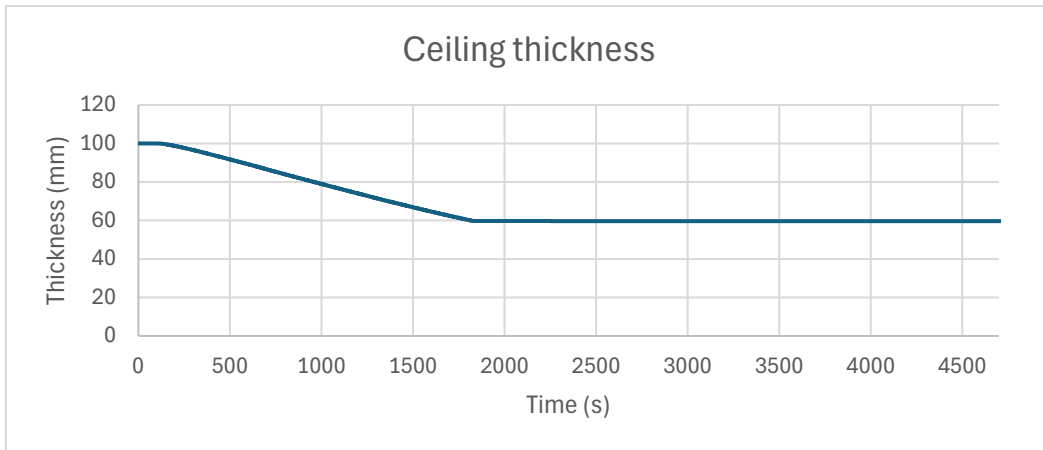


Figure 81: Simulation 3 decreasing ceiling thickness

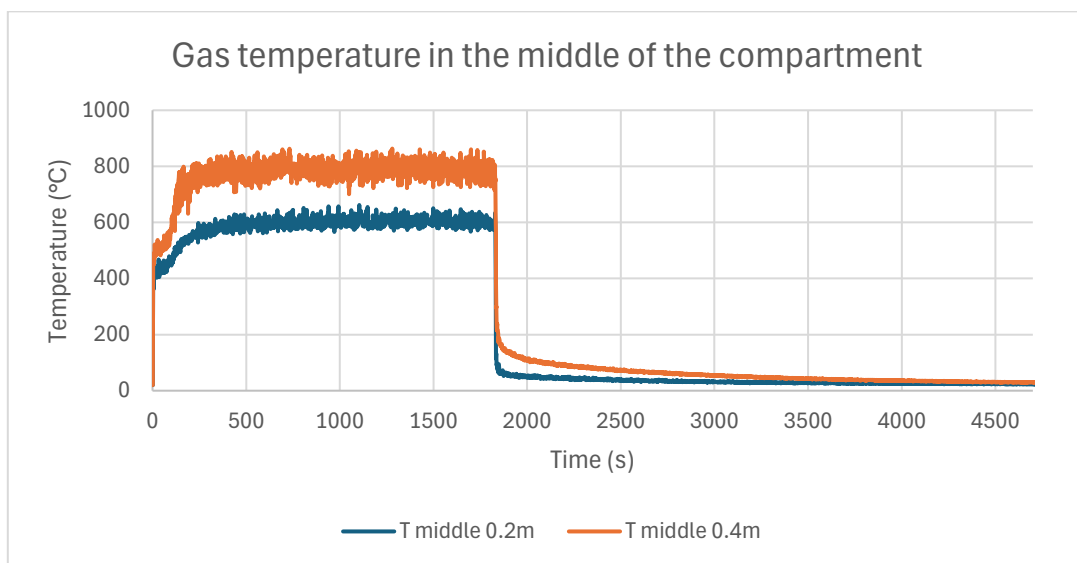


Figure 82: Simulation 3 gas temperatures in middle of compartment

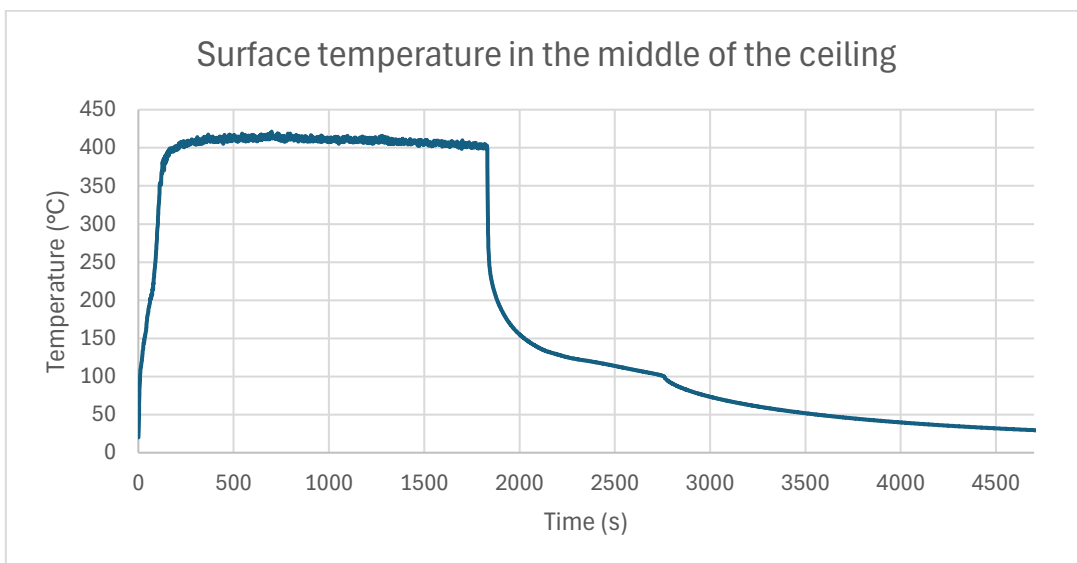


Figure 83: Simulation 3 CLT surface temperature

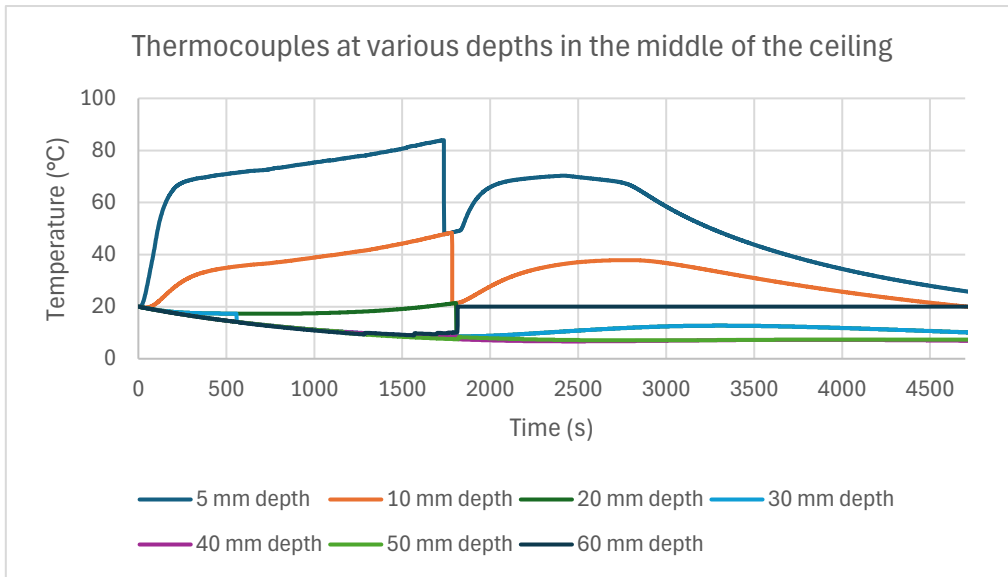


Figure 84: Simulation 3 thermocouples

F ANALYSIS NON-COMBUSTIBLE SURFACES FDS

Appendix F elaborates on the modelling of non-combustible surfaces in the FDS model. The modelling process is extensively discussed, resulting in the choice for PromatectH as non-combustible surface.

The reference test series by Olivier (2019), as presented in Chapter 6.1.8, consists of exposed CLT panels, while the remaining non-combustible surfaces are made from PromatectH. For replicating the test setup by Olivier (2019), it came to the attention that not only the input of the combustible timber surfaces is important. The input for the remaining non-combustible surfaces also influences the simulation results due to their thermal properties. The thermal properties influence the heat dissipation within the compartment and therefore directly influence the combustion conditions for the exposed timber. This appendix presents a comparison of simulation results replicating configuration 3 by Olivier (2019) with an exposed left sidewall. The following surface properties are assessed: INERT, ADIABATIC and PromatectH.

By default, surfaces in FDS are modelled as 'INERT'. INERT surfaces are specified such that the surface temperature always remains at the ambient temperature of 20°C. In the FDS user guide INERT surfaces are referred to as the ultimate ambient temperature heat sink, which resembles a cooling element. At the start of this thesis, the goal was to keep the model as simple as possible which meant to stick with most default settings in the FDS model. However, once it came to the attention that INERT surfaces act as a cooling element, the choice was made to opt for different surface properties.

Another predefined setting for surfaces in FDS is labelled 'ADIABATIC'. Setting a surface to be ADIABATIC forces it to be perfectly insulated. The surface temperature adjusts itself during the simulation such that there is no net heat transfer from the compartment gas to the solid surface. It is important to note that no surface is fully ADIABATIC in reality. Therefore, it is advised in the FDS user guide to limit the use of this surface property to diagnostic purposes.

The last assessed alternative is a surface with self-specified properties, resembling the PromatectH material. PromatectH is a non-combustible calcium-silicate material with adequate thermal properties to withstand fire induced loads. PromatectH is used for the non-combustible surfaces in the reference experiment as presented in Chapter 8.2.3. Table 36 gives an overview of the material properties of the PromatectH surfaces in the FDS model

Table 36: Properties PromatectH surface in FDS model

Parameter	Input for PromatectH surface
Surface thickness	20 mm
Density	870 kg/m ³
Thermal conductivity	0,18 W/(m*K)
Specific heat capacity	0,92 kJ/(kg*K)

For analysing the influence of the varying non-combustible surfaces, the HRR and the gas temperature in the middle of the compartment is assessed. Table 37 provides an overview of the simulation results.

When looking at the HRR, given in Figure 85, it can be noted that the INERT simulation underestimates the growth phase of the fire due to a slower ignition of the exposed CLT wall. Eventually, the HRR levels out around 50 kW. On the other hand, the ADIABATIC simulation overestimates the speed at which the timber ignites. The PromatectH simulation approximates the experimental result well in the early stages but increases a bit further than the experimental HRR, levelling out around 65 kW. On average, the INERT and PromatectH simulations differ approximately the same from the experimental result.

However, the shape of the HRR graph should also be taken into account which scores better for the PromatectH simulation.

When looking at the gas temperatures, given in Figure 86, it can be seen that all simulations highly underestimate the temperature in the middle of the compartment. The INERT simulation approximates the temperature the worst, followed by the PromatectH and ADIABATIC simulations. The cooling effect of the INERT surfaces can thus clearly be identified. In the decay phase, it can be seen that the temperature decay goes more gradually for the PromatectH simulation. The ADIABATIC and INERT simulations barely show any temperature decay because temperature drops quickly back to ambient conditions.

Conclusively, based on combining the HRR and temperature observations, the PromatectH surface properties are chosen for the final FDS model, used for the simulations in Chapter 9 and 10. Self-specifying the material properties from the reference experiment is preferred for replicating the test conditions in the best way possible. Additionally, for extrapolating to different compartment configurations, the results can be better understood with self-defined properties as it is more difficult to extract the mathematics behind INERT and ADIABATIC simulations.

Table 37: Overview simulation results for varying non-combustible surfaces

	INERT	ADIABATIC	PromatectH	Configuration 3 (Olivier, 2019)
Average HRR in heating phase	50,4 kW	70,9 kW	64,3 kW	56,3 kW
Average T 0,2 m in middle of compartment	434°C	636°C	581°C	747°C
Average T 0,4 m in middle of compartment	521°C	742°C	688°C	930°C
Max temperature	612°C	795°C	769°C	1008°C

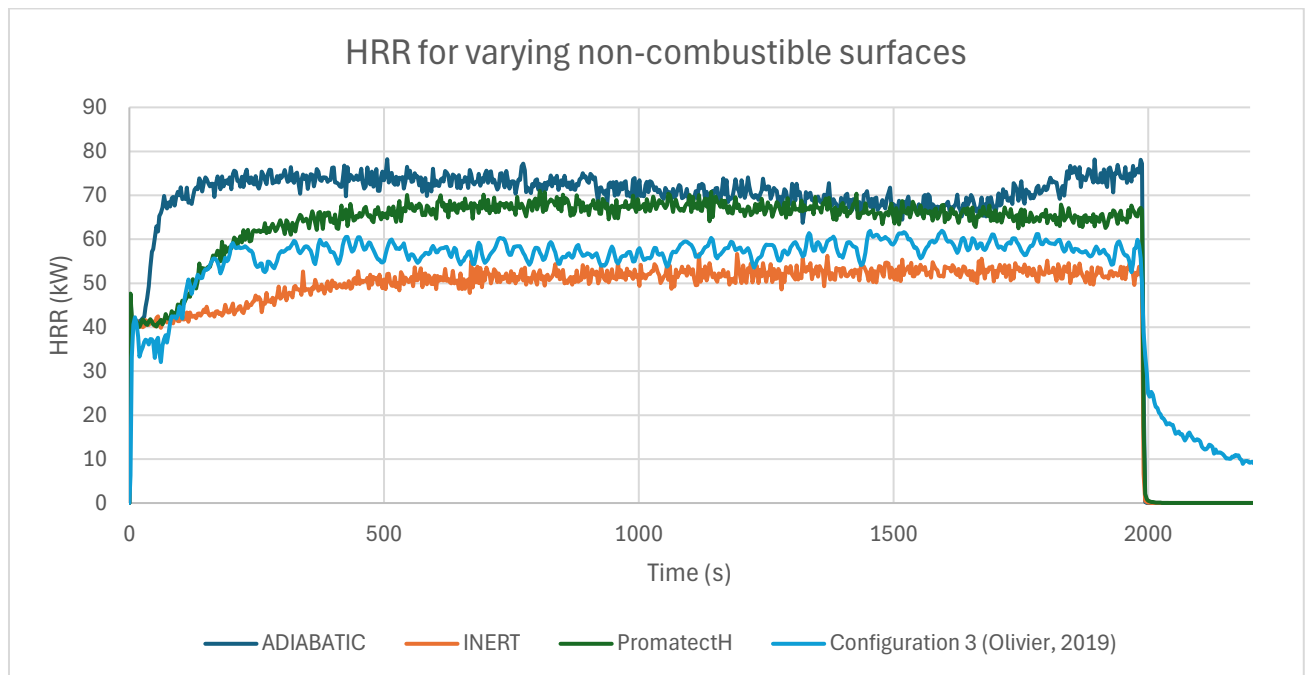


Figure 85: HRR for varying non-combustible surfaces in heating phase

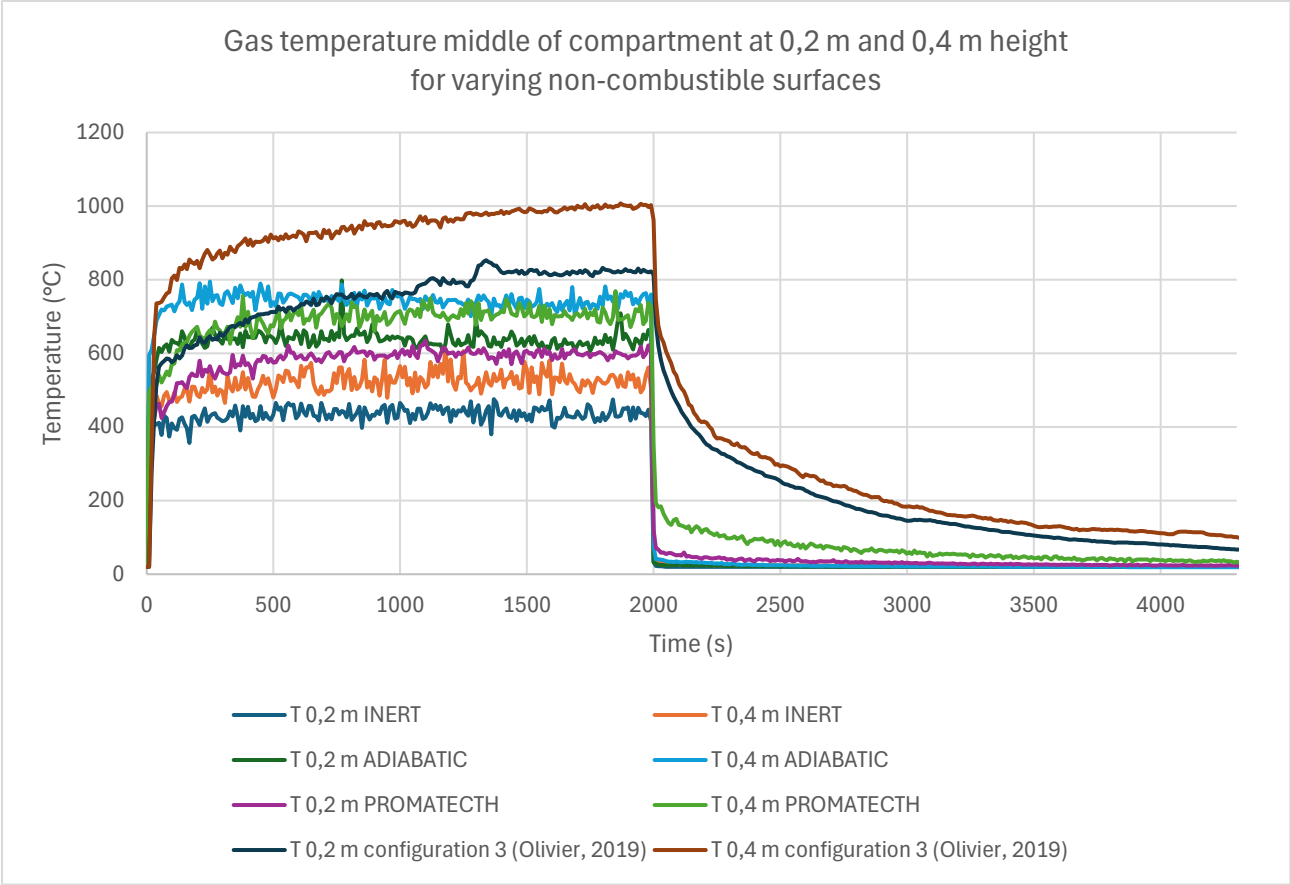


Figure 86: Gas temperatures for varying non-combustible surfaces

G ANALYSIS CHAR LAYER IN FDS MODEL

Appendix G elaborates on the modelling process of the char layer in the FDS model and the choice to exclude the formation of a physical char layer in the pyrolysis process in the final FDS model. This appendix adds to the information presented in Chapter 8.3. As explained, the char layer forms due to a not fully efficient combustion process of wood. A certain percentage of the burning wood remains on the surface in the form of a carbonaceous char layer. This layer slows down the heating from the underlying unaffected wood and works partly as a barrier for pyrolysis gases.

Initially, in the FDS model it was assumed that 15% of the pyrolyzing wood is left behind as char layer, while the remaining 85% is released as pyrolysis gases into the compartment which is based on the research by Hejtmánek et al. (2017). Subsequently, the char ratio was gradually reduced to 10%, 5% and 0% to assess the influence of the char layer on the simulated HRR and temperature development. This appendix provides a comparison between the simulations with varying char ratios.

The char layer is modelled with material properties derived from graphs in prEN 1995-1-2 as presented in Appendix C, specifically for CLT panels. An average value is taken for each material property within the temperature range above 300°C, which is often taken as the point where the char layer forms. Table 38 provides an overview of all used properties for modelling the char layer in FDS with the goal to imitate the insulating effect of the char layer.

Table 38: FDS input properties char layer

	Input value FDS model
Density	100 kg/m ³
Thermal conductivity	1,0 W/(m*K)
Specific heat capacity	1,6 kJ/(kg*K)

The simulations with varying char ratios are using the same test setup as configuration 3 by Olivier (2019) with an exposed left side wall. In Figure 87 the simulations are compared with the experimental data during the heating phase. The first thing to be noticed is the wavy HRR pattern for the simulations with char formation. A higher char ratio results in more fluctuating HRR results. It can be seen that the simulation with 0% char and the experimental result both show a very steady HRR after the initial growth phase. After turning the gas burner off, a slightly more gradual decay phase can be observed in the simulation with 5% char.

When looking at the average HRR, the simulations with char layer approximate the experimental result better than the 0% char simulation, which can be seen in Table 39. However, the shape of the HRR graph is also important for analysing if the FDS model works similar to the burning behaviour in real life experiments.

Table 39: HRR results for varying char ratio

	Average HRR	Percentual difference with configuration 3 (Olivier, 2019)
Simulation 0% char	64,3 kW	+14,2%
Simulation 5% char	59,0 kW	+4,8%
Simulation 10% char	55,5 kW	-1,3%
Simulation 15% char	51,8 kW	-8,6%
Configuration 3 (Olivier, 2019)	56,3 kW	/

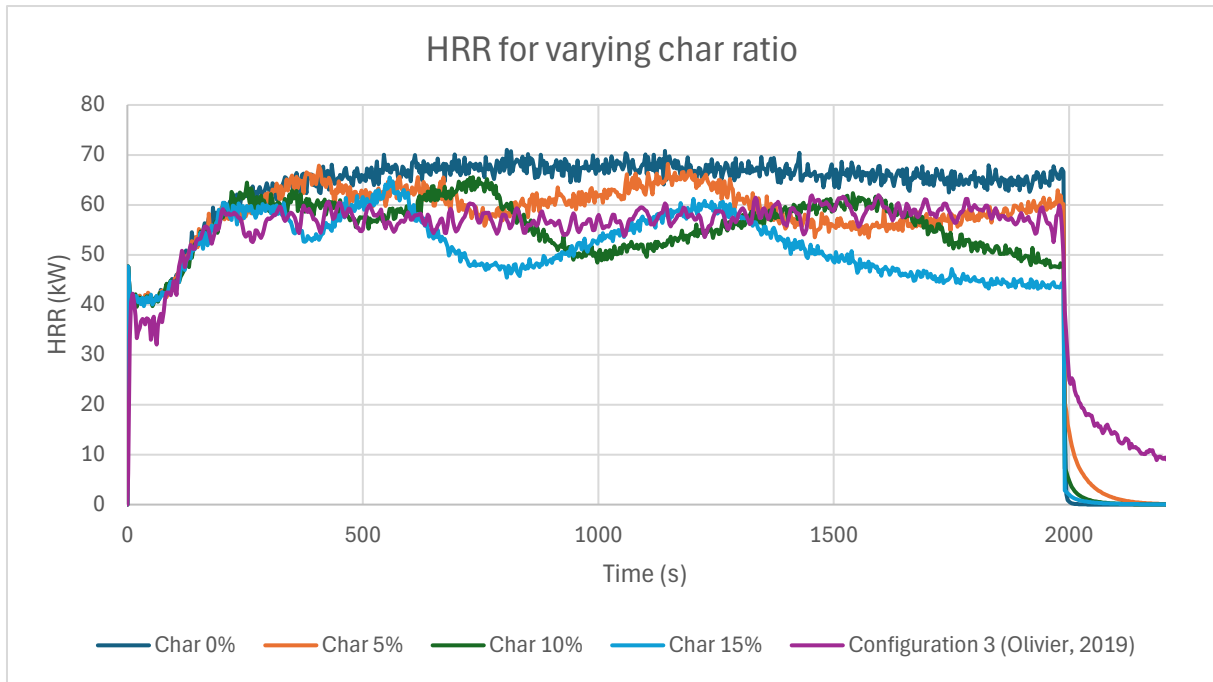


Figure 87: HRR for varying char ratio in heating phase

For assessing what happens with the burning behaviour of the exposed left side wall, the results are analysed in more detail focussing on the mass loss rate (MLR) of the wall. The MLR is measured in FDS in the middle of the exposed wall, outputting the burning rate in $\text{kg}/(\text{m}^2 \cdot \text{s})$. Figure 88 shows the MLR for the various simulations. In the initial stages, all simulations follow the same trend. However, the MLR subsequently drops for all simulations with a char layer. The MLR maintains a very irregular pattern for the remainder of the simulation which is difficult to explain. On the other hand, the simulation without char layer shows a relatively stable MLR which is in line with the stable HRR as presented in Figure 87.

A possible reason for the irregular MLR can be that once the char layer forms, the model cools down due to a lower surface temperature of the char layer. The combustion process of the underlying CLT will be affected by the char layer forming a barrier between the compartment gas and the timber. Subsequently, the char layer is heating up and the MLR increases again. In the FDS model, the char layer increases in thickness over time because no fall-off criteria are specified for the char layer. This can be part of future research. If the char layer keeps increasing in thickness, it would be expected that the MLR gradually decreases over time. However, the occasional steep increases in MLR contradict this theory.

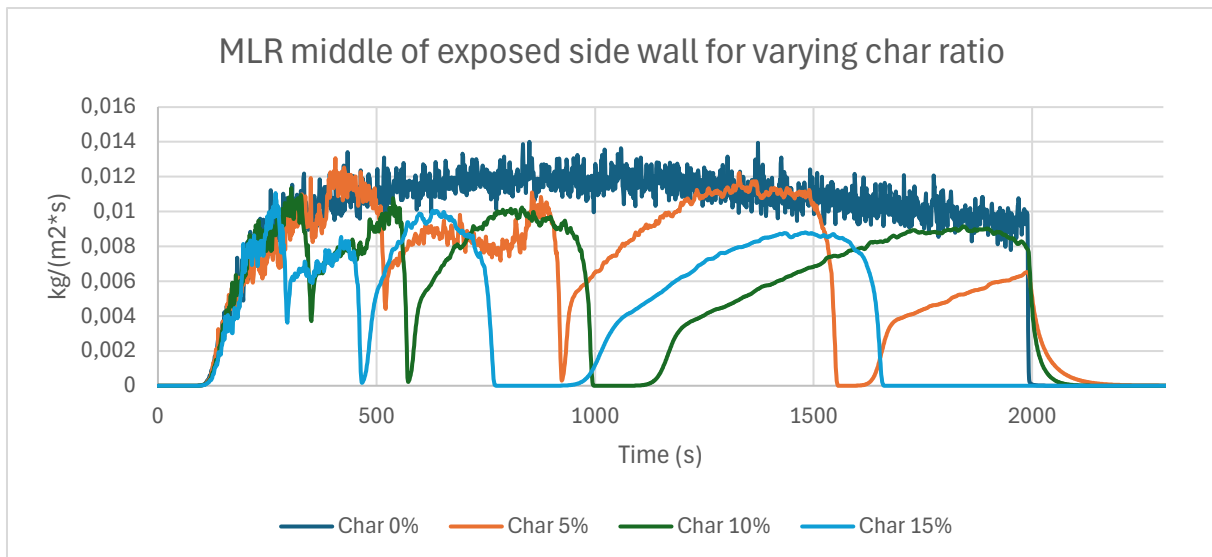


Figure 88: Mass loss rate exposed CLT wall for varying char ratio

Conclusively, no clear reasoning is found within the scope of this thesis to explain the irregular burning behaviour of wood in simulations where a physical char layer is formed in the FDS model. Due to the unexplainable HRR development, the reliability of the simulation results could not be verified. Therefore, it was decided to exclude the char layer from the final FDS model.

To account for a realistic energy release due to the burning CLT, the incomplete combustion is considered by using an effective heat of combustion value. The heat of combustion is defined as the amount of energy that is released when a unit mass is fully oxidised, which assumes a fully effective combustion process. Heat of combustion of wood ranges between 16-20 MJ/kg depending on the wood composition (MacLeod et al., 2023). In the FDS model presented in this thesis an effective heat of combustion value of 10 MJ/kg is applied, which is in line with values used in existing research as presented in Chapter 7.3.

The implications of excluding the char layer in the FDS model can be divided into two stages:

- In the heating phase, excluding the char layer should not notably influence the HRR development because the released energy is corrected by applying a lower effective heat of combustion value.
- In the decay phase, the char layer does have a notable influence in real life tests as explained in Chapter 6.1. The insulating effect of the char layer allows for sustained smouldering combustion of the underlying wood. The decay phase can therefore not be approximated in a realistic manner. Additional reasons for the bad representation of the decay phase are explained in Chapter 10.1.

For future research, it is advisable to look into fall off criteria for the char layer to approximate the real-life behaviour in a better way than in the modelling approach discussed in this thesis.

NATHAN
REMANS

